



Title	Stochastic-geometrical analysis to investigate critical behavior for statistical-mechanical models
Author(s)	半田, 悟
Citation	北海道大学. 博士(理学) 甲第13554号
Issue Date	2019-03-25
DOI	10.14943/doctoral.k13554
Doc URL	http://hdl.handle.net/2115/74215
Type	theses (doctoral)
File Information	Satoshi_Handa.pdf



[Instructions for use](#)

**Stochastic-geometrical analysis
to investigate critical behavior
for statistical-mechanical models**
(統計力学模型の臨界現象に対する確率幾何学的な解析)

Satoshi HANDA

Department of Mathematics
Hokkaido University

March. 2019.

Stochastic-geometrical analysis to investigate critical behavior for statistical-mechanical models

Satoshi HANDA
Department of Mathematics
Hokkaido University

Supervisor(Principal referee): Prof. Dr. Akira Sakai (Hokkaido University)

Other referees: Prof. Dr. Akihito Hora (Hokkaido University)

Prof. Dr. Michiko Yuri (Hokkaido University)

Prof. Dr. Tadahiro Miyao (Hokkaido University)

Contents

Preface	7
1 Introduction	9
1.1 Background	9
1.1.1 Critical behavior	9
1.1.2 The mean-field theory	10
1.1.3 The infrared bound	11
1.1.4 Other critical exponents	12
1.2 The main results	13
1.3 Organization	14
2 The mean-field behavior for the Ising model	15
2.1 The general setting and background for the Ising model	15
2.2 Other topics for the Ising model	18
2.3 Upper bound on the 1-arm exponent ρ in high dimensions	22
2.3.1 The setting for the mean-field bound on ρ	22
2.3.2 Mean-field bound on the 1-arm exponent ρ	23
2.3.3 Derivation of the mean-field bound for percolation	25
2.3.4 The random-current representation	27
2.3.5 A new correlation inequality	28
2.3.6 Proof of Theorem 2.3.1	31
2.3.7 Further discussion	33
2.4 Lower bound on the 1-arm exponent ρ in high dimensions	34
3 The lace expansion analysis for the nearest-neighbor models on the BCC lattice	37
3.1 Background	37
3.1.1 The lace expansion	37
3.1.2 The motivation for the lace expansion analysis on the BCC lattice .	38
3.2 The models and the main result	39
3.2.1 The body-centered cubic (BCC) lattice	39
3.2.2 Self-avoiding walk	40
3.2.3 Percolation	41
3.2.4 The infrared bound on the BCC lattice	41
3.2.5 Where and how to use the lace expansion	46

3.2.6	Organization	51
3.3	Lace-expansion analysis for self-avoiding walk	51
3.3.1	Derivation of the lace expansion	51
3.3.2	Diagrammatic bounds on the expansion coefficients	54
3.3.3	Diagrammatic bounds on the bootstrapping functions	58
3.3.4	Bounds on diagrams in terms of random-walk quantities	60
3.3.5	Further discussion	63
4	The mean-field behavior for the quantum Ising model	65
4.1	Background for the quantum Ising model	65
4.2	Setting and preliminaries	66
4.2.1	Definition of the quantum Ising model	66
4.2.2	The Suzuki-Trotter transformation	67
4.2.3	The random-current representation, the source-switching lemma and the correlation inequalities	69
4.2.4	The magnetization and the susceptibility	71
4.3	Mean-field behavior of the susceptibility	74
4.3.1	The main results	75
4.3.2	Proof of the item (a) in Theorem 4.3.1.	75
4.3.3	Proof of the item (b) in Theorem 4.3.1.	77
4.3.4	Further discussion	81
	Acknowledgements	83
	Bibliography	85

Preface

Statistical mechanics is a branch of mathematical physics developed in 19 century. The purpose of this theory is to extract macroscopic features from microscopic system of a numerous number of interacting particles. It is completely impossible to solve all Newtonian equations of motion for each particle. Probability theory and statistics play a great role in statistical mechanics to deal with such a large number of degrees of freedom.

As a result of cooperation of those interacting particles, intriguing phenomena like phase transitions and critical phenomena occur. For example, the Ising model (on the d -dimensional Euclidean lattice) is a statistical-mechanical model of ferromagnets and exhibits a phase transition in $d \geq 2$. While the spontaneous magnetization is zero in the high temperature phase, it is strictly positive in the low temperature phase. This means that there is a non-trivial temperature, called the critical temperature, around which a physical property on the system drastically changes. Other observables also show singular behavior around or at the critical temperature and those phenomena are called critical behavior. We believe that critical behavior is identified by the so-called critical exponent and this exponent depends only on the dimension and the symmetry of the system. Moreover, we believe that the universality classes of physical systems are classified by those universal exponents. Therefore, the main important objects to be investigated are about the existence of phase transitions and the critical behavior or the critical exponents.

As explained above, we have to consider extremely large number of interacting particles which cannot be treated just by independent random variables. Many mathematicians and physicists have been making efforts to overcome this difficulty. One of the ways is a stochastic-geometrical analysis based on the random walk theory. Although an interacting system does not have the independence like a random walk, we can predict approximate behaviors of the interacting system and have some ideas from the random walk analysis in terms of a stochastic-geometrical language (the Ising model is defined in terms of spin language, but has various stochastic-geometrical representations). Many important results have been proven in such a way. However, it is still far way from the fully understanding of interacting systems mathematically-rigorously.

In this thesis, we consider the four models; the classical Ising model, self-avoiding walk (SAW), percolation and the quantum Ising model. In Chapter 1, we will give a conceptual background of critical behavior. In Chapter 2, we will introduce the classical Ising model along with the historical accumulation of knowledge and the recent developments. We prove the quantitative estimate on the unknown critical exponent of the Ising model. This work is based on the preprint [48]. In Chapter 3, we will introduce SAW and percolation and show the results on the lace expansion analysis for the body-centered cubic lattice.

This work is based on the paper [49]. In Chapter 4, we will introduce the quantum Ising model, especially focusing on the graphical representations of it. By using the Suzuki-Trotter transformation and a graphical representation based on the classical Ising model, we will analyze the susceptibility of the quantum Ising model. This is an ongoing work with Kamijima and Sakai and based on the preprint [50].

Chapter 1

Introduction

1.1 Background

1.1.1 Critical behavior

Cooperation of infinitely many particles results in various intriguing and challenging problems. One of those is to understand phase transitions and critical behavior of statistical-mechanical models, such as percolation and the ferromagnetic Ising model. For percolation, for example, it exhibits a phase transition when the bond-occupation parameter p crosses its critical value p_c . If p is far below p_c , each cluster of occupied vertices is so small that we may use standard probabilistic techniques for i.i.d. random variables to predict what happens in the subcritical phase. If p is far above p_c , on the other hand, vacant vertices can only form tiny islands and most of the other vertices are connected to form a single gigantic cluster. However, when p is close to p_c , the cluster of connected vertices from the origin may be extremely large but porous in a nontrivial way, and therefore naive perturbation methods fail.

A similar phenomenon occurs for self-avoiding walk (SAW), a century-old statistical-mechanical model for linear polymers. Consider a locally finite, amenable and transitive graph as space. A standard example is the d -dimensional integer lattice \mathbb{Z}^d . The main observable to be investigated is the SAW two-point function, which is the following generating function with fugacity $p \geq 0$:

$$G_p(x) = \sum_{\omega: o \rightarrow x} p^{|\omega|} \prod_{j=1}^{|\omega|} D(\omega_j - \omega_{j-1}) \prod_{0 \leq s < t \leq |\omega|} (1 - \lambda \delta_{\omega_s, \omega_t}), \quad (1.1.1)$$

where the sum is over the nearest-neighbor paths ω on the concerned lattice from the origin o to x , $|\omega|$ is the number of steps along ω , and D is the 1-step distribution of simple random walk (RW): $D(x) = (2d)^{-1} \delta_{|x|,1}$ on \mathbb{Z}^d . The parameter $\lambda \in [0, 1]$ is the intensity of self-avoidance; the model with $\lambda = 1$ is called strictly SAW, while the one with $\lambda \in (0, 1)$ is called weakly SAW. The two-point function with $\lambda = 0$ is equivalent to the RW Green function $S_p(x) \equiv \sum_{n=0}^{\infty} p^n D^{*n}(x)$, where D^{*n} is the n -fold convolution of D . The critical point (= the radius of convergence) for RW is $p = 1$. For SAW, because of subadditivity, there is a critical point $p_c \geq 1$ such that the susceptibility $\chi_p \equiv \sum_x G_p(x)$ is finite if and only if $p < p_c$ and diverges as $p \uparrow p_c$ (see, e.g., [71]).

The way χ_p diverges is intriguing, as it shows power-law behavior as $(p_c - p)^{-\gamma}$ with the critical exponent γ . It is considered to be universal in the sense that the value of γ depends only on d and is insensitive to $\lambda \in (0, 1]$ and the detail lattice structure. For example, the value of γ for strictly SAW on \mathbb{Z}^2 is believed to be $\frac{43}{32}$ and equal to that for weakly SAW on the 2-dimensional triangular lattice. This is not the case for the critical point p_c , as its value may vary depending on $\lambda \in (0, 1]$ and the detail lattice structure. Other statistical-mechanical models, such as percolation, Ising model and the quantum Ising model, which exhibit divergence of the susceptibility, are also characterized by the critical exponent γ , and many physicists as well as mathematicians have been trying hard to identify the value of γ and classify the models into different universality classes since last century.

1.1.2 The mean-field theory

Because of the nonlocal self-avoidance constraint $\prod_{0 \leq s < t \leq |\omega|} (1 - \lambda \delta_{\omega_s, \omega_t})$ in (1.1.1), SAW does not enjoy the Markovian property, which holds only when $\lambda = 0$. If there is a way to average out the self-avoidance effect and absorb it into the fugacity p , then $G_p(x)$ may be approximated by the RW Green function $S_\mu(x)$ with a mean-field fugacity $\mu = \mu(\mathbb{Z}^d, \lambda, p)$, and therefore χ_p may be approximated by $\sum_x S_\mu(x) = (1 - \mu)^{-1}$. Presumably, $\mu(p_c) = 1$. If μ is left-differentiable at p_c , then this implies $\chi_p \asymp (p_c - p)^{-1}$ (i.e., χ_p is bounded above and below by positive multiples of $(p_c - p)^{-1}$) as $p \uparrow p_c$. In this respect, the mean-field value for the critical exponent γ is 1.

However, realizing the above idea is highly nontrivial. As a first step, one may want to use perturbation theory from the mean-field model (i.e., $\lambda = 0$). The expansion of the self-avoidance constraint in powers of $\lambda > 0$ yields

$$\prod_{0 \leq s < t \leq |\omega|} (1 - \lambda \delta_{\omega_s, \omega_t}) = \sum_{\Gamma \in \mathcal{G}[0, |\omega|]} (-\lambda)^{|\Gamma|} \prod_{\{s, t\} \in \Gamma} \delta_{\omega_s, \omega_t}, \quad (1.1.2)$$

where Γ , which is called a graph, is a set of pairs of indices on $[0, |\omega|] \equiv \{0, 1, \dots, |\omega|\}$, $\mathcal{G}[0, |\omega|]$ is a set of such graphs, and $|\Gamma|$ is the cardinality of Γ . The trivial contribution from $\Gamma \equiv \emptyset$ is the unperturbed solution $S_p(x)$, which is already bad because its radius of convergence is 1, while $p_c \geq 1$. The first correction term proportional to λ is

$$-\lambda \sum_{\omega: o \rightarrow x} p^{|\omega|} \prod_{j=1}^{|\omega|} D(\omega_j - \omega_{j-1}) \sum_{0 \leq s < t \leq |\omega|} \delta_{\omega_s, \omega_t} = -\lambda (S_p(o) - 1) S_p^{*2}(x). \quad (1.1.3)$$

The higher-order correction terms are more involved, but the radius of convergence of each term is always $p = 1$. What is worse, the alternating series of those terms is absolutely convergent only when p is close to zero, because the sum over $\Gamma \in \mathcal{G}[0, |\omega|]$ is potentially huge as long as $\lambda > 0$. As a result, this naive expansion cannot be applied near p_c in order to justify the mean-field behavior.

1.1.3 The infrared bound

Instead of deriving the exact solution for χ_p , one may seek bounds on χ_p or its derivative. Indeed, it is not so difficult to show that [71]

$$\frac{\chi_p^2}{1 + \lambda p_c^2 G_{p_c}^{*2}(o)} \leq \frac{d(p\chi_p)}{dp} \leq \chi_p^2. \quad (1.1.4)$$

The second inequality implies that χ_p is always bounded below by $(1 - p/p_c)^{-1}$. Moreover, the first inequality implies that χ_p is also bounded above by a multiple of $(1 - p/p_c)^{-1}$, hence $\gamma = 1$, if

$$G_{p_c}^{*2}(o) = \lim_{p \uparrow p_c} \int_{\mathbb{T}^d} \hat{G}_p(k)^2 \frac{d^d k}{(2\pi)^d} < \infty, \quad (1.1.5)$$

where $\hat{G}_p(k)$ is the Fourier transform of the SAW two-point function and $\mathbb{T}^d \equiv [-\pi, \pi]^d$ is the d -dimensional torus of side length 2π in the Fourier space. It is a sufficient condition for the mean-field behavior for χ_p and is called the bubble condition, named after the shape of the diagram consisting of two line segments. Whether or not the bubble condition holds depends on the behavior of $\hat{G}_p(k)$ in the infrared regime (i.e., around $k = 0$).

For the Ising model, we can show a similar differential inequality for the susceptibility of the Ising model. The critical bubble $G_{p_c}^{*2}(o)$ also appears in the denominator in the lower bound.

For percolation, we can also show a similar differential inequalities, but in the denominator in the lower bound, $G_{p_c}^{*3}(o)$ appears instead of $G_{p_c}^{*2}(o)$. Thus, the cubic integrability of $\hat{G}_p(k)$ (we can prove the non-negativity of $\hat{G}_p(k)$, see (3.2.49) below) is the so-called the triangle condition [8] which is a sufficient condition for γ and other critical exponents to take on their mean-field values. Again, whether or not the triangle condition holds depends on the infrared behavior of $\hat{G}_p(k)$.

Usually, there is no a priori bounds on $\hat{G}_p(k)$. However, for some spin models with a strong symmetry condition called reflection-positivity (e.g., the ferromagnetic Ising model with symmetric nearest-neighbor couplings satisfies this condition), the two-point function enjoys the following infrared bound [37]:

Theorem 1.1.1. *For any $d > 2$, there is a constant $K < \infty$ such that*

$$\|(1 - \hat{D})\hat{G}_p\|_\infty \equiv \sup_{k \in \mathbb{T}^d} (1 - \hat{D}(k))|\hat{G}_p(k)| \leq K \quad \text{uniformly in } p \text{ close to } p_c. \quad (1.1.6)$$

If D is a symmetric, non-degenerate and finite-range distribution with variance σ^2 , then $1 - \hat{D}(k) \sim \frac{\sigma^2}{2d}|k|^2$ as $|k| \rightarrow 0$. Suppose that the infrared bound holds for SAW, the Ising model and percolation. Then

$$G_{p_c}^{*2}(o) \leq \int_{\mathbb{T}^d} \left(\frac{K}{1 - \hat{D}(k)} \right)^2 \frac{d^d k}{(2\pi)^d} \asymp \int_{\mathbb{T}^d} \frac{d^d k}{|k|^4} \quad (\text{SAW and the Ising model}), \quad (1.1.7)$$

$$G_{p_c}^{*3}(o) \leq \int_{\mathbb{T}^d} \left(\frac{K}{1 - \hat{D}(k)} \right)^3 \frac{d^d k}{(2\pi)^d} \asymp \int_{\mathbb{T}^d} \frac{d^d k}{|k|^6} \quad (\text{percolation}), \quad (1.1.8)$$

which imply that the bubble condition holds in all dimensions $d > 4$ and the triangle condition holds in all dimensions $d > 6$.

On the other hand, there is some evidence (from hyperscaling inequalities, numerical simulations, conformal field theory and so on) to suggest that the critical exponents (if they exist) can not take on their mean-field values simultaneously if $d < 4$ for SAW and Ising model, and $d < 6$ for percolation. In this respect, the (upper) critical dimension d_c is said to be 4 for SAW and the Ising model, and 6 for percolation.

To complete the mean-field picture in high dimensions, it thus remains to show that the infrared bound (1.1.6) holds for all dimensions $d > d_c$. Here, the lace expansion comes into play. We will present the work on the lace expansion in Chapter 3.

We have mentioned only the classical models so far. There are the following results about the quantum Ising model. In particular, Björnberg [16] established an infrared bound for the Schwinger function, which is one of the main quantities for the space-time Ising model, assuming reflection-positivity. He also derived a similar differential inequality for the susceptibility with the critical bubble. As a consequence, he showed that the critical exponent γ for the susceptibility takes the mean-field value 1 by using the infrared bound to show the finiteness of the critical bubble and solving the differential inequality. It should be noted here that he analyzed the critical behavior when varying the ratio between the parameters of the coupling constant and of the quantum effect with fixed parameter p , which corresponds to the inverse temperature β . However, we are also interested in the critical behavior when varying the inverse temperature with fixed parameter of the quantum effect. In Chapter 4, we will consider more the quantum effect on the critical temperature and/or the critical exponents.

1.1.4 Other critical exponents

As explained in the above subsection, the bubble and triangle conditions are sufficient conditions for γ to take its mean-field value. However, there are other critical exponents which could not be identified by those conditions.

The first one is the critical exponent η called the anomalous dimension for the critical two-point function, defined as $G_{p_c}(x) \asymp |x|^{2-d-\eta}$ for $|x| \uparrow \infty$. In 2003, Hara, van der Hofstad and Slade [52] showed that the anomalous dimension $\eta = 0$ for SAW on the the spread-out lattice $\bar{\mathbb{Z}}_L^{d>d_c=4}$ and percolation on $\bar{\mathbb{Z}}_L^{d>d_c=6}$, which means that the critical two-point function of SAW and percolation asymptotically behaves like $|x|^{2-d}$ for the sufficiently large spread-out parameter L (they also showed the same results for lattice trees and lattice animals on $\bar{\mathbb{Z}}_L^{d>d_c=8}$). In 2008, Hara showed the same results for the nearest-neighbor SAW on $\mathbb{Z}^{d \geq 5(=d_c+1)}$ and percolation on $\mathbb{Z}^{d \geq 19(>d_c+1=7)}$. In 2007, Sakai showed the same result for the critical two-point function of the nearest-neighbor Ising model in sufficiently high dimensions and on the the spread-out lattice $\bar{\mathbb{Z}}_L^{d>d_c=4}$ for the sufficiently large L [80]. If $\eta = 0$, then the bubble condition (1.1.5) or the triangle condition hold in $d > 4$ or $d > 6$, respectively. Therefore, the results for the anomalous dimension in high dimensions are quite powerful.

The second critical exponent which could not be identified by the bubble and triangle conditions is the 1-arm exponent ρ . For the precise definition of the 1-arm exponent, see Section 2.3. For percolation, it is showed that ρ takes on the mean-field value 2, first by

Sakai [78] in $d > 7$ assuming that $\eta = 0$ and another condition, and then by Kozma and Nachmias [67] in $d > 6$ only assuming $\eta = 0$. For the Ising model, it is showed that ρ has the mean-field bound 1 in $d > 4$ assuming $\eta = 0$ in [48]. We will present this work in Chapter 2. We believe that the opposite inequality $\rho \geq 1$ holds in $d > 4$ for the Ising model. In a similar manner to [78], we strongly expect $\rho \geq 1$ in $d > 4$ as a conditional result. We will have a discussion about the lower bound for the Ising 1-arm exponent ρ in Section 2.4.

1.2 The main results

As explained in the previous section, there are some open problems.

1. Does the 1-arm exponent of the Ising model take mean-field value 1 in high dimensions? Is it possible to give optimal bounds for it?
2. Does the infrared bound hold for the nearest-neighbor percolation and Ising model in all dimensions $d > 6$ and $d > 4$, respectively without assuming reflection-positivity?
3. Do critical exponents change depending on the quantum effect?

For those questions, we obtain the following results.

Theorem 1.2.1 (Mean-field bound for the 1-arm exponent). *For the ferromagnetic Ising model on \mathbb{Z}^d , $d > 4$, defined by a translation-invariant, \mathbb{Z}^d -symmetric and finite-range spin-spin coupling satisfying $\eta = 0$,*

$$\liminf_{r \rightarrow \infty} r^{1+\varepsilon} \langle \sigma_o \rangle_r^+ = \infty \quad (1.2.1)$$

whenever $\varepsilon > 0$. Consequently, the critical exponent ρ satisfies $\rho \leq 1$.

Theorem 1.2.2 (Infrared bound). *For SAW on the d -dimensional body-centered cubic lattice $\mathbb{L}^{d \geq 6}$ and percolation on $\mathbb{L}^{d \geq 9}$, there exists a model-dependent constant $K \in (0, \infty)$ such that*

$$\|(1 - \hat{D})\hat{G}_p\|_\infty \leq K \quad \text{uniformly in } p \in [1, p_c), \quad (1.2.2)$$

which implies the mean-field behavior, e.g., $\gamma = 1$.

In the theorem below, the critical inverse temperature β_c appears and corresponds to p_c in the above subsection. See Chapter 4 in more detail.

Theorem 1.2.3 (The critical behavior of the Ising susceptibility with quantum effect). *Let the spin-spin coupling be non-negative and summable. For the ferromagnetic Ising model with the sufficiently small quantum effect $\delta \geq 0$, sufficiently small the space-time bubble diagram B and for $0 < \beta < \beta_c(\delta)$, the following holds.*

(a) *We have the lower bound for the susceptibility,*

$$\chi(\beta, \delta) \geq \frac{C_1}{\beta_c - \beta}. \quad (1.2.3)$$

where $0 < C_1 < \infty$ is a constant. Thus, if the critical exponent γ exists, then $\gamma \leq 1$.

(b) *We have the upper bound for the susceptibility,*

$$\chi(\beta, \delta) \leq \frac{C_2}{\beta_c - \beta}, \quad (1.2.4)$$

where $0 < C_2 < \infty$ is a constant. Thus, if the critical exponent γ exists, then $\gamma \geq 1$.

1.3 Organization

1. In Chapter 2, we will present the work based on the paper [48]. In Section 2.1 and 2.2, we will introduce the classical Ising model along with the historical accumulation of knowledge and the recent developments. In Section 2.3, we will introduce the 1-arm exponent ρ and prove that ρ has the mean-field bound 1 in $d > 4$ assuming the anomalous dimension $\eta = 0$, especially comparing with the 1-arm exponent of percolation. In Section 2.4, we will mention the lower bound for ρ also comparing with the percolation case.
2. In Chapter 3, we will present the work based on the preprint [49]. In Section 3.1, we will give a short history about the lace expansion. In Section 3.2, we will introduce the definition of the body-centered cubic (BCC) lattice and SAW and percolation on BCC lattice, and show the main result on the infrared bound based on the lace expansion analysis for the BCC lattice. In Section 3.3, we will give a full detail of lace-expansion analysis for self-avoiding walk.
3. In Chapter 4, we will present the ongoing work based on the preprint [50]. In Section 4.1, we will give a short summary for the quantum Ising model, especially focusing on the graphical representation. In Section 4.2, we will introduce the definition of the quantum Ising model and the key ingredients, Suauki-Trotter transformation and the random-current representation, to analyze the some physical quantities. In Section 4.3, we will identify the critical exponent for the susceptibility in high dimensions by deriving the two differential inequalities.

Chapter 2

The mean-field behavior for the Ising model

2.1 The general setting and background for the Ising model

In 1920, Lenz first invented a statistical-mechanical model for ferromagnets, which is nowadays known as the Ising model named after his student Ising, who began to work on it. We consider the d -dimensional Euclidean lattice \mathbb{Z}^d . The model consists of magnetic atoms on a finite subset $\Lambda \subset \mathbb{Z}^d$. Each magnetic atom has a spin which can be in either upward or downward state. Mathematically, each site $x \in \Lambda$ is associated to a spin variable σ_x which takes values either $+1$ (for the upward state) or -1 (for the downward state). For each spin configuration $\boldsymbol{\sigma} = \{\sigma_x\}_{x \in \Lambda}$, we define the Hamiltonian $H_\Lambda^{\vec{h}}$, which is the total energy for the spin configuration,

$$H_\Lambda^{\vec{h}}(\boldsymbol{\sigma}) = - \sum_{\{u,v\} \subset \Lambda} J_{u,v} \sigma_u \sigma_v - \sum_{v \in \Lambda} h_v \sigma_v, \quad (2.1.1)$$

where $\{J_{u,v}\}_{u,v \in \mathbb{Z}^d}$ is a collection of coupling constants and $\vec{h} = \{h_v\}_{v \in \mathbb{Z}^d}$ is a collection of external magnetic fields. If we assume that $J_{u,v} \geq 0$, then a spin tends to align with spins of its neighbors to keep $H_\Lambda^{\vec{h}}(\boldsymbol{\sigma})$ smaller. This is why the system is called ferromagnetic.

We introduce the Gibbs measure $\mu_{T;\Lambda}$ for a spin configuration $\boldsymbol{\sigma}$, which is the probability that $\boldsymbol{\sigma}$ is realized as a spin configuration,

$$\mu_{T;\Lambda}(\boldsymbol{\sigma}) = \frac{e^{-H_\Lambda^{\vec{h}}(\boldsymbol{\sigma})/T}}{Z_{T;\Lambda}^{\vec{h}}}, \quad (2.1.2)$$

where $T > 0$ is the temperature and the partition function $Z_{T;\Lambda}^{\vec{h}}$ is the normalization constant, defined by

$$Z_{T;\Lambda}^{\vec{h}} = \sum_{\boldsymbol{\sigma} \in \{\pm 1\}^\Lambda} e^{-H_\Lambda^{\vec{h}}(\boldsymbol{\sigma})/T}. \quad (2.1.3)$$

We define the thermal expectation of a function f on spin configurations by

$$\langle f \rangle_{T;\Lambda}^{\vec{h}} = \sum_{\sigma \in \{\pm 1\}^\Lambda} f(\sigma) \frac{e^{-H_\Lambda^{\vec{h}}(\sigma)/T}}{Z_{T;\Lambda}^{\vec{h}}}. \quad (2.1.4)$$

Now, we have prepared to define physical quantities to analyze phase transitions and critical behaviors. The following three are the basic physical quantities; the magnetization, the truncated two-point function and the susceptibility, respectively,

$$m(T, \vec{h}) = \lim_{\Lambda \rightarrow \mathbb{Z}^d} \langle \sigma_o \rangle_{T;\Lambda}^{\vec{h}}, \quad (2.1.5)$$

$$G_T(x, y) = \lim_{h \downarrow 0} \lim_{\Lambda \uparrow \mathbb{Z}^d} (\langle \sigma_o \sigma_x \rangle_{T;\Lambda}^{\vec{h} \equiv h} - \langle \sigma_o \rangle_{T;\Lambda}^{\vec{h} \equiv h} \langle \sigma_x \rangle_{T;\Lambda}^{\vec{h} \equiv h}), \quad (2.1.6)$$

$$\chi(T) = \sum_{x \in \mathbb{Z}^d} G_T(o, x). \quad (2.1.7)$$

And the spontaneous magnetization $m_s(T)$ is also important quantity, defined by

$$m_s(T) = \lim_{h \downarrow 0} m(T, \vec{h} \equiv h). \quad (2.1.8)$$

From now on, we suppose that coupling constant $J_{u,v} \geq 0$ is a translation-invariant, \mathbb{Z}^d -symmetric and finite-range (i.e., the support of J is finite), and $\vec{h} \equiv h \geq 0$. The existence of those limits are guaranteed by Griffiths' inequalities [41], [42] [43] and [39] (see also Proposition 4.2.3 in this thesis).

It is well known that if the system is finite then $\lim_{h \downarrow 0} \langle \sigma_o \rangle_{T;\Lambda}^{\vec{h}} = 0$ for any $0 < T < \infty$, which means that there is no phase transition. Moreover, other physical quantities are infinitely differentiable with respect to T and h , thus have no singular point. In order to catch phase transitions and critical behaviors, we should take the infinite-volume limit although we do not know whether it can show singular behaviors at first.

In 1925, Ising [47] proved that the 1-dimensional Ising model does not show phase transition, i.e., $m_s(T) = 0$ for any $0 < T < \infty$. In 1936, Peierls [75] implied that the spontaneous magnetization of the Ising model with $d \geq 2$ is positive at sufficiently low temperature (it was not mathematically rigorous at that time, but nowadays his method is called the Peierls contour argument and used for showing the existence of phase transition). Since then, many mathematician and physicists have become enthusiastic and been studying it.

In 1944, Onsager [74] solved the free-energy density of the Ising model with $d = 2$ and $h \equiv 0$ and showed the existence of phase transition. In 1952, Lee and Yang [69] showed that if $h \neq 0$ then the Ising model has no phase transition at any $T > 0$, which means that we only need to consider the case $h = 0$ for critical phenomena.

There are some characterizations for the critical temperature T_c . We can use the physical quantities above as the order parameters. For example, we can characterize the critical temperature T_c by the spontaneous magnetization,

$$T_c = \sup\{T > 0 : m_s(T) > 0\}. \quad (2.1.9)$$

Since G_T just becomes the two-point function for $T > T_c$, the monotonicity of the $\chi(T)$ holds thanks to Griffiths' inequality. Thus we can use the susceptibility as another characterization for the critical temperature,

$$\tilde{T}_c = \inf\{T > 0 : \chi(T) < \infty\}. \quad (2.1.10)$$

It is not obvious whether $T_c = \tilde{T}_c$. In fact, for another spin model, $T_c \neq \tilde{T}_c$ (e.g., Berezinskii-Kosterlitz-Thouless transition). However in 1987, Aizenman, Barsky and Fernández [3] showed that $T_c = \tilde{T}_c$ for the Ising model.

Once the model shows phase transitions, we are next interested in the behavior of order parameters around or at T_c , which is called critical behaviors. We believe that there exist power exponents β, η (anomalous dimension), γ, γ' such that

$$m_s(T) \underset{T \uparrow T_c}{\asymp} (T_c - T)^\beta, \quad G_{T_c}(x, y) \underset{|x-y| \uparrow \infty}{\asymp} |x-y|^{2-d-\eta}, \quad \chi(T) \begin{cases} \underset{T \downarrow T_c}{\asymp} (T - T_c)^{-\gamma} \\ \underset{T \uparrow T_c}{\asymp} (T_c - T)^{-\gamma'}. \end{cases} \quad (2.1.11)$$

For $d = 2$, Onsager's exact solution [74], Yang, Wu et al. [89] implies that $\beta = 1/8, \eta = 1/4$ and $\gamma = 7/4$. For $d = 3$, although there are some numerical results and approximate values, there are no rigorous result. For $d > 4$, we believe that the critical exponents take on the mean-field values, $\beta = 1/2, \eta = 0$ and $\gamma = 1$. Thus, $d = 4$ is threshold dimension and called the upper critical dimension, denoted by d_c . In 1982 and 1986, Aizenman [1] showed that $\gamma = 1$ and Aizenman and Fernández [5] showed that $\beta = 1/2$ under the bubble condition (see (1.1.5)). In 1976, Fröhlich, Simon and Spencer [37] showed that if the spin model satisfies reflection-positivity, then the infrared bound holds. This infrared bound and the Parseval's identity imply that the bubble condition holds. However, we believe that we do not need to assume reflection-positivity in order to show the mean-field behaviors (or the bubble condition), e.g., the next-nearest-neighbor model does not satisfy reflection-positivity. Note that the bubble condition does not imply that the anomalous dimension $\eta = 0$. Conversely if $\eta = 0$, the bubble condition holds. In 2007, Sakai [79] invented the lace expansion for the Ising model and showed that $\eta = 0$ under the suitable condition for coupling constants for $d > 4$. This means that the bubble condition holds for a quite large class of coupling constants without assuming reflection-positivity.

About the critical exponent γ' , we also believe that $\gamma = \gamma'$ by the symmetry. In the low temperature phase, the spontaneous magnetization is not 0. Thus, we have to treat the truncated two-point function in the definition of G_T . Recently, Duminil-Copin et al. [29] showed the exponential decay for the truncated two-point function G_T for $T < T_c$ and $d \geq 3$. For $d = 2$, the exponential decay is also known by Onsager's exact solution. For $T > T_c$, the exponential decay is also proved in [3]. Therefore, the truncated two-point function decays exponentially fast for all but the critical temperature T_c in any dimensions $d \geq 2$. This result also shows the finiteness of the susceptibility. However, identifying the speed of divergence as T goes to T_c from below, which the critical exponent γ' represents, is still an open problem.

There is another unknown critical exponent, which is called the 1-arm exponent ρ , defined by

$$\langle \sigma_o \rangle_r^+ \underset{r \uparrow \infty}{\asymp} r^{-\rho}, \quad (2.1.12)$$

where $\langle \sigma_o \rangle_r^+$ is the 1-spin expectation at the center of a ball of radius r surrounded by plus spins. The bubble condition also does not identify the value of ρ . In Section 2.3, we will present the work on the 1-arm exponent.

2.2 Other topics for the Ising model

1. *Critical behaviors for $d = d_c = 4$.* In the upper critical dimension $d_c = 4$, we believe that some order parameters have logarithmic correction. For example, we believe that for $d = d_c = 4$ the susceptibility diverges like,

$$\chi(T) \underset{T \downarrow T_c}{\sim} (T - T_c)^{-1} |\log(T - T_c)|^{1/3}. \quad (2.2.1)$$

The logarithmic correction appears via the logarithmic divergence of the bubble diagram for $d = 4$. This prediction is highly expected by the renormalization group method. In fact, for the n -component $|\phi|^4$ model, this asymptotic behavior holds by the mathematically rigorous renormalization group method, which Bauerschmidt, Brydges, and Slade have recently developed [9, 10], inspired by the original Wilson's idea. Their method can be applied to the n -component $|\phi|^4$ model and weakly self-avoiding walk via a functional integral representation with boson and fermion fields. The Ising model can be rewritten by a functional integral with boson fields with the potential (or the Boltzmann weight) $V(\varphi)$,

$$V(\varphi) = \frac{1}{2} \varphi^2 - \log \cosh(T^{-1/2} \varphi + h) + \text{Constant}, \quad (2.2.2)$$

where $\varphi \in \mathbb{R}$ [36, 11]. This transformation, known as the sine-Gordon transformation, allows us to translate the discrete Ising-spin σ on ± 1 into the continuous unbounded boson-spin φ on \mathbb{R} . The shape of this function of φ looks like the 1-component $|\phi|^4$ model. However, The control of the error terms arising from the renormalisation group maps has not been dealt properly yet.

2. *The infinite-volume Gibbs measure.* There is another way to characterize phase transition (or the critical temperature). We have already defined the Gibbs measure $\mu_{T;\Lambda}$ on a finite set $\Lambda \subset \mathbb{Z}^d$ and the thermal expectation, and then we take the infinite-volume limit of physical quantities to catch phase transition or critical behavior. How about the Gibbs measure after taking the infinite-volume limit? We have not introduced the boundary conditions so far, but physical quantities have the boundary effect. If there is no spin on the outside of a finite set Λ , we say the boundary is free. This corresponds to just (2.1.1). If the outside of Λ is occupied by plus or minus spins, we say the boundary is plus or minus, respectively. To define the plus or minus boundary, we put the extra term into the Hamiltonian (2.1.1); $\pm \sum_{u \in \Lambda, v \in \Lambda^c} J_{u,v} \sigma_u$ for plus or minus boundary. If we regard Λ as a torus, we say the boundary is periodic. For a general boundary condition ω , we denote the Gibbs measure with boundary condition ω by $\mu_{T;\Lambda}^\omega$. We take an increasing sequence $\{\Lambda_n\}_{n=1}^\infty$ to \mathbb{Z}^d . If the weak limit of $\mu_{T;\Lambda_n}^\omega$ as $n \uparrow \infty$ exists, we call the limit the infinite-volume Gibbs measure μ_T^ω (i.e., for any local function f of a spin

configuration, $\mu_T^\omega(f) := \lim_{n \uparrow \infty} \mu_{T; \Lambda_n}^\omega(f)$). We denote by $\mathcal{G}(T)$ the closed convex hull of a family of the infinite-volume Gibbs measures. If the number of measures in $\mathcal{G}(T)$ is 1 (i.e., $|\mathcal{G}(T)| = 1$) for any temperature $T > 0$, we say there is no phase transition (uniqueness of the infinite-volume Gibbs measure holds). If $|\mathcal{G}(T)| > 1$ for some small T , we say phase transition occurs. We can also define the critical temperature T'_c by

$$T'_c = \sup\{T > 0 : |\mathcal{G}(T)| > 1\}. \quad (2.2.3)$$

It is well-known that for the ferromagnetic Ising model with $h \geq 0$, the uniqueness of the infinite-volume Gibbs measure and the analyticity of the free-energy density are equivalent. Thus, $T'_c = T_c$. Moreover, by FKG-inequality, we have

$$\mu_T^-(f) \leq \mu_T^\omega(f) \leq \mu_T^+(f) \quad (2.2.4)$$

for any non-decreasing function f . Thus, the uniqueness of the infinite-volume Gibbs measure is equivalent to that $\mu_T^-(f) = \mu_T^+(f)$. In the other topics of the Ising model below in this section, we use a word phase transition in this sense.

3. *Phase transition on tree graphs.* The Ising model on trees, for example on the Cayley tree or the Bethe lattice, has been rigorously studied since the 1970's [66, 76]. The Cayley tree or the Bethe lattice, denoted by $\Gamma^d = (G, E)$, where G is a vertex set and E is a edge set, is an infinite $(d+1)$ -regular tree. This graph is non-amenable, i.e., $\inf\{\frac{|\partial K|}{|K|} : K \subset V, |K| < \infty\} \neq 0$, where ∂K is an inner boundary of K . By Lee-Yang, there is no phase transition with homogeneous magnetic fields on \mathbb{Z}^d , which is an amenable graph. However, due to the non-amenableity for the Cayley tree or the Bethe lattice, the phase transition can occur even when there is a non-zero homogeneous external magnetic field, cf. [65]. Preston [76] showed the following result:

Theorem 2.2.1 ([76]). *For the ferromagnetic Ising model on the Cayley tree or the Bethe lattice with coupling constants $J_{x,y} \equiv J > 0$ and with external magnetic fields $h_x \equiv h > 0$, there exists a critical temperature $T_c = T_c(d) > 0$ and $h_c = h_c(T, d)$ such that,*

$$\left\{ \begin{array}{ll} \text{(i)} & \text{there is no phase transition if } T \geq T_c(d) \text{ or } |h| > h_c(T, d), \\ \text{(ii)} & \text{there is a phase transition otherwise.} \end{array} \right.$$

As a recent work, there is a result for the critical-field Ising model on the Cayley tree under the influence of inhomogeneous external magnetic fields, for which we refer to the discussion in [15].

4. *Inhomogeneous external magnetic fields.* As mentioned above, we know that there is no phase transition for the nearest-neighbor Ising model with non-zero homogeneous external magnetic fields by Lee and Yang. However, for an inhomogeneous external magnetic field, the situation is different. Bissacot and Cioletti showed the following results [14]:

Theorem 2.2.2 ([14]). *Let $d \geq 2$. If the external magnetic field $\vec{h} = \{h_v\}_{v \in \mathbb{Z}^d}$ is summable, i.e., $\sum_{v \in \mathbb{Z}^d} |h_v| < \infty$, then there is a phase transition.*

Theorem 2.2.3 ([14]). *Let $d \geq 1$. If the external magnetic field $\vec{h} = \{h_v\}_{v \in \mathbb{Z}^d}$ satisfies $\liminf_{v \in \mathbb{Z}^d} h_v > 0$, then there is no phase transition (the uniqueness of the infinite-volume Gibbs measure holds).*

Especially, if the fields behave like the power decay, i.e.,

$$h_v = \begin{cases} h^*, & \text{if } v = 0, \\ \frac{h^*}{|v|^\gamma}, & \text{if } v \neq 0, \end{cases} \quad (2.2.5)$$

where $h^* > 0$ and $\gamma > 0$ (this is not the critical exponent for the susceptibility), by Theorem 2.2.2 above, there is a phase transition for $\gamma > d$. However, there are stronger results by Bissacot et al. [13], and Cioletti and Vila [20]:

Theorem 2.2.4 ([13] and [20]). *Let $d \geq 2$. For the ferromagnetic nearest-neighbor Ising model,*

$$\begin{cases} \text{(i) there is no phase transition} & \text{if } 0 < \gamma < 1, \\ \text{(ii) there is a phase transition} & \text{if } \gamma > 1, \\ \text{(iii) there is a phase transition} & \text{if } \gamma = 1 \text{ and } h^* \ll 1. \end{cases} \quad (2.2.6)$$

The second case claims that even for the non-summable case $1 < \gamma \leq d$, phase transition occurs. For the case $\gamma = 1$, the regime for large $h^* > 0$ is still an open problem. If the model shows phase transition, we are naturally interested in its critical behavior or the critical exponents for order parameters. However, there is almost no result in such a research direction. Presence of inhomogeneous external magnetic fields seems to deprive the system of translation-invariance and make the analysis much harder.

5. *The long-range Ising model (the Dyson model).* We consider the d -dimensional Ising model without the external magnetic fields and with long-range coupling constants $\{J_{u,v}\}_{u,v \in \mathbb{Z}^d}$ defined by

$$J_{u,v} = \begin{cases} J, & \text{if } |u - v| = 1, \\ \frac{1}{|u - v|^\alpha}, & \text{if } |u - v| \neq 1, \end{cases} \quad (2.2.7)$$

where $J > 0$ and $\alpha > d$ (the condition for α is for the total energy of the system not to diverge; the so-called regularity condition). For $d = 1$, it is well known that if $\alpha > 2$, there is no phase transition since the free-energy density is analytic in the thermodynamic parameters for any finite temperature. In 1969, Dyson showed the existence of a phase transition for $1 < \alpha < 2$ [31] and then in 1982, Fröhlich and Spencer showed the existence of a phase transition for $\alpha = 2$ [38].

On the other hand, for $d \geq 2$ with the nearest-neighbor coupling and without the external magnetic fields, there is a phase transition. Thus, by the Griffiths' inequality,

there is a phase transition for any $\alpha > d$. What happens if we put the inhomogeneous external magnetic field like (2.2.5)? By heuristic argument by Imry and Ma, we conjecture that there is a phase transition for the following two cases:

$$\begin{cases} \text{(i)} & \alpha > d + 1 \text{ and } \gamma > 1, \\ \text{(ii)} & d < \alpha < d + 1 \text{ and } \gamma > \alpha - d. \end{cases} \quad (2.2.8)$$

Since if $\alpha > d + 1$ then the energy of long-range interaction between a finite box and the outside of the box is smaller than the order of the surface of the box. Thus, the system is like the nearest neighbor case. Therefore, the item (i) is consistent with the case (ii) in Theorem 2.2.4. The item (ii) means that it is possible to impose the external magnetic fields a little bit more since $\alpha - d < 1$, due to the long-range effect, compared with the nearest-neighbor case. The existence of phase transition is shown by using the Peierls contour argument, but due to the long-range effect, the construction of the contour is not easy compared with the nearest-neighbor case. Moreover, we need to control the interaction between two contours due to also the long-range effect. To show the above conjecture by using Pirogov-Sinai contour is an ongoing project with Bissacot, Endo and Affonso.

There are a series of results about critical behavior for long-range models by Chen and Sakai [22, 23, 24, 25, 26]. In particular, they analyzed the critical two-point function for self-avoiding walk, percolation and the Ising model on \mathbb{Z}^d and proved its asymptotic behavior in high dimensions in [25, 26]. The models have the 1-step distribution $D(x) \asymp |x|^{-d-\alpha}$ with $\alpha > 0$ and the upper-critical dimension $d_c = 2(\alpha \wedge 2)$ for self-avoiding walk and the Ising model, and $d_c = 3(\alpha \wedge 3)$ for percolation, where $s \wedge t = \min\{s, t\}$. For the Ising model, there are the following relationships between $(T, J_{o,x}) = (p, D(x))$ such that $p = \sum_{x \in \mathbb{Z}^d} \tanh(J_{o,x}/T)$ and $pD(x) = \tanh(J_{o,x}/T)$. The statements are the following:

Theorem 2.2.5 ([25]). *Let $\alpha \neq 2$ and $d > d_c$. For sufficiently spread-out models of self-avoiding walk, percolation and the Ising model, the following holds.*

$$G_{p_c}(x) \underset{|x| \uparrow \infty}{\asymp} |x|^{\alpha \wedge 2 - d}. \quad (2.2.9)$$

Theorem 2.2.6 ([26]). *Let $\alpha = 2$ and $d > d_c$. For sufficiently spread-out models of self-avoiding walk, percolation and the Ising model, the following holds.*

$$G_{p_c}(x) \underset{|x| \uparrow \infty}{\asymp} \frac{|x|^{2-d}}{\log |x|}. \quad (2.2.10)$$

The prefactor of the dominant term of $G_{p_c}(x)$ has more concrete form in the statement in the papers [25] and [26]. The proofs are based on the lace expansion analysis.

2.3 Upper bound on the 1-arm exponent ρ in high dimensions

2.3.1 The setting for the mean-field bound on ρ

First, we introduce the special setting of the Ising model for proving the mean-field bound on the 1-arm exponent. It seems to be slightly unusual setting due to the technical reason for the proof of the main result. We consider the Ising model on V_R , which is the d -dimensional ball of radius $R > 0$:

$$V_R = \{v \in \mathbb{Z}^d : |v| \leq R\}. \quad (2.3.1)$$

It is convenient to use the Euclidean distance $|\cdot|$ here, but the results hold for any norm on the lattice \mathbb{Z}^d . Let ∂V_r ($r < R$) be the boundary of V_r :

$$\partial V_r = \{v \in V_R \setminus V_r : \exists u \in V_r \text{ such that } J_{u,v} > 0\}. \quad (2.3.2)$$

The Hamiltonian for a spin configuration $\sigma \equiv \{\sigma_v\}_{v \in V_R} \in \{\pm 1\}^{V_R}$ is defined as

$$H_{r,R}^h(\sigma) = - \sum_{\{u,v\} \subset V_R} J_{u,v} \sigma_u \sigma_v - h \sum_{v \in \partial V_r} \sigma_v, \quad (2.3.3)$$

where $J_{u,v} \geq 0$ is a translation-invariant, \mathbb{Z}^d -symmetric and finite-range coupling, and h is the strength of the external magnetic field. We note that it is crucial to impose the external magnetic field only on ∂V_r . Due to this slightly unusual setup, we will eventually be able to derive an essential correlation inequality that differs from the one for percolation.

The thermal expectation of a function f on spin configurations at the critical temperature T_c is given by

$$\langle f \rangle_{r,R}^h = \frac{1}{2^{|V_R|}} \sum_{\sigma \in \{\pm 1\}^{V_R}} f(\sigma) \frac{e^{-H_{r,R}^h(\sigma)/T_c}}{Z_{r,R}^h}, \quad Z_{r,R}^h = \frac{1}{2^{|V_R|}} \sum_{\sigma \in \{\pm 1\}^{V_R}} e^{-H_{r,R}^h(\sigma)/T_c}. \quad (2.3.4)$$

The major quantities to be investigated are the 1-spin and 2-spin expectations. Since they are increasing in h by Griffiths' inequality [41], [42] [43] and [39] (see also Proposition 4.2.3 in this thesis), we simply denote their limits by

$$\langle \sigma_x \rangle_r^+ = \lim_{h \uparrow \infty} \langle \sigma_x \rangle_{r,R}^h \quad [x \in V_r \cup \partial V_r], \quad (2.3.5)$$

$$\langle \sigma_x \sigma_y \rangle_R = \lim_{h \downarrow 0} \langle \sigma_x \sigma_y \rangle_{r,R}^h \quad [x, y \in V_R]. \quad (2.3.6)$$

Since $\langle \sigma_x \sigma_y \rangle_R$ is also increasing in R by Griffiths' inequality, we denote its limit by

$$\langle \sigma_x \sigma_y \rangle = \lim_{R \uparrow \infty} \langle \sigma_x \sigma_y \rangle_R. \quad (2.3.7)$$

In the following statement (as well as later in the proofs) we use the notation $f \asymp g$ to mean that the ratio f/g is bounded away from zero and infinity (in the prescribed limit).

One assumption that we shall make throughout is the mean-field decay for the critical two-point function

$$\langle \sigma_o \sigma_x \rangle \asymp |x|^{2-d} \quad \text{as } |x| \uparrow \infty. \quad (2.3.8)$$

A sharp asymptotic expression that implies (2.3.8) is proven by the lace expansion for a fairly general class of J , whenever the support of J is sufficiently large [79]. We note that reflection-positivity has not succeeded in providing the above two-sided x -space bound; only one exception is the nearest-neighbor model, for which a one-sided x -space bound is proven [85]. In dimensions $d < 4$, the exponent on the right-hand side may change. An exact solution for $d = 2$ was identified by Wu et al. [89], which implies $\langle \sigma_o \sigma_x \rangle \asymp |x|^{-1/4}$ as $|x| \uparrow \infty$.

We consider the ferromagnetic Ising model at its critical temperature $T = T_c$, and study the 1-spin expectation $\langle \sigma_o \rangle_r^+$ at the center of a ball of radius r surrounded by plus spins. The decreasing limit of $\langle \sigma_o \rangle_r^+$ as $r \uparrow \infty$ is the spontaneous magnetization. Recently, Aizenman, Duminil-Copin and Sidoravicius [4] showed that, if the spin-spin coupling satisfies a strong symmetry condition called reflection-positivity, then the spontaneous magnetization is a continuous function of temperature in all dimensions $d > 2$, in particular $\lim_{r \uparrow \infty} \langle \sigma_o \rangle_r^+ = 0$ at criticality. The present paper gives quantitative bounds on the rate of convergence. The nearest-neighbor model is an example that satisfies reflection-positivity. Also, its spontaneous magnetization on \mathbb{Z}^2 is known to be zero at criticality [90]. However, in general, finite-range models do not satisfy reflection-positivity, and therefore we cannot automatically justify continuity of the spontaneous magnetization for, e.g., the next-nearest-neighbor model. Fortunately, by using the lace expansion [25, 79], we can avoid assuming reflection-positivity to ensure $\eta = 0$ (as well as $\beta = 1/2$, $\gamma = 1$, $\delta = 3$) and $\lim_{r \uparrow \infty} \langle \sigma_o \rangle_r^+ = 0$ at criticality in dimensions $d > 4$ if the support of J is large enough.

In this section, we prove that it does not approach very fast whenever $d > 4$; in this case we prove $\langle \sigma_o \rangle_r^+ \geq r^{-1+o(1)}$. The proof relies on the random-current representation, which is a sophisticated version of the high-temperature expansion. It was initiated in [44] to show the GHS inequality. Then, in 1980's, Aizenman revived it to show that the bubble condition (i.e., square-summability of the critical 2-spin expectation, see (1.1.5)) is a sufficient condition for the mean-field behavior [1, 3, 5] as we have already explained in the in the previous chapter (around the subsection 1.1.3). It is also used in [4, 79, 81] to obtain many useful results for the Ising and φ^4 models. In combination with the second-moment method, we prove a correlation inequality that involves $\langle \sigma_o \rangle_r^+$ and free-boundary 2-spin expectations. Then, by using this correlation inequality, we derive the desired result.

2.3.2 Mean-field bound on the 1-arm exponent ρ

We are investigating the 1-arm exponent for the Ising model at criticality, informally described as $\langle \sigma_o \rangle_r^+ \approx r^{-\rho}$ as $r \uparrow \infty$. In order to make the symbol \approx precise, we give the formal definition

$$\rho = -\liminf_{r \rightarrow \infty} \frac{\log \langle \sigma_o \rangle_r^+}{\log r}. \quad (2.3.9)$$

A more conventional way of defining ρ is by letting $\langle \sigma_o \rangle_r^+ \asymp r^{-\rho}$ as $r \uparrow \infty$, which was used to define the percolation 1-arm exponent [67, 78]. However, the latter definition does not necessarily guarantee the existence of ρ . To avoid this existence issue, we adopt the former definition (2.3.9).

The main result is the one-sided bound $\rho \leq 1$ in the mean-field regime, i.e., when $d > 4$ and (2.3.8) holds. Folklore of statistical physics predicts that (2.3.9) is actually a limit. The use of limit inferior is somewhat arbitrary (limsup would be also possible), but this choice gives the strongest result.

Theorem 2.3.1. *For the ferromagnetic Ising model on \mathbb{Z}^d , $d > 4$, defined by a translation-invariant, \mathbb{Z}^d -symmetric and finite-range spin-spin coupling satisfying (2.3.8),*

$$\liminf_{r \rightarrow \infty} r^{1+\varepsilon} \langle \sigma_o \rangle_r^+ = \infty \quad (2.3.10)$$

whenever $\varepsilon > 0$. Consequently, the critical exponent ρ defined in (2.3.9) satisfies $\rho \leq 1$.

Tasaki [88] derive the hyperscaling inequality as follows. This gives us an upper bound for the 1-arm exponent.

Theorem 2.3.2. *The critical exponents η and ρ satisfy*

$$d - 2 + \eta \geq 2\rho. \quad (2.3.11)$$

Proof of Theorem 2.3.2. We impose the external magnetic field $h > 0$ on the boundary at a distance $|x|/3$ from the origin o and x . Then, by the Griffiths' inequality, we obtain $\langle \sigma_o \sigma_x \rangle \leq \langle \sigma_o \sigma_x \rangle_h$. Then by taking the limit as $h \uparrow \infty$, $\langle \sigma_o \sigma_x \rangle \leq \langle \sigma_o \rangle_{|x|/3}^+ \langle \sigma_x \rangle_{|x|/3}^+ = (\langle \sigma_o \rangle_{|x|/3}^+)^2$ if for sufficiently large $|x|$ (so that $|x|/3$ is larger than the range of the spin-spin coupling). At the last equality, we have used translation-invariance. By the definitions of the critical exponents, we obtain the hyperscaling inequality. ■

In dimensions $d > 4$, this implies the hyperscaling inequality $\rho \leq (d - 2)/2$, and the bound in 2.3.1 improves on Tasaki's result.

Remark 2.3.3. It is a challenge now to prove

$$\limsup_{r \rightarrow \infty} r^{1-\varepsilon} \langle \sigma_o \rangle_r^+ = 0 \quad (2.3.12)$$

for any $\varepsilon > 0$, which implies readily (together with our theorem) that (2.3.9) is actually a limit and $\rho = 1$.

Our proof of $\rho \leq 1$ uses (2.3.8), which requires $d > 4$ (and the support of J to be large), even though the result is believed to be true for all dimensions $d \geq 2$. The aforementioned correlation inequality $\langle \sigma_o \rangle_{|x|/3}^+ \geq \sqrt{\langle \sigma_o \sigma_x \rangle}$ combined with the exact solution for $d = 2$ [89] and numerical predictions for $d = 3, 4$ supports this belief. This is why we call $\rho \leq 1$ the optimal mean-field bound.

Another key ingredient for the proof of $\rho \leq 1$ is the random-current representation, which provides a translation between spin correlations and percolation-like connectivity events. Then, by applying the second-moment method to the connectivity events as

explained below for percolation, we can derive a crucial correlation inequality (cf. (2.3.28)) that relates 1-spin and 2-spin expectations. To explain what the second-moment method is and to compare the resulting correlation inequalities for the two models, we spend the next subsection to explain the derivation of the mean-field bound on the percolation 1-arm exponent, i.e., $\rho \leq 2$ for $d > 6$.

2.3.3 Derivation of the mean-field bound for percolation

We consider the following bond percolation on \mathbb{Z}^d . Each bond $\{u, v\} \subset \mathbb{Z}^d$ is either occupied or vacant with probability $pJ_{u,v}$ or $1 - pJ_{u,v}$, independently of the other bonds, where $p \geq 0$ is the percolation parameter. The two-point function $G_p(x, y)$ is the probability that x is connected to y by a path of occupied bonds ($G_p(x, x) = 1$ by convention), i.e.,

$$G_p(x, y) = \mathbb{P}_p(x \text{ is connected to } y). \quad (2.3.13)$$

It is well-known that, for any $d \geq 2$, there is a nontrivial critical point p_c such that the susceptibility $\sum_x G_p(o, x)$ is finite if and only if $p < p_c$ [8]. We define the 1-arm probability θ_r , which is the probability that the center of the ball of radius r is connected to its surface by a path of occupied bonds, i.e.,

$$\theta_r = \mathbb{P}_p(o \text{ is connected to } \partial V_r). \quad (2.3.14)$$

This probability also exhibits a phase transition at p_c [2]: $\theta(p) \equiv \lim_{r \uparrow \infty} \theta_r = 0$ if $p < p_c$ and $\theta(p) > 0$ if $p > p_c$. Although the continuity $\theta(p_c) = 0$ has not yet been proven in full generality, it is shown by the lace expansion [35, 54] that, if $d > 6$ and the support of J is sufficiently large, then $\theta(p_c) = 0$ and $G_{p_c}(o, x) \asymp |x|^{2-d}$ as $|x| \uparrow \infty$. This Newtonian behavior of G_{p_c} is believed not to hold in lower dimensions (we are working on a research in this direction and see the next chapter and [49]).

Fix $p = p_c$ and define the percolation 1-arm exponent ρ by letting $\theta_r \asymp r^{-\rho}$ as $r \uparrow \infty$. It is known that the following inequality called the hyperscaling inequality holds in [88].

Theorem 2.3.4. *The critical exponents η and ρ satisfy*

$$d - 2 + \eta \geq 2\rho. \quad (2.3.15)$$

Since $\eta = 0$ for $d > 6$, the above inequality implies that $\rho \leq (d - 2)/2$ for $d > 6$, which gives us an upper bound for the 1-arm exponent.

Proof of Theorem 2.3.4 Since if the origin o is connected to x , then both sites are connected to the boundary at a distance $|x|/3$ from them. Thus, $G_p(o, x) \leq \theta_{|x|/3}^2$ for sufficiently large $|x|$ (so that $|x|/3$ is larger than the range of the spin-spin coupling). By the definitions of the critical exponents, we obtain the hyperscaling inequality. ■

In [78], we were able to improve this to the optimal mean-field bound $\rho \leq 2$ for $d > 6$ by using the second-moment method.

Theorem 2.3.5. *If $d > 6$, the support of J is sufficiently large and ρ exists, then $\rho \geq 2$.*

Proof. Let X_r be the random number of vertices on ∂V_r that are connected to the origin o . We note that X_r can be positive only when o is connected to ∂V_r . Then, by the Schwarz inequality,

$$\mathbb{E}_p[X_r]^2 = \mathbb{E}_p\left[X_r \mathbb{1}_{\{o \text{ is connected to } \partial V_r\}}\right]^2 \leq \underbrace{\mathbb{E}_p\left[\mathbb{1}_{\{o \text{ is connected to } \partial V_r\}}\right]}_{=\theta_r} \mathbb{E}_p[X_r^2], \quad (2.3.16)$$

which implies $\theta_r \geq \mathbb{E}_p[X_r]^2 / \mathbb{E}_p[X_r^2]$. Notice that $\mathbb{E}_p[X_r] = \sum_{x \in \partial V_r} G_p(o, x)$. If o is connected to x and y , then there exists a site $u \in \mathbb{Z}^d$ such that o is connected to u , x is connected to u and y is connected to u bond-disjointly, By the BK inequality, (this kind of bound is called the tree-graph inequality [8]),

$$\mathbb{E}_p[X_r^2] = \sum_{x, y \in \partial V_r} \mathbb{P}_p(o \text{ is connected to } x, y) \leq \sum_{\substack{u \in \mathbb{Z}^d \\ x, y \in \partial V_r}} G_p(o, u) G_p(u, x) G_p(u, y). \quad (2.3.17)$$

As a result, we arrive at the correlation inequality

$$\theta_r \geq \frac{\left(\sum_{x \in \partial V_r} G_p(o, x) \right)^2}{\sum_{\substack{u \in \mathbb{Z}^d \\ x, y \in \partial V_r}} G_p(o, u) G_p(u, x) G_p(u, y)}. \quad (2.3.18)$$

Using $G_{p_c}(x, y) \asymp \|x - y\|^{2-d}$, where $\|\cdot\| = |\cdot| \vee 1$ is to avoid singularity around zero, we can show that the right-hand side of the above inequality is bounded from below by a multiple of r^{-2} , resulting in $\rho \leq 2$ for $d > 6$. In fact, the numerator is of the order r^2 since

$$\sum_{x \in \partial V_r} G_{p_c}(o, x) \asymp \sum_{x \in \partial V_r} |x|^{2-d} \asymp r^{d-1} r^{2-d} = r. \quad (2.3.19)$$

For bounding the denominator, we split the sum over z into two cases, $u \in V_{r/2}$ and $u \notin V_{r/2}$. For the first case,

$$\sum_{\substack{u \in V_{r/2} \\ x, y \in \partial V_r}} G_{p_c}(o, u) G_{p_c}(u, x) G_{p_c}(u, y) \leq C r^{2(2-d)+2(d-1)} \sum_{u \in V_{r/2}} \|u\|^{2-d} \leq C r^4, \quad (2.3.20)$$

where $C > 0$ is a constant which does not depend on r , and might change when we bound above, but we use the same letter C . For the second case, by using the convolution bound in Proposition 1.7 (i) in [52] at the second inequality,

$$\begin{aligned} \sum_{\substack{u \notin V_{r/2} \\ x, y \in \partial V_r}} G_{p_c}(o, u) G_{p_c}(u, x) G_{p_c}(u, y) &\leq C r^{2-d} \sum_{\substack{u \in \mathbb{Z}^d \\ x, y \in \partial V_r}} \|x - u\|^{2-d} \|y - u\|^{2-d} \\ &\leq C r^{2-d} \sum_{x, y \in \partial V_r} \|x - y\|^{4-d} \\ &\leq C r^{2-d+4-d+2(d-1)} = C r^4. \end{aligned} \quad (2.3.21)$$

Therefore, the denominator is of order r^4 and this complete the proof of Theorem 2.3.5. \blacksquare

In order to prove the opposite inequality $\rho \geq 2$ for $d > 6$ to conclude the equality, Kozma and Nachmias [67] use another correlation inequality that involves not only θ_r and G_p but also the mean-field cluster-size distribution. The Ising cluster-size distribution under the random-current representation is not available yet, and we are currently heading in that direction. We will have a discussion on the lower bound of the Ising 1-arm in Section 2.4.

2.3.4 The random-current representation

A current configuration $\mathbf{n} \equiv \{n_b\}$ is a set of nonnegative integers on bonds $b \in B_R \equiv \{\{u, v\} \subset V_R : J_{u,v} > 0\}$ or $b \in G_r \equiv \{\{v, g\} : v \in \partial V_r\}$, where g is an imaginary ghost site. Given a current configuration \mathbf{n} , we define the source set $\partial \mathbf{n}$ as

$$\partial \mathbf{n} = \left\{ v \in V_R \cup \{g\} : \sum_{b \ni v} n_b \text{ is odd} \right\}, \quad (2.3.22)$$

and the weight functions $w_{r,R}^h(\mathbf{n})$ and $w_R(\mathbf{n})$ as

$$w_{r,R}^h(\mathbf{n}) = \prod_{b \in B_R} \frac{(J_b/T_c)^{n_b}}{n_b!} \prod_{b' \in G_r} \frac{(h/T_c)^{n_{b'}}}{n_{b'}!}, \quad w_R(\mathbf{n}) = w_{r,R}^0(\mathbf{n}). \quad (2.3.23)$$

Then, we obtain the following random current representation (cf. Figure 2.1):

$$Z_{r,R}^h = \sum_{\partial \mathbf{n} = \emptyset} w_{r,R}^h(\mathbf{n}), \quad Z_R = \sum_{\partial \mathbf{n} = \emptyset} w_R(\mathbf{n}), \quad (2.3.24)$$

and for $x, y \in V_R$,

$$\langle \sigma_x \rangle_{r,R}^h = \sum_{\partial \mathbf{n} = \{x, g\}} \frac{w_{r,R}^h(\mathbf{n})}{Z_{r,R}^h}, \quad \langle \sigma_x \sigma_y \rangle_R = \sum_{\partial \mathbf{n} = \{x\} \triangle \{y\}} \frac{w_R(\mathbf{n})}{Z_R}. \quad (2.3.25)$$

Given a current configuration $\mathbf{n} = \{n_b\}$, we say that x is \mathbf{n} -connected to y , denoted $x \xleftrightarrow{\mathbf{n}} y$ if either $x = y \in V_R \cup \{g\}$ or there is a path from x to y consisting of bonds $b \in B_R \cup G_r$ with $n_b > 0$. For $A \subset V_R \cup \{g\}$, we also say that x is \mathbf{n} -connected to y in A , denoted $x \xleftrightarrow{\mathbf{n}} y$ in A , if either $x = y \in A$ or there is a path from x to y consisting of bonds $b \subset A$ with $n_b > 0$.

Given a subset $A \subset V_R$, we define

$$W_A(\mathbf{m}) = \prod_{b \in A} \frac{(J_b/T_c)^{m_b}}{m_b!}, \quad \mathcal{Z}_A = \sum_{\partial \mathbf{m} = \emptyset} W_A(\mathbf{m}). \quad (2.3.26)$$

The most important feature of the random-current representation is the so-called source-switching lemma (e.g., [79, Lemma 2.3]). We state the version we use the most in this paper as below. This is an immediate consequence from the source-switching lemma.

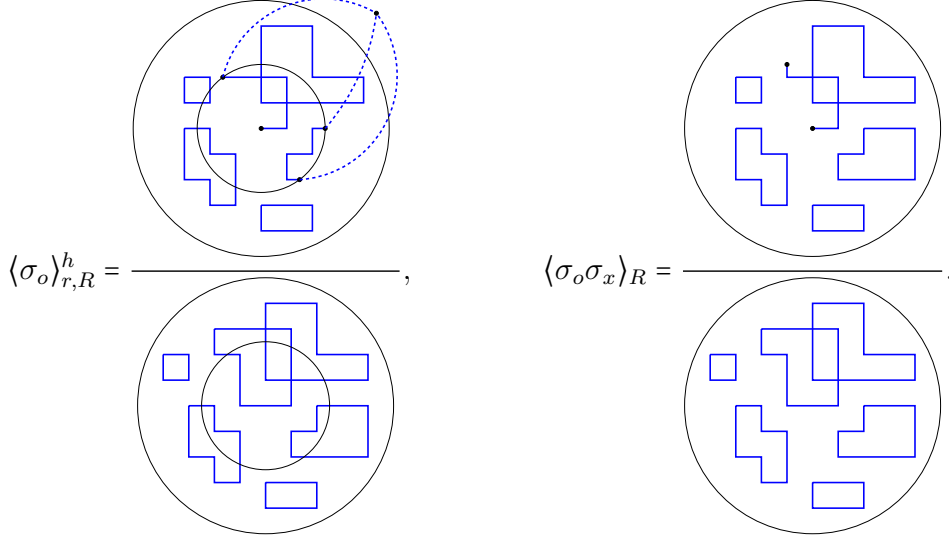


Figure 2.1: The random-current representation for $\langle \sigma_o \rangle_{r,R}^h$ and $\langle \sigma_o \sigma_x \rangle_R$. The bonds with even current are all omitted. The vertex connected by dashed line segments is the ghost site g .

Lemma 2.3.6 (Consequence from the source-switching lemma, [79]). *For any subsets $A \subset V_R$ and $B \subset V_R \cup \{g\}$, any $x, y \in V_R$ and any function f on current configurations,*

$$\sum_{\substack{\partial \mathbf{n} = B \\ \partial \mathbf{m} = \emptyset}} w_{r,R}^h(\mathbf{n}) W_A(\mathbf{m}) \mathbb{1}\{x \xleftrightarrow{\mathbf{n}+\mathbf{m}} y \text{ in } A\} f(\mathbf{n} + \mathbf{m}) = \sum_{\substack{\partial \mathbf{n} = B \Delta \{x\} \Delta \{y\} \\ \partial \mathbf{m} = \{x\} \Delta \{y\}}} w_{r,R}^h(\mathbf{n}) W_A(\mathbf{m}) f(\mathbf{n} + \mathbf{m}). \quad (2.3.27)$$

For a proof, we refer to [79, Lemma 2.3].

2.3.5 A new correlation inequality

The main technical vehicle in the proof of Theorem 2.3.1 is the following correlation inequality that relates $\langle \sigma_o \rangle_r^+$ to the sum of 2-spin expectations.

Proposition 2.3.7. *For the ferromagnetic Ising model,*

$$\langle \sigma_o \rangle_r^+ \geq \frac{\left(\sum_{x \in \partial V_r} \langle \sigma_o \sigma_x \rangle \right)^2}{\sum_{x,y \in \partial V_r} \langle \sigma_o \sigma_x \rangle \langle \sigma_x \sigma_y \rangle + \sum_{\substack{u \in \mathbb{Z}^d \\ x,y \in \partial V_r}} \langle \sigma_o \sigma_u \rangle \langle \sigma_u \sigma_x \rangle \langle \sigma_u \sigma_y \rangle \langle \sigma_o \rangle_{\text{dist}(u, \partial V_r)}^+}. \quad (2.3.28)$$

Compare this with the correlation inequality (2.3.18) for percolation. The extra factor in the denominator of (2.3.28), $\langle \sigma_o \rangle_{\text{dist}(u, \partial V_r)}^+$, will eventually be the key to obtain the optimal mean-field bound on the Ising 1-arm exponent.

Proof of Proposition 2.3.7. The proof is carried out in four steps.

Step 1: The second-moment method. Let

$$X_r(\mathbf{n}) = \sum_{x \in \partial V_r} \mathbb{1}\{o \longleftrightarrow_{\mathbf{n}} x \text{ in } V_R\}. \quad (2.3.29)$$

Then, by the Schwarz inequality, we obtain

$$\begin{aligned} \sum_{\substack{\partial \mathbf{n} = \{o, g\} \\ \partial \mathbf{m} = \emptyset}} \frac{w_{r,R}^h(\mathbf{n})}{Z_{r,R}^h} \frac{w_R(\mathbf{m})}{Z_R} X_r(\mathbf{n} + \mathbf{m}) &\leq \left(\underbrace{\sum_{\partial \mathbf{n} = \{o, g\}} \frac{w_{r,R}^h(\mathbf{n})}{Z_{r,R}^h}}_{=\langle \sigma_o \rangle_{r,R}^h} \underbrace{\sum_{\partial \mathbf{m} = \emptyset} \frac{w_R(\mathbf{m})}{Z_R}}_{=1} \right)^{1/2} \\ &\quad \times \left(\sum_{\substack{\partial \mathbf{n} = \{o, g\} \\ \partial \mathbf{m} = \emptyset}} \frac{w_{r,R}^h(\mathbf{n})}{Z_{r,R}^h} \frac{w_R(\mathbf{m})}{Z_R} X_r(\mathbf{n} + \mathbf{m})^2 \right)^{1/2}. \end{aligned} \quad (2.3.30)$$

By Lemma 2.3.6, we can rewrite the left-hand side as

$$\begin{aligned} \sum_{x \in \partial V_r} \sum_{\substack{\partial \mathbf{n} = \{o, g\} \\ \partial \mathbf{m} = \emptyset}} \frac{w_R(\mathbf{n})}{Z_{r,R}} \frac{w_R(\mathbf{m})}{Z_R} \mathbb{1}\{o \longleftrightarrow_{\mathbf{n}+\mathbf{m}} x \text{ in } V_R\} &= \sum_{x \in \partial V_r} \sum_{\substack{\partial \mathbf{n} = \{x, g\} \\ \partial \mathbf{m} = \{o, x\}}} \frac{w_{r,R}^h(\mathbf{n})}{Z_{r,R}^h} \frac{w_R(\mathbf{m})}{Z_R} \\ &= \sum_{x \in \partial V_r} \langle \sigma_x \rangle_{r,R}^h \langle \sigma_o \sigma_x \rangle_R. \end{aligned} \quad (2.3.31)$$

As a result, we obtain

$$\langle \sigma_o \rangle_{r,R}^h \geq \frac{\left(\sum_{x \in \partial V_r} \langle \sigma_x \rangle_{r,R}^h \langle \sigma_o \sigma_x \rangle_R \right)^2}{\sum_{\substack{\partial \mathbf{n} = \{o, g\} \\ \partial \mathbf{m} = \emptyset}} \frac{w_{r,R}^h(\mathbf{n})}{Z_{r,R}^h} \frac{w_R(\mathbf{m})}{Z_R} X_r(\mathbf{n} + \mathbf{m})^2}. \quad (2.3.32)$$

Step 2: Switching sources. Next, we investigate the denominator of the right-hand side of (2.3.32), which equals

$$\sum_{x, y \in \partial V_r} \sum_{\substack{\partial \mathbf{n} = \{o, g\} \\ \partial \mathbf{m} = \emptyset}} \frac{w_{r,R}^h(\mathbf{n})}{Z_{r,R}^h} \frac{w_R(\mathbf{m})}{Z_R} \mathbb{1}\{o \longleftrightarrow_{\mathbf{n}+\mathbf{m}} x, y \text{ in } V_R\}. \quad (2.3.33)$$

The contribution from the summands $x = y$ may be rewritten as in (2.3.31). Similarly, for the case of $x \neq y$, we use Lemma 2.3.6 to obtain

$$\begin{aligned} &\sum_{\substack{x, y \in \partial V_r \\ (x \neq y)}} \sum_{\substack{\partial \mathbf{n} = \{o, g\} \\ \partial \mathbf{m} = \emptyset}} \frac{w_{r,R}^h(\mathbf{n})}{Z_{r,R}^h} \frac{w_R(\mathbf{m})}{Z_R} \mathbb{1}\{o \longleftrightarrow_{\mathbf{n}+\mathbf{m}} x, y \text{ in } V_R\} \\ &= \sum_{\substack{x, y \in \partial V_r \\ (x \neq y)}} \sum_{\substack{\partial \mathbf{n} = \{x, g\} \\ \partial \mathbf{m} = \{o, x\}}} \frac{w_{r,R}^h(\mathbf{n})}{Z_{r,R}^h} \frac{w_R(\mathbf{m})}{Z_R} \mathbb{1}\{o \longleftrightarrow_{\mathbf{n}+\mathbf{m}} y \text{ in } V_R\}. \end{aligned} \quad (2.3.34)$$

For the event $o \xleftrightarrow[n+\mathbf{m}]{} y$ in V_R to occur under the source constraint $\partial \mathbf{n} = \{x, g\}$, $\partial \mathbf{m} = \{o, x\}$, either one of the following must be the case:

- (i) $\{o \xleftrightarrow[\mathbf{m}]{} y\}$.
- (ii) $\{o \xleftrightarrow[\mathbf{m}]{} y\}^c$ and $\exists u \in \overline{\mathcal{C}_{\mathbf{m}}(o)} \equiv \{v \in V_R : o \xleftrightarrow[\mathbf{m}]{} v\}$ that is $(\mathbf{n} + \mathbf{m}')$ -connected to y in $V_R \setminus \overline{\mathcal{C}_{\mathbf{m}}(o)}$, where \mathbf{m}' is the restriction of \mathbf{m} on bonds $b \in V_R \setminus \overline{\mathcal{C}_{\mathbf{m}}(o)}$.

Case (i) is easy; by Lemma 2.3.6, the contribution to (2.3.34) is bounded as

$$\begin{aligned}
& \sum_{\substack{x, y \in \partial V_r \\ (x \neq y)}} \sum_{\partial \mathbf{n} = \{x, g\}} \underbrace{\frac{w_{r,R}^h(\mathbf{n})}{Z_{r,R}^h}}_{= \langle \sigma_x \rangle_{r,R}^h \leq 1} \sum_{\partial \mathbf{m} = \{o, x\}} \frac{w_R(\mathbf{m})}{Z_R} \mathbb{1}\{o \xleftrightarrow[\mathbf{m}]{} y\} \\
& \leq \sum_{\substack{x, y \in \partial V_r \\ (x \neq y)}} \sum_{\substack{\partial \mathbf{m} = \{o, x\} \\ \partial l = \emptyset}} \frac{w_R(\mathbf{m})}{Z_R} \frac{w_R(l)}{Z_R} \mathbb{1}\{o \xleftrightarrow[\mathbf{m}+l]{} y\} \\
& = \sum_{\substack{x, y \in \partial V_r \\ (x \neq y)}} \underbrace{\sum_{\partial \mathbf{m} = \{x, y\}} \frac{w_R(\mathbf{m})}{Z_R}}_{= \langle \sigma_x \sigma_y \rangle_R} \underbrace{\sum_{\partial l = \{o, y\}} \frac{w_R(l)}{Z_R}}_{= \langle \sigma_o \sigma_y \rangle_R}. \tag{2.3.35}
\end{aligned}$$

Step 3: Conditioning on clusters. Case (ii) is a bit harder and needs extra care. Here we use the conditioning-on-clusters argument. First, by conditioning on $\overline{\mathcal{C}_{\mathbf{m}}(o)}$, we can rewrite the contribution to (2.3.34) from case (ii) as

$$\sum_{\substack{u \in V_R \\ x, y \in \partial V_r \\ (x \neq y)}} \sum_{\substack{A \subset V_R \\ (o, u, x \in A)}} \sum_{\substack{\partial \mathbf{n} = \{x, g\} \\ \partial \mathbf{m} = \{o, x\}}} \frac{w_{r,R}^h(\mathbf{n})}{Z_{r,R}^h} \frac{w_R(\mathbf{m})}{Z_R} \mathbb{1}\{\overline{\mathcal{C}_{\mathbf{m}}(o)} = A\} \mathbb{1}\{u \xleftrightarrow[\mathbf{n}+\mathbf{m}']{} y \text{ in } V_R \setminus A\}. \tag{2.3.36}$$

Then, the sum over the current configurations in (2.3.36) can be rewritten as

$$\sum_{\partial \mathbf{m} = \{o, x\}} \frac{W_A(\mathbf{m}) \mathcal{Z}_{V_R \setminus A}}{Z_R} \mathbb{1}\{\overline{\mathcal{C}_{\mathbf{m}}(o)} = A\} \sum_{\substack{\partial \mathbf{n} = \{x, g\} \\ \partial \mathbf{m}' = \emptyset}} \frac{w_{r,R}^h(\mathbf{n})}{Z_{r,R}^h} \frac{W_{V_R \setminus A}(\mathbf{m}')}{\mathcal{Z}_{V_R \setminus A}} \mathbb{1}\{u \xleftrightarrow[\mathbf{n}+\mathbf{m}']{} y \text{ in } V_R \setminus A\}. \tag{2.3.37}$$

Now, by using Lemma 2.3.6, the above expression is equal to

$$\sum_{\partial \mathbf{m} = \{o, x\}} \frac{W_A(\mathbf{m}) \mathcal{Z}_{V_R \setminus A}}{Z_R} \mathbb{1}\{\overline{\mathcal{C}_{\mathbf{m}}(o)} = A\} \underbrace{\sum_{\partial \mathbf{n} = \{u, x, y, g\}} \frac{w_{r,R}^h(\mathbf{n})}{Z_{r,R}^h}}_{= \langle \sigma_u \sigma_x \sigma_y \rangle_{r,R}^h} \underbrace{\sum_{\partial \mathbf{m}' = \{u, y\}} \frac{W_{V_R \setminus A}(\mathbf{m}')}{\mathcal{Z}_{V_R \setminus A}}}_{= \langle \sigma_u \sigma_y \rangle_{V_R \setminus A}}, \tag{2.3.38}$$

where $\langle \sigma_u \sigma_y \rangle_{V_R \setminus A}$ is the 2-spin expectation on the vertex set $V_R \setminus A$ under the free-boundary condition, and is bounded by $\langle \sigma_u \sigma_y \rangle_R$ due to monotonicity. As a result, we obtain

$$\begin{aligned}
(2.3.36) &\leq \sum_{\substack{u \in V_R \\ x, y \in \partial V_r \\ (x \neq y)}} \langle \sigma_u \sigma_x \sigma_y \rangle_{r, R}^h \langle \sigma_u \sigma_y \rangle_R \sum_{\substack{A \subset V_R \\ (o, u, x \in A)}} \sum_{\partial \mathbf{m} = \{o, x\}} \frac{W_A(\mathbf{m}) Z_{V_R \setminus A}}{Z_R} \mathbb{1}\{\overline{\mathcal{C}_{\mathbf{m}}(o)} = A\} \\
&= \sum_{\substack{u \in V_R \\ x, y \in \partial V_r \\ (x \neq y)}} \langle \sigma_u \sigma_x \sigma_y \rangle_{r, R}^h \langle \sigma_u \sigma_y \rangle_R \sum_{\partial \mathbf{m} = \{o, x\}} \frac{w_R(\mathbf{m})}{Z_R} \mathbb{1}\{o \xleftrightarrow{\mathbf{m}} u\} \\
&\leq \sum_{\substack{u \in V_R \\ x, y \in \partial V_r \\ (x \neq y)}} \langle \sigma_u \sigma_x \sigma_y \rangle_{r, R}^h \langle \sigma_u \sigma_y \rangle_R \sum_{\substack{\partial \mathbf{m} = \{o, x\} \\ \partial \mathbf{l} = \emptyset}} \frac{w_R(\mathbf{m})}{Z_R} \frac{w_R(\mathbf{l})}{Z_R} \mathbb{1}\{o \xleftrightarrow{\mathbf{m} + \mathbf{l}} u\} \\
&= \sum_{\substack{u \in V_R \\ x, y \in \partial V_r \\ (x \neq y)}} \langle \sigma_u \sigma_x \sigma_y \rangle_{r, R}^h \langle \sigma_u \sigma_y \rangle_R \underbrace{\sum_{\partial \mathbf{m} = \{u, x\}} \frac{w_R(\mathbf{m})}{Z_R}}_{= \langle \sigma_u \sigma_x \rangle_R} \underbrace{\sum_{\partial \mathbf{l} = \{o, u\}} \frac{w_R(\mathbf{l})}{Z_R}}_{= \langle \sigma_o \sigma_u \rangle_R}, \tag{2.3.39}
\end{aligned}$$

where, in the last line, we have used Lemma 2.3.6 again.

Step 4: Conclusion. Summarizing (2.3.32), (2.3.35) and (2.3.39), we arrive at

$$\langle \sigma_o \rangle_{r, R}^h \geq \frac{\left(\sum_{x \in \partial V_r} \langle \sigma_x \rangle_{r, R}^h \langle \sigma_o \sigma_x \rangle_R \right)^2}{\sum_{x, y \in \partial V_r} \langle \sigma_o \sigma_x \rangle_R \langle \sigma_x \sigma_y \rangle_R + \sum_{\substack{u \in V_R \\ x, y \in \partial V_r}} \langle \sigma_o \sigma_u \rangle_R \langle \sigma_u \sigma_x \rangle_R \langle \sigma_u \sigma_y \rangle_R \langle \sigma_u \sigma_x \sigma_y \rangle_{r, R}^h}. \tag{2.3.40}$$

Now we take $h \uparrow \infty$ in both sides. In this limit, the spins on ∂V_r take on $+1$. Moreover, by Griffiths' inequality, we have $\lim_{h \uparrow \infty} \langle \sigma_u \sigma_x \sigma_y \rangle_{r, R}^h = \langle \sigma_u \rangle_{r, R}^\infty \leq \langle \sigma_o \rangle_{\text{dist}(u, \partial V_r)}^+$. Therefore,

$$\langle \sigma_o \rangle_r^+ \geq \frac{\left(\sum_{x \in \partial V_r} \langle \sigma_o \sigma_x \rangle_R \right)^2}{\sum_{x, y \in \partial V_r} \langle \sigma_o \sigma_x \rangle_R \langle \sigma_x \sigma_y \rangle_R + \sum_{\substack{u \in V_R \\ x, y \in \partial V_r}} \langle \sigma_o \sigma_u \rangle_R \langle \sigma_u \sigma_x \rangle_R \langle \sigma_u \sigma_y \rangle_R \langle \sigma_o \rangle_{\text{dist}(u, \partial V_r)}^+}. \tag{2.3.41}$$

Taking $R \uparrow \infty$, we finally obtain (2.3.28). ■

2.3.6 Proof of Theorem 2.3.1

Proof of Theorem 2.3.1. We proceed indirectly and assume, by contradiction, that (2.3.10) is false. Then there exists a monotone sequence $(r_k)_{k \in \mathbb{N}}$ diverging to ∞ such that

$$\langle \sigma_o \rangle_{r_k}^+ \leq K r_k^{-(1+\varepsilon)} \tag{2.3.42}$$

whenever k is large enough.

We are starting from Proposition 2.3.7. We estimate every term in the numerator and the denominator of (2.3.28) using (2.3.8). Firstly, the numerator of (2.3.28) is of the order r^2 since

$$\sum_{x \in \partial V_r} \langle \sigma_o \sigma_x \rangle \asymp \sum_{x \in \partial V_r} |x|^{2-d} \asymp r^{d-1} r^{2-d} = r. \quad (2.3.43)$$

Secondly, the first term in the denominator is of order r^2 since

$$\sum_{x, y \in \partial V_r} \langle \sigma_o \sigma_x \rangle \langle \sigma_x \sigma_y \rangle \asymp \sum_{x \in \partial V_r} \|x\|^{2-d} \sum_{y \in \partial V_r} \|x - y\|^{2-d} \asymp r^{d-1} r^{2-d} r = r^2, \quad (2.3.44)$$

where we have used $\|\cdot\| = |\cdot| \vee 1$ (cf. below (2.3.18)). The second term in the denominator is the dominant one. To this end, we fix a sequence r_k satisfying (2.3.42). We split the sum over u into three cases: (i) $|u| < r_k/2$, (ii) $r_k/2 \leq |u| < 3r_k/2$, (iii) $3r_k/2 \leq |u|$, and show that it is $O(r_k^3)$ for any $\varepsilon > 0$.

Case (i):

$$\begin{aligned} & \sum_{\substack{|u| < r_k/2 \\ x, y \in \partial V_{r_k}}} \|u\|^{2-d} \|u - x\|^{2-d} \|u - y\|^{2-d} \|r_k - |u|\|^{-(1+\varepsilon)} \\ & \asymp r_k^{2(2-d)-(1+\varepsilon)} \underbrace{\sum_{x, y \in \partial V_{r_k}} \sum_{|u| < r_k/2} \|u\|^{2-d}}_{\asymp r_k^{2(d-1)+2}} \\ & \asymp r_k^{3-\varepsilon}. \end{aligned} \quad (2.3.45)$$

Case (ii):

$$\begin{aligned} & \sum_{\substack{r_k/2 \leq |u| < 3r_k/2 \\ x, y \in \partial V_{r_k}}} |u|^{2-d} \|u - x\|^{2-d} \|u - y\|^{2-d} \|r_k - |u|\|^{-(1+\varepsilon)} \\ & \asymp r_k^{2-d} \sum_{r_k/2 \leq |u| < 3r_k/2} \|r_k - |u|\|^{-(1+\varepsilon)} \underbrace{\sum_{x \in \partial V_{r_k}} \|u - x\|^{2-d} \sum_{y \in \partial V_{r_k}} \|u - y\|^{2-d}}_{\asymp r_k^2} \\ & \asymp r_k^{4-d} \int_{r_k/2}^{3r_k/2} \|r_k - l\|^{-(1+\varepsilon)} l^{d-1} dl \\ & \asymp r_k^3 \int_0^{r_k/2} \|l\|^{-(1+\varepsilon)} dl \asymp r_k^3. \end{aligned} \quad (2.3.46)$$

Case (iii): By the Schwarz inequality,

$$\begin{aligned}
& \sum_{\substack{|u| \geq 3r_k/2 \\ x, y \in \partial V_{r_k}}} |u|^{2-d} |u-x|^{2-d} |u-y|^{2-d} (|u| - r_k)^{-(1+\varepsilon)} \\
& \asymp r_k^{2-d-(1+\varepsilon)} \underbrace{\sum_{x, y \in \partial V_{r_k}} \sqrt{\sum_{|u| \geq 3r_k/2} |u-x|^{4-2d}} \sqrt{\sum_{|u| \geq 3r_k/2} |u-y|^{4-2d}}} \\
& \hspace{15em} \asymp r_k^{2(d-1)+4-d} \\
& \asymp r_k^{3-\varepsilon}.
\end{aligned} \tag{2.3.47}$$

Plugging these estimates into the bound of Proposition 2.3.7 obtains

$$\langle \sigma_o \rangle_{r_k}^+ \geq C \frac{r_k^2}{r_k^2 + r_k^3} \asymp r_k^{-1} \tag{2.3.48}$$

for any large k and for some C (independent of k), which contradicts (2.3.42), and (2.3.10) follows.

The claim $\rho \leq 1$ follows straightforwardly: Suppose $\rho > 1 + \varepsilon$ for some $\varepsilon > 0$, then there exists a sequence $(r_k)_{k \in \mathbb{N}}$ such that

$$\frac{\log \langle \sigma_o \rangle_{r_k}^+}{\log r_k} < -1 - \varepsilon,$$

and this contradicts (2.3.10). ■

2.3.7 Further discussion

1. *On trees.* The absence of loops in the underlying graph makes it easier to analyze, and a number of critical exponents are known to take on their mean-field values, see [82, Section 4.2]. For the Ising model on a regular tree, it is shown [61] that

$$\langle \sigma_o \rangle_r^+ \asymp r^{-1/2} \quad \text{as } r \uparrow \infty, \tag{2.3.49}$$

where, instead of the ball V_r , we are using the subtree of depth r from the root (with the plus-boundary condition). This seems to hint on $\rho = 1/2$ on trees. The discrepancy to the high-dimensional setting can be resolved by adjusting the notion of distance in the tree, that is, one should rather work with the metric $\text{dist}(o, x) := \sqrt{\text{depth}(x)}$ incorporating spatial effects when embedding the tree into the lattice \mathbb{Z}^d . With this notion of distance, we get the mean-field value $\rho = 1$. The same situation occurs for percolation, where we refer to [45, Chapter 10.1] for a discussion of this issue.

2. *Long-range models.* In our result, we assumed that the spin-spin coupling J is finite-range, that is, there is an $M > 0$ such that $J_{o,x} = 0$ whenever $|x| > M$. We believe that $\rho = 1$ is true even for infinite-range couplings with sufficiently fast decaying tails, although the boundary ∂V_r on which the external magnetic field is imposed

under the current setting is no longer bounded. The situation may change when we consider couplings with regularly-varying tails, and we focus now on the situation when

$$J_{o,x} \asymp |x|^{-d-\alpha} \quad \text{as } |x| \uparrow \infty, \quad (2.3.50)$$

for some $\alpha > 0$. In the earlier work [25], it shows that, under a suitable spread-out condition, the critical 2-spin expectation scales as

$$\langle \sigma_o \sigma_x \rangle \asymp |x|^{\alpha \wedge 2 - d} \quad \text{as } |x| \uparrow \infty, \quad (2.3.51)$$

in contrast to (2.3.8). In particular, there is a crossover at $\alpha = 2$ between a “finite-range regime” and a “long-range regime”.

For the critical exponent ρ , it is tempting to believe that this crossover happens for $\alpha = 4$. The reason for this is again a comparable result for percolation: Hulshof [63] proved that, if $G_{p_c}(o, x) \asymp |x|^{\alpha \wedge 2 - d}$ as $|x| \uparrow \infty$, then the critical 1-arm probability scales as $\theta_r \asymp r^{-(\alpha \wedge 4)/2}$ as $r \uparrow \infty$. In view of Hulshof’s result, it is plausible that, for the long-range Ising model with couplings like in (2.3.50), it is the case that $\rho = (\alpha \wedge 4)/4$.

3. *The (1-component) φ^4 model.* This spin model is considered to be in the same universality class as Ising ferromagnets [1]. It can be constructed as an $N \uparrow \infty$ limit of a properly coupled N ferromagnetic Ising systems [84], and therefore we can apply the random-current representation for the Ising model. By virtue of this representation, we can use the lace expansion to show that the critical 2-spin expectation satisfies (2.3.8) for a large class of short-range models [81]. It is natural to be interested in the critical 1-spin expectation similar to $\langle \sigma_o \rangle_r^+$ for the Ising model. However, since the φ^4 spin is an unbounded variable, we cannot simply take $h \uparrow \infty$ to define the 1-spin expectation under the “plus-boundary” condition. Once it is defined appropriately, we believe that its 1-arm exponent also satisfies the mean-field bound $\rho \leq 1$ for $d > 4$.

2.4 Lower bound on the 1-arm exponent ρ in high dimensions

In this section, we discuss the lower bound on the 1-arm exponent $\rho > 0$. For percolation, Kozma and Nachmias [67] proved the opposite inequality $\rho \geq 2$ for $d > 6$ in order to conclude the equality. They use another correlation inequality that involves not only θ_r and G_p but also the mean-field cluster-size distribution. However, we do not have the information on the Ising cluster-size distribution under the random-current representation so far, and if we could obtain it, to translate the method by Kozma and Nachmias into the Ising language via the random-current representation seems to be pretty tough.

In the paper [78], Sakai also proved $\rho \geq 2$ for $d > 6$ for percolation with some assumptions.

1. (The lower bound for the critical restricted 2-point function; far from the boundary)

$$\sum_{x \in \partial V_{r/2}} \mathbb{P}_{p_c}(o \text{ is connected to } x, o \text{ is NOT connected to } \partial V_r) \geq c \|x\|^2, \quad (2.4.1)$$

where $c > 0$ is a constant.

2. (The upper bound for the critical restricted 2-point function; close to the boundary)
If there exists a parameter $\kappa \geq 1$ such that,

$$\mathbb{P}_{p_c}(o \text{ is connected to } x, o \text{ is NOT connected to } \partial V_r) \leq c \|x\|^{2-d-\kappa} \|r - |x|\|^\kappa, \quad (2.4.2)$$

for $r/2 \leq |x| \leq r$.

The first assumption is used to show that $\rho \geq 2$ for $d > 7$ and the second assumption is used for the result to go down to $d > 6$. In fact, for the random walk, the second assumption holds with $\kappa = 1$ at $|x| = r$. The $\kappa \geq 1$ can be understood as a crossover parameter from $2 - d$ to $1 - d$ in high dimensions.

Quite recently, Chatterjee and Hanson showed the result which corresponds to the first assumption in Theorem 2 in [21] for percolation. Moreover, by the result on the half-space critical 2-point function in Theorem 1, we can immediately imply the second assumption only at $|x| = r$ with $\kappa = 1$. Their method seems to be based on the argument by Kozma and Nachmias. Thus, to derive the lower bound for the percolation 1-arm needs almost the same amount of efforts as to derive the behaviors for the restricted 2-point function. However, we can separate the problem into two; one is to obtain the behaviors of the full or restricted 2-point function and the other one is derive the mean-field value of the 1-arm exponent in high dimensions. This means that if we assume the behaviors of the full 2-point function proved by the heavy lace expansion analysis and of the restricted 2-point function proved by the heavy argument by Kozma and Nachmias (although the second assumption has been partially proved when x is on the boundary), we can conclude that $\rho=2$ for $d > 6$ for percolation.

We also believe that the same result by Chatterjee and Hanson for the Ising model. Therefore, we are interested in whether we can imply that $\rho \geq 1$ for $d > 4$ for the Ising model by assuming the same conditions above. This is an ongoing project with Heydenreich and Sakai. We are roughly doing the calculation for the Ising model via the random-current representation, and we expect that $\rho \geq 1$ for $d > 4$ with both assumptions (although we can show that $\rho \geq 2$ for $d > 7$ only with the first assumption for percolation, we need both assumptions in order to conclude the result for the meaningful dimensions). To close this chapter, we claim the following conjecture on the lower bound for the Ising 1-arm.

Conjecture 2.4.1. *For the ferromagnetic Ising model on \mathbb{Z}^d , $d > 4$, defined by a translation-invariant, \mathbb{Z}^d -symmetric and finite-range spin-spin coupling with the two assumptions below, $\rho \geq 1$ if the critical exponent ρ exists.*

1. (The lower bound for the critical restricted 2-point function; far from the boundary)

$$\sum_{x \in \partial V_{r/2}} \langle \sigma_o \sigma_x \rangle_{T_c; V_r} \geq c \|x\|^2, \quad (2.4.3)$$

where $c > 0$ is a constant.

2. (The upper bound for the critical restricted 2-point function; close to the boundary)

If there exists a parameter $\kappa \geq 1$ such that,

$$\langle \sigma_o \sigma_x \rangle_{T_c; V_r} \leq c \|x\|^{2-d-\kappa} \|r - |x|\|^\kappa, \quad (2.4.4)$$

for $r/2 \leq |x| \leq r$.

Chapter 3

The lace expansion analysis for the nearest-neighbor models on the BCC lattice

3.1 Background

3.1.1 The lace expansion

The lace expansion is one of the few mathematically rigorous methods to prove critical behavior for various statistical-mechanical models in high dimensions. In 1985, Brydges and Spencer [19] came up to a fascinating idea for weakly SAW. First, they looked at the naive expansion (1.1.2). Next, from each $\Gamma \in \mathcal{G}[0, |\omega|]$, they isolated a connected graph $\Gamma_0 \subset \Gamma$ of the origin. Then, they extracted a minimally connected graph $\mathcal{L} \subset \Gamma_0$ called a lace, and resummed all the other edges in $\Gamma \setminus \mathcal{L}$ to partially restore the self-avoidance constraint. This is what we nowadays call the algebraic lace expansion, named after the shape of the aforesaid minimally connected graph. Since then, the algebraic lace expansion has been successfully applied to other models, such as oriented percolation [73], lattice trees and lattice animals [53].

Later in 1990s, Hara and Slade (e.g., [55]) came up to a more intuitively understandable way of deriving the lace expansion. To distinguish it from the algebraic lace expansion, we sometimes call it the inclusion-exclusion lace expansion. This opened up the possibility of applying the lace expansion to a wider class of models, including (unoriented) percolation [54], the contact process [82], the Ising model [79] and the (one-component) φ^4 model [81].

From now on, we simply call the latter the lace expansion. We will only show its derivation for strictly SAW in Section 3.3.1.

The result of the lace expansion is formally explained by the following recursion equation similar to that for the RW Green function: for any $p < p_c$, there are functions I_p and J_p such that

$$G_p(x) = I_p(x) + (J_p * G_p)(x). \quad (3.1.1)$$

If I_p and J_p satisfy certain regularity conditions, then it is natural to believe that the

global behavior of G_p is also similar to that of the RW Green function and therefore the infrared bound (1.1.6) holds.

However, since I_p and J_p are described by an alternating series of the lace-expansion coefficients $\{\pi_p^{(n)}\}_{n=0}^N$, each of which involves complicated local interaction (n represents the degree of complexity), it is certainly not true that the aforesaid regularity conditions always hold. In fact, the regularity conditions require the critical bubble $(D^{*2} * G_{p_c}^{*2})(o)$ for SAW and the critical triangle $(D^{*2} * G_{p_c}^{*3})(o)$ for percolation to be small, not to be merely finite. This seemingly tautological statement (i.e., the critical bubble/triangle have to be small in order to prove them to be finite) is taken care of by the so-called bootstrapping argument, which will be explained in the later section.

During the course of the bootstrapping argument, we often assume that the number of neighbors per vertex is sufficiently large. Since each vertex has $2d$ neighbors on \mathbb{Z}^d , it means that d is assumed to be large. For SAW, Hara and Slade [55, 56] succeeded in showing that $d \geq 5$ is large enough to prove mean-field results. For percolation, however, the situation is not as good as for SAW. The best results so far were obtained by Fitzner and van der Hofstad [35], in which they proved mean-field results for $d \geq 11$ by using NoBLE, a perturbation method from non-backtracking random walk (= memory-2 SAW).

There is another way to increase the number of neighbors per vertex. Instead of taking d large, we may enlarge the range L of neighbors. One such example is the spread-out lattice $\bar{\mathbb{Z}}_L^d$, in which two distinct vertices $x, y \in \mathbb{Z}^d$ satisfying $\|x - y\|_\infty \leq L$ are defined to be neighbors, hence $(2L + 1)^d - 1$ neighbors per vertex. By taking L sufficiently large, all the models for which the lace expansion was obtained are proven to exhibit mean-field behavior for all d above the predicted upper-critical dimensions [53, 54, 71, 73, 82, 79, 81].

3.1.2 The motivation for the lace expansion analysis on the BCC lattice

Since we believe in universality, the mean-field results on the spread-out lattice $\bar{\mathbb{Z}}_L^d$, as long as $L < \infty$, are believed to hold on \mathbb{Z}^d as well. This is proven to be true for SAW, but not yet for percolation. We want to get rid of the artificial parameter L and come up to a decent nearest-neighbor lattice, on which 7-dimensional percolation is proven to exhibit the mean-field behavior. In an ongoing project with Lung-Chi Chen and Markus Heydenreich [27], we analyze the lace expansion for percolation on a d -dimensional version of the body-centered cubic (BCC) lattice, which has better features than the standard \mathbb{Z}^d , as explained in the next section. Thanks to those features, enumeration of RW quantities relevant to the lace-expansion analysis becomes extremely simple. Also, since those RW quantities are much smaller¹ than the \mathbb{Z}^d -counterparts, it is easy to get closer to the predicted upper-critical dimension without introducing too much technical complexity. One of the purposes of the survey [49] is to explain the current status of the BCC work and reveal the potential problems to overcome for completion of the mean-field picture in high dimensions.

¹A d -dimensional version of the face-centered cubic (FCC) lattice has $d2^{d-1}$ neighbors per vertex, more neighbors than on the BCC lattice, and therefore the RW quantities should be much smaller on the FCC lattice. However, since enumeration of those quantities on the FCC lattice is not so simple (in fact, it is rather complicated!), we decided to use the more charming BCC lattice.

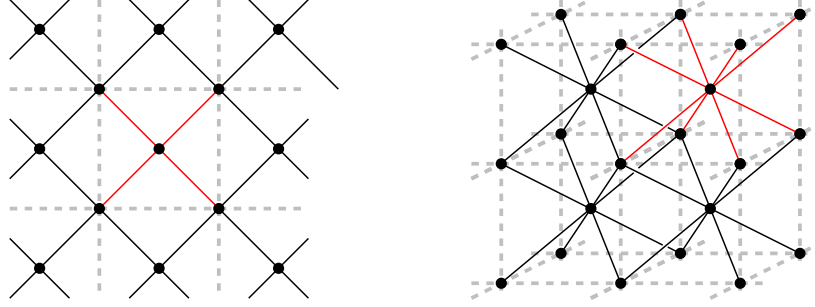


Figure 3.1: The basic structure (in red) of the BCC lattice \mathbb{L}^d for $d = 2, 3$.

Another purpose of the survey [49] is to provide a relatively short, self-contained note on the lace expansion for the nearest-neighbor models. Currently, the best references on \mathbb{Z}^d are [55, 56] for SAW and [34, 35] for percolation. However, they are not necessarily accessible to beginners, due to their length (36 + 93 pages for SAW and 79 + 92 pages for percolation) and complexity. This is really unfortunate because, as mentioned earlier, the lace expansion can provide a good playground for, e.g., graduate students who may want to apply mathematical concepts and skills they learned to interesting and important problems. Considering this situation, we will keep the material as simple as possible, instead of making all-out efforts to go down to the predicted upper-critical dimensions. That will be the final goal of [27].

The lace expansion is one of the few mathematically rigorous methods to prove critical behavior for various statistical-mechanical models in high dimensions. It can show that the two-point function for the concerned model, up to the critical point, is bounded by the Green function for the underlying random walk in high dimensions.

3.2 The models and the main result

First, we provide precise definitions of the BCC lattice, self-avoiding walk and percolation. Then, we show the main result and explain its proof assuming key propositions.

3.2.1 The body-centered cubic (BCC) lattice

The d -dimensional BCC lattice \mathbb{L}^d is a graph that contains the origin $o = (0, \dots, 0)$ and is generated by the set of neighbors $\{x = (x_1, \dots, x_d) : \prod_{j=1}^d |x_j| = 1\}$. It is equivalent to \mathbb{Z}^d when $d = 1$ and 2 (modulo rotation by $\pi/4$) but is more crowded in higher dimensions in the sense that the degree of each vertex is 2^d on \mathbb{L}^d , while it is $2d$ on \mathbb{Z}^d . We write $x \sim y$ if $x, y \in \mathbb{L}^d$ are neighbors, i.e., $\prod_{j=1}^d |x_j - y_j| = 1$. It is a natural extension of the standard 3-dimensional BCC structure (see Figure 3.1). The d -dimensional Brownian motion with the identity covariance matrix can be constructed as the scaling limit of random walk (RW) on \mathbb{L}^d generated by the 1-step distribution

$$D(x) = \frac{1}{2^d} \mathbb{1}_{\{x \sim o\}} = \prod_{j=1}^d \frac{1}{2} \delta_{|x_j|, 1}. \quad (3.2.1)$$

Due to this factorization and Stirling's formula², we can obtain a rather sharp bound on the $2n$ -step return probability for all $n \in \mathbb{N}$, as

$$0 \leq (\pi n)^{-d/2} - D^{*2n}(o) \leq \left(1 - e^{d(\frac{1}{24n+1} - \frac{1}{6n})}\right) (\pi n)^{-d/2} \leq \frac{2d}{15n} (\pi n)^{-d/2}. \quad (3.2.2)$$

Using this, we can easily evaluate various RW quantities, such as the RW loop ε_1 , the RW bubble ε_2 and the RW triangle ε_3 , defined as

$$\varepsilon_j = (D^{*2} * S_1^{*j})(o) = \sum_{n=1}^{\infty} D^{*2n}(o) \times \begin{cases} 1 & [j = 1], \\ (2n-1) & [j = 2], \\ (2n-1)n & [j = 3]. \end{cases} \quad (3.2.3)$$

For example, if we split the sum into two at $n = N$, then the RW bubble ε_2 in dimensions $d > 4$ can be estimated as

$$0 \leq \varepsilon_2 - \sum_{n=1}^N (2n-1) D^{*2n}(o) \leq 2\pi^{-d/2} \int_N^{\infty} t^{1-d/2} dt = \frac{4\pi^{-d/2}}{d-4} N^{(4-d)/2}. \quad (3.2.4)$$

If we choose $d = 5$ and $N = 100$ and use a calculator to evaluate the sum over $n \leq N$, then we obtain $\varepsilon_2 \leq 0.178465$. Table 3.1 summarizes the bounds on those RW quantities in different dimensions by choosing $N = 500$ (so that, by (3.2.2), we can show that the RW triangle ε_3 for $d = 7$ takes a value around the indicated number within 10^{-6}).

Table 3.1: Upper bounds on the RW loop, bubble and triangle for $3 \leq d \leq 9$.

	$d = 3$	$d = 4$	$d = 5$	$d = 6$	$d = 7$	$d = 8$	$d = 9$
ε_1	0.393216	0.118637	0.046826	0.020461	0.009406	0.004451	0.002144
ε_2	∞	∞	0.178332	0.044004	0.015302	0.006156	0.002678
ε_3	∞	∞	∞	∞	0.052689	0.012354	0.004148

3.2.2 Self-avoiding walk

As declared at the end of Section 3.1, we restrict our attention to strictly SAW, which we simply call SAW from now on. Let $\Omega(x, y)$ be the set of self-avoiding paths on \mathbb{L}^d from x to y . By convention, $\Omega(x, x)$ is considered to be a singleton: a zero-step SAW at x . Then, the SAW two-point function defined in the previous section can be simplified as

$$G_p(x) = \sum_{\omega \in \Omega(o, x)} p^{|\omega|} \prod_{j=1}^{|\omega|} D(\omega_j - \omega_{j-1}), \quad (3.2.5)$$

²The two-sided bound $\frac{1}{12n+1} \leq \log \frac{n!}{\sqrt{2\pi n} \left(\frac{n}{e}\right)^n} \leq \frac{1}{12n}$ holds for all $n \in \mathbb{N}$ [33, Section II.9].

where the empty product is regarded as 1. Recall that the susceptibility and its critical point are defined as

$$\chi_p = \sum_{x \in \mathbb{L}^d} G_p(x), \quad p_c = \sup\{p \geq 0 : \chi_p < \infty\}. \quad (3.2.6)$$

For more background and related results before 1993, we refer to the “green” book by Madras and Slade [71]. For recent progress in various important problems, we refer to the monograph by Bauerschmidt et al. [12].

3.2.3 Percolation

Here, we introduce bond percolation on \mathbb{L}^d . Each bond $\{u, v\} \subset \mathbb{L}^d$ randomly takes either one of the two states, occupied or vacant, independently of the other bonds. We define the bond-occupation probability of a bond $\{u, v\}$ as $pD(v - u)$, where $p \in [0, 2^d]$ is the percolation parameter, which is equal to the expected number of occupied bonds per vertex. Let \mathbb{P}_p be the associated probability measure, and denote its expectation by \mathbb{E}_p .

Next, we define the percolation two-point function. In order to do so, we first introduce the notion of connectivity. We say that a self-avoiding path $\omega = (\omega_0, \dots, \omega_{|\omega|}) \in \Omega(x, y)$ is occupied if either $x = y$ or every $b_j(\omega) \equiv \{\omega_{j-1}, \omega_j\}$ for $j = 1, \dots, |\omega|$ is occupied. We say that x is connected to y , denoted by $x \longleftrightarrow y$, if there is an occupied self-avoiding path $\omega \in \Omega(x, y)$. Then, we define the percolation two-point function as

$$G_p(x) = \mathbb{P}_p(o \longleftrightarrow x) = \mathbb{P}_p\left(\bigcup_{\omega \in \Omega(o, x)} \{\omega \text{ is occupied}\}\right). \quad (3.2.7)$$

The susceptibility χ_p and its critical point p_c are defined as in (3.2.6). Menshikov [72] and Aizenman and Barsky [2] independently proved that p_c is unique in the sense that it can also be characterized by the emergence of an infinite cluster of the origin:

$$p_c = \inf\{p \in [0, 2^d] : \mathbb{P}_p(o \longleftrightarrow \infty) > 0\}. \quad (3.2.8)$$

Recently, Duminil-Copin and Tassion [30] came up to a particularly simple proof of the uniqueness. They also extended the idea to the Ising model and dramatically simplified the proof of the uniqueness of the critical temperature, first proven by Aizenman, Barsky and Fernández [3].

For more background and related results before 1999, we refer to the excellent book by Grimmett [45]. The book by Bollobás and Riordan [18] also contains progress after publication of Grimmett’s book.

3.2.4 The infrared bound on the BCC lattice

On the BCC lattice \mathbb{L}^d , we can prove the following result without introducing too much technical complexity.

Theorem 3.2.1 (Infrared bound). *For SAW on $\mathbb{L}^{d \geq 6}$ and percolation on $\mathbb{L}^{d \geq 9}$, there exists a model-dependent constant $K \in (0, \infty)$ such that*

$$\|(1 - \hat{D})\hat{G}_p\|_\infty \leq K \quad \text{uniformly in } p \in [1, p_c), \quad (3.2.9)$$

which implies the mean-field behavior, e.g., $\gamma = 1$.

In the proof of a key proposition necessary for the above theorem, we will also show that $\chi_1 < \infty$. This automatically implies the infrared bound for $p \in [0, 1)$, since

$$\|(1 - \hat{D})\hat{G}_p\|_\infty \leq 2\chi_1 < \infty. \quad (3.2.10)$$

The above result for SAW is not as sharp as the result in [55, 56], where Hara and Slade proved the infrared bound on $\mathbb{Z}^{d \geq 5}$. If we simply follow their analysis with the same amount of work, then we should be able to extend the above result to $\mathbb{L}^{d \geq 5}$. However, as is mentioned earlier, this is not our intention. We include the result for SAW as an example, just to show how easy to prove the infrared bound in such low dimensions with relatively small effort. Going down from 9 to 7 for percolation will require more serious effort. This will be the pursuit of the joint work [27].

The proof of the above theorem is rather straightforward, assuming the following three propositions. To state those propositions, we first define

$$g_1(p) = p, \quad g_2(p) = \|(1 - \hat{D})\hat{G}_p\|_\infty. \quad (3.2.11)$$

Obviously, what we want to do is to show that $g_2(p)$ is bounded uniformly in $p \in [1, p_c]$. To define one more relevant function $g_3(p)$, we introduce the notation for a sort of second derivative in the Fourier space, in a particular direction. For a function \hat{f} on \mathbb{T}^d and $k, l \in \mathbb{T}^d$, we let

$$\hat{\Delta}_k \hat{f}(l) = \frac{\hat{f}(l+k) + \hat{f}(l-k)}{2} - \hat{f}(l). \quad (3.2.12)$$

By simple trigonometric calculation, it is shown in [86, (5.17)] that the Fourier transform of the RW Green function $\hat{S}_1(k) \equiv (1 - \hat{D}(k))^{-1}$, which is well-defined in a proper limit when $d > 2$, obeys the inequality

$$\begin{aligned} & |\hat{\Delta}_k \hat{S}_1(l)| \\ & \leq \hat{U}(k, l) \equiv (1 - \hat{D}(k)) \left(\frac{\hat{S}_1(l+k) + \hat{S}_1(l-k)}{2} \hat{S}_1(l) + 4\hat{S}_1(l+k)\hat{S}_1(l-k) \right). \end{aligned} \quad (3.2.13)$$

Finally, we define, by using this $\hat{U}(k, l)$,

$$g_3(p) = \sup_{k, l} \frac{1}{\hat{U}(k, l)} \times \begin{cases} |\hat{\Delta}_k \hat{G}_p(l)| & [\text{SAW}], \\ |\hat{\Delta}_k(\hat{G}_p(l)p\hat{D}(l))| & [\text{percolation}], \end{cases} \quad (3.2.14)$$

where the supremum near $k = 0$ should be interpreted as the supremum over the limit as $|k| \rightarrow 0$. It will be clear that g_3 is defined in slightly different ways between the two models, due to the difference in the recursion equations obtained by the lace expansion.

For the self-consistency, we recall [86, Lemma 5.7] and its proof. We will also use this lemma in the lace expansion analysis later.

Lemma 3.2.2. *Let a function $\hat{A}(k) = (1 - \hat{a}(k))^{-1}$, where \hat{a} is the Fourier transform of a symmetric function $a(x) = a(-x)$ for all $x \in \mathbb{Z}^d$. Then for all $k, l \in \mathbb{T}^d$,*

$$\begin{aligned} |\hat{\Delta}_k \hat{A}(l)| & \leq \frac{\hat{A}(l+k) + \hat{A}(l-k)}{2} \hat{A}(l) |\hat{\Delta}_k \hat{a}(l)| \\ & \quad + \hat{A}(l+k)\hat{A}(l-k)\hat{A}(l)(-\hat{\Delta}_l |\hat{a}|(0))(-\hat{\Delta}_k |\hat{a}|(0)). \end{aligned} \quad (3.2.15)$$

Proof. At first, we will show the following identity by simple computation,

$$\begin{aligned}\hat{\Delta}_k \hat{A}(l) &= \frac{\hat{A}(l+k) + \hat{A}(l-k)}{2} \hat{A}(l) \hat{\Delta}_k \hat{a}(l) \\ &\quad + \hat{A}(l+k) \hat{A}(l-k) \hat{A}(l) \left(\sum_x a(x) (\sin l \cdot x) (\sin k \cdot x) \right)^2.\end{aligned}\quad (3.2.16)$$

By the definition of a second derivative in the Fourier space (3.2.12),

$$\begin{aligned}\hat{\Delta}_k \hat{A}(l) &= \frac{1}{2} \hat{A}(l+k) \hat{A}(l-k) \hat{A}(l) \left(\frac{1}{\hat{A}(l+k) \hat{A}(l)} + \frac{1}{\hat{A}(l-k) \hat{A}(l)} - 2 \frac{1}{\hat{A}(l+k) \hat{A}(l-k)} \right)\end{aligned}\quad (3.2.17)$$

Note that a is a symmetric function, $\hat{a}(l) = \sum_x a(x) \cos k \cdot x$. By the definition of $\hat{A}(l)$, the terms in the above parenthesis become

$$\underbrace{-2\hat{a}(l) + \hat{a}(l+k) + \hat{a}(l-k) - 2\hat{a}(l+k)\hat{a}(l-k) + \hat{a}(l-k)\hat{a}(l) + \hat{a}(l+k)\hat{a}(l)}_{=2\hat{\Delta}_k \hat{a}(l)}.\quad (3.2.18)$$

By using the basic trigonometric identities $\cos(\alpha \pm \beta) = \cos(\alpha) \cos(\beta) \mp \sin(\alpha) \sin(\beta)$,

$$\hat{a}(l+k) \hat{a}(l-k) = \left(\sum_x a(x) (\cos l \cdot x) (\cos k \cdot x) \right)^2 - \left(\sum_x a(x) (\sin l \cdot x) (\sin k \cdot x) \right)^2, \quad (3.2.19)$$

$$\hat{a}(l+k) + \hat{a}(l-k) = 2 \sum_x a(x) (\cos l \cdot x) (\cos k \cdot x). \quad (3.2.20)$$

Thus, the latter terms in (3.2.18) become

$$\begin{aligned}2 \underbrace{\left(\hat{a}(l) - \sum_x a(x) (\cos l \cdot x) (\cos k \cdot x) \right)}_{=-\hat{\Delta}_k \hat{a}(l)} \left(\sum_x a(x) (\cos l \cdot x) (\cos k \cdot x) \right) \\ + 2 \left(\sum_x a(x) (\sin l \cdot x) (\sin k \cdot x) \right)^2.\end{aligned}\quad (3.2.21)$$

Therefore,

$$\begin{aligned}\hat{\Delta}_k \hat{A}(l) &= \hat{A}(l+k) \hat{A}(l-k) \hat{A}(l) \hat{\Delta}_k \hat{a}(l) \left(1 - \sum_x a(x) (\cos l \cdot x) (\cos k \cdot x) \right) \\ &\quad + \hat{A}(l+k) \hat{A}(l-k) \hat{A}(l) \left(\sum_x a(x) (\sin l \cdot x) (\sin k \cdot x) \right)^2.\end{aligned}\quad (3.2.22)$$

Noting that the quantity in the parenthesis in the first term above becomes $\frac{1}{2}((1 - \hat{a}(l+k)) + (1 - \hat{a}(l-k)))$, we obtain the identity (3.2.16). The upper bound in (3.2.15) is obtained by applying the Schwarz inequality to the sum in the identity (3.2.16) and using

the basic inequality $\sin^2 t = (1 + \cos t)(1 - \cos t) \leq 2(1 - \cos t)$. This completes the proof of Lemma 3.2.2. \blacksquare

Now, we state the aforementioned three propositions and show that they indeed imply Theorem 3.2.1.

Proposition 3.2.3 (Continuity). *The functions $\{g_i(p)\}_{i=1}^3$ are continuous in $p \in [1, p_c)$.*

Proposition 3.2.4 (Initial conditions). *For SAW on $\mathbb{L}^{d \geq 6}$ and percolation on $\mathbb{L}^{d \geq 8}$, there are model-dependent finite constants $\{K_i\}_{i=1}^3$ such that $g_i(1) < K_i$ for $i = 1, 2, 3$.*

Proposition 3.2.5 (Bootstrapping argument). *For SAW on $\mathbb{L}^{d \geq 6}$ and percolation on $\mathbb{L}^{d \geq 9}$, we fix $p \in (1, p_c)$ and assume $g_i(p) \leq K_i$, $i = 1, 2, 3$, where $\{K_i\}_{i=1}^3$ are the same constants as in Proposition 3.2.4. Then, the stronger inequalities $g_i(p) < K_i$, $i = 1, 2, 3$, hold.*

Here we prove the main result Theorem 3.2.1 and Proposition 3.2.3, whose proofs are separated from the lace expansion analysis.

Proof of Theorem 3.2.1. Since $g_2(p)$ is continuous in $p \in [1, p_c)$, with the initial value $g_2(1) < K_2$, and cannot be equal to K_2 for $p \in (1, p_c \wedge K_1)$, we can say that the strict inequality $g_2(p) < K_2$ holds for all $p \in [1, p_c \wedge K_1)$. Since the same argument applies to $g_1(p)$, we can conclude $p_c \leq K_1$, hence $g_2(p) < K_2$ for all $p \in [1, p_c)$ (see Figure 3.2). This completes the proof of Theorem 3.2.1 assuming Propositions 3.2.3–3.2.5. \blacksquare

Proof of Proposition 3.2.3. First, we recall (3.2.11) and (3.2.14) for the bootstrapping functions $\{g_i(p)\}_{i=1}^3$. Obviously, $g_1(p) \equiv p$ is continuous. To prove continuity of the other two, we introduce

$$\tilde{g}_{2,k}(p) = (1 - \hat{D}(k))\hat{G}_p(k), \quad (3.2.23)$$

$$\tilde{g}_{3,k,l}(p) = \frac{1}{\hat{U}(k,l)} \times \begin{cases} \hat{\Delta}_k \hat{G}_p(l) & [\text{SAW}], \\ \hat{\Delta}_k (\hat{G}_p(l) \hat{D}(l)) & [\text{percolation}], \end{cases} \quad (3.2.24)$$

and show that they are continuous in $p \in [1, p_c)$ for every $k, l \in \mathbb{T}^d$. However, since

$$g_2(p) = \sup_{k \in \mathbb{T}^d} |\tilde{g}_{2,k}(p)|, \quad g_3(p) = \sup_{k,l \in \mathbb{T}^d} |\tilde{g}_{3,k,l}(p)|, \quad (3.2.25)$$

and the supremum of continuous functions is not necessarily continuous, we must be a bit more cautious here. The following elementary lemma provides a sufficient condition for the supremum to be continuous.

Lemma 3.2.6 (Lemma 5.13 of [86], in our language). *Fix $p_0 \in [1, p_c)$ and let $\{\hat{f}_k(p)\}_{k \in \mathbb{T}^d}$ be an equicontinuous family of functions in $p \in [1, p_0]$. Suppose that $\sup_{k \in \mathbb{T}^d} \hat{f}_k(p) < \infty$ for every $p \in [1, p_0]$. Then, $\sup_{k \in \mathbb{T}^d} \hat{f}_k(p) < \infty$ is continuous in $p \in [1, p_0]$.*

Therefore, in order to prove continuity of $\{g_i(p)\}_{i=2,3}$ in $p \in [1, p_c)$, we want to show that $\{\tilde{g}_{2,k}(p)\}_{k \in \mathbb{T}^d}$ and $\{\tilde{g}_{3,k,l}(p)\}_{k,l \in \mathbb{T}^d}$ are equicontinuous families of functions in $p \in [1, p_0]$ for each $p_0 \in [1, p_c)$. To prove this, it then suffices to show that the following (i) and (ii) hold.

- (i) $\tilde{g}_{2,k}(p)$ and $\partial_p \tilde{g}_{2,k}(p)$ are finite uniformly in $k \in \mathbb{T}^d$ and $p \in [1, p_0]$.

(ii) $\tilde{g}_{3,k,l}(p)$ and $\partial_p \tilde{g}_{3,k,l}(p)$ are finite uniformly in $k, l \in \mathbb{T}^d$ and $p \in [1, p_0]$.

To prove (i) is not so hard. By $0 \leq 1 - \hat{D}(k) \leq 2$, $|\hat{G}_p(k)| \leq \chi_p$ and the monotonicity of χ_p in p , we obtain $|\tilde{g}_{2,k}(p)| \leq 2\chi_{p_0} < \infty$ uniformly in $k \in \mathbb{T}^d$ and $p \in [1, p_0]$. Moreover, by subadditivity for SAW, Russo's formula and the BK inequality for percolation (see, e.g., [45]), and then using translation-invariance, we obtain

$$0 \leq \partial_p G_p(x) \leq (D * G_p^{*2})(x), \quad (3.2.26)$$

hence

$$|\partial_p \tilde{g}_{2,k}(p)| \leq 2 \sum_x (D * G_p^{*2})(x) \leq 2\chi_{p_0}^2 < \infty, \quad (3.2.27)$$

uniformly in $k \in \mathbb{T}^d$ and $p \in [1, p_0]$, as required.

To prove (ii) needs extra care, especially near $k = 0$, because of the factor $1 - \hat{D}(k)$ in $\hat{U}(k, l)$. Here, we prove (ii) only for SAW. See [49] for the proof for percolation.

Proof of (ii) for SAW. First, we use the following lemma in [34, Appendix A].

Lemma 3.2.7. *Let $J \in \mathbb{N}$ and $t_j \in \mathbb{R}$ for $j = 1, \dots, J$. Then*

$$0 \leq 1 - \cos \sum_{j=1}^J t_j \leq J \sum_{j=1}^J (1 - \cos t_j). \quad (3.2.28)$$

By using this telescopic inequality, we obtain

$$\begin{aligned} |\hat{\Delta}_k \hat{G}_p(l)| &\leq \sum_x (1 - \cos k \cdot x) G_p(x) \\ &= \sum_x \sum_{\omega \in \Omega(o, x)} \left(1 - \cos \sum_{i=1}^{|\omega|} k \cdot (\omega_i - \omega_{i-1}) \right) p^{|\omega|} \prod_{j=1}^{|\omega|} D(\omega_j - \omega_{j-1}) \\ &\leq \sum_{u, v, x} (1 - \cos k \cdot (v - u)) \sum_{\omega \in \Omega(o, x)} |\omega| \sum_{i=1}^{|\omega|} \mathbb{1}_{\{b_i(\omega) = (u, v)\}} p^{|\omega|} \prod_{j=1}^{|\omega|} D(\omega_j - \omega_{j-1}). \end{aligned} \quad (3.2.29)$$

Ignoring the self-avoidance constraint between $\eta \equiv (\omega_0, \dots, \omega_{i-1})$ and $\xi \equiv (\omega_i, \dots, \omega_{|\omega|})$ and using translation-invariance, we can further bound $|\hat{\Delta}_k \hat{G}_p(l)|$ as

$$\begin{aligned} |\hat{\Delta}_k \hat{G}_p(l)| &\leq \sum_{u, v, x} (1 - \cos k \cdot (v - u)) p D(v - u) \sum_{\substack{\eta \in \Omega(o, u) \\ \xi \in \Omega(v, x)}} (|\eta| + |\xi| + 1) \\ &\quad \times p^{|\eta|} \prod_{i=1}^{|\eta|} D(\eta_i - \eta_{i-1}) p^{|\xi|} \prod_{j=1}^{|\xi|} D(\xi_j - \xi_{j-1}) \\ &\leq 2p(1 - \hat{D}(k)) \chi_p \sum_x \sum_{\omega \in \Omega(o, x)} (|\omega| + 1) p^{|\omega|} \prod_{j=1}^{|\omega|} D(\omega_j - \omega_{j-1}). \end{aligned} \quad (3.2.30)$$

However, by the identity $|\omega| + 1 = \sum_y \mathbb{1}_{\{y \in \omega\}}$ for a self-avoiding path ω , subadditivity and translation-invariance, the sum in the last line is bounded as

$$\sum_x \sum_{\omega \in \Omega(o, x)} (|\omega| + 1) p^{|\omega|} \prod_{j=1}^{|\omega|} D(\omega_j - \omega_{j-1}) \leq \sum_{x, y} G_p(y) G_p(x - y) = \chi_p^2. \quad (3.2.31)$$

As a result, we arrive at

$$|\hat{\Delta}_k \hat{G}_p(l)| \leq 2p_0(1 - \hat{D}(k))\chi_{p_0}^3, \quad (3.2.32)$$

which implies that $\tilde{g}_{3,k,l}(p)$ is finite uniformly in $k, l \in \mathbb{T}^d$ and $p \in [1, p_0]$.

For the derivative $\partial_p \tilde{g}_{3,k,l}(p) \equiv \hat{U}(k, l)^{-1} \hat{\Delta}_k \partial_p \hat{G}_p(l)$, we note that

$$\begin{aligned} |\hat{\Delta}_k \partial_p \hat{G}_p(l)| &\stackrel{(3.2.26)}{\leq} \sum_x (1 - \cos k \cdot x) (D * G_p^{*2})(x) \\ &\stackrel{(3.2.28)}{\leq} 3 \left((1 - \hat{D}(k))\chi_p^2 + 2\chi_p \underbrace{\sum_v (1 - \cos k \cdot v) G_p(v)}_{=\hat{\Delta}_k \hat{G}_p(0)} \right) \\ &\stackrel{(3.2.32)}{\leq} 3(1 - \hat{D}(k))\chi_{p_0}^2 (1 + 4p_0\chi_{p_0}^2). \end{aligned} \quad (3.2.33)$$

Therefore, $\partial_p \tilde{g}_{3,k,l}(p)$ is also finite uniformly in $k, l \in \mathbb{T}^d$ and $p \in [1, p_0]$. \blacksquare

To close this subsection, we recall the actual proof of Lemma 3.2.7 for completeness.

Proof of Lemma 3.2.7. First, we take the real part of the telescopic identity

$$1 - \exp(i \sum_{j=1}^J t_j) = \sum_{j=1}^J (1 - e^{it_j}) \exp(i \sum_{h=1}^{j-1} t_h), \quad (3.2.34)$$

where the empty sum for $j = 1$ is regarded as zero. Then, we use the basic three inequalities

$$\begin{aligned} \left| \sin \sum_{h=1}^{j-1} t_h \right| &\leq \sum_{h=1}^{j-1} |\sin t_h|, \quad |\sin t_j| |\sin t_h| \leq (\sin^2 t_j + \sin^2 t_h)/2, \\ \sin^2 t_j &= (1 + \cos t_j)(1 - \cos t_j) \leq 2(1 - \cos t_j), \end{aligned} \quad (3.2.35)$$

to obtain

$$\begin{aligned} 1 - \cos \left(\sum_{j=1}^J t_j \right) - \sum_{j=1}^J (1 - \cos t_j) &= - \sum_{j=1}^J (1 - \cos t_j) \underbrace{\left(1 - \cos \sum_{h=1}^{j-1} t_h \right)}_{\geq 0} + \sum_{j=1}^J (\sin t_j) \sin \sum_{h=1}^{j-1} t_h \\ &\leq \sum_{j=1}^J \sum_{h=1}^{j-1} \frac{\sin^2 t_j + \sin^2 t_h}{2} \leq (J-1) \sum_{j=1}^J (1 - \cos t_j), \end{aligned} \quad (3.2.36)$$

which implies (3.2.28). This completes the proof of Lemma 3.2.7 \blacksquare

3.2.5 Where and how to use the lace expansion

It remains to prove Propositions 3.2.4 and 3.2.5. To prove remaning two propositions, we will use the following lace expansion.

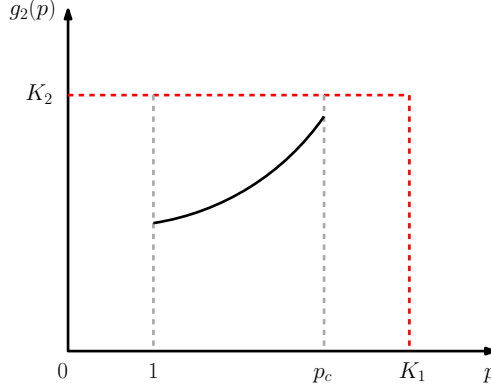


Figure 3.2: Depiction of the proof of Theorem 3.2.1 assuming Propositions 3.2.3–3.2.5.

Proposition 3.2.8 (Lace expansion). *For any $p < p_c$ and $N \in \mathbb{Z}_+ \equiv \{0\} \cup \mathbb{N}$, there exist model-dependent nonnegative functions $\{\pi_p^{(n)}\}_{n=0}^N$ on \mathbb{L}^d ($\pi_p^{(0)} \equiv 0$ for SAW) such that, if we define $I_p^{(N)}$ and $J_p^{(N)}$ as*

$$I_p^{(N)}(x) = \delta_{o,x} + \begin{cases} 0 & [\text{SAW}], \\ \sum_{n=0}^N (-1)^n \pi_p^{(n)}(x) & [\text{percolation}], \end{cases} \quad (3.2.37)$$

$$J_p^{(N)}(x) = pD(x) + \begin{cases} \sum_{n=1}^N (-1)^n \pi_p^{(n)}(x) & [\text{SAW}], \\ \sum_{n=0}^N (-1)^n (\pi_p^{(n)} * pD)(x) & [\text{percolation}], \end{cases} \quad (3.2.38)$$

then we obtain the recursion equation

$$G_p(x) = I_p^{(N)}(x) + (J_p^{(N)} * G_p)(x) + (-1)^{N+1} R_p^{(N+1)}(x), \quad (3.2.39)$$

where the remainder $R_p^{(N)}$ obeys the bound

$$0 \leq R_p^{(N)}(x) \leq (\pi_p^{(N)} * G_p)(x). \quad (3.2.40)$$

The derivation of the lace expansion is model-dependent and is explained for SAW in the next section. See [49] for percolation for explanation.

Here, we briefly explain where and how to use the lace expansion to prove Propositions 3.2.4–3.2.5. The details will be given in later section.

Step 1. First, we evaluate $\{g_i(p)\}_{i=1}^3$ in terms of sums of $\hat{\pi}_p^{(n)}(k) \equiv \sum_x e^{ik \cdot x} \pi_p^{(n)}(x)$.

(i) Let $p \in [1, p_c)$ and suppose $\sum_{n=0}^\infty \hat{\pi}_p^{(n)}(0)$ is small enough to ensure that

$$\lim_{N \rightarrow \infty} \hat{\pi}_p^{(N)}(0) = 0, \quad \hat{I}_p(k) \equiv \lim_{N \rightarrow \infty} \hat{I}_p^{(N)}(k) > 0 \quad \text{uniformly in } p \text{ and } k. \quad (3.2.41)$$

The latter is always true for SAW since $\hat{I}_p(k) \equiv 1$. The former implies that

$$0 \leq \sum_{x \in \mathbb{L}^d} R_p^{(N)}(x) \leq \hat{\pi}_p^{(N)}(0) \chi_p \xrightarrow{N \rightarrow \infty} 0. \quad (3.2.42)$$

Let (n.b. $\pi_p^{(0)} \equiv 0$ for SAW)

$$\hat{\Pi}_p(k) = \sum_{n=0}^{\infty} (-1)^n \hat{\pi}_p^{(n)}(k), \quad \hat{J}_p(k) = p\hat{D}(k) + \begin{cases} \hat{\Pi}_p(k) & [\text{SAW}], \\ \hat{\Pi}_p(k)p\hat{D}(k) & [\text{percolation}]. \end{cases} \quad (3.2.43)$$

Then, by using (3.2.39), we obtain

$$\chi_p \equiv \hat{G}_p(0) = \hat{I}_p(0) + \hat{J}_p(0)\chi_p = \frac{\hat{I}_p(0)}{1 - \hat{J}_p(0)}. \quad (3.2.44)$$

Since $\chi_p \geq 0$ and $\hat{I}_p(0) > 0$, we can conclude $\hat{J}_p(0) \leq 1$, which implies

$$g_1(p) \leq \begin{cases} 1 - \hat{\Pi}_p(0) & [\text{SAW}], \\ (1 + \hat{\Pi}_p(0))^{-1} & [\text{percolation}]. \end{cases} \quad (3.2.45)$$

(ii) Next, by (3.2.39) and (3.2.44), we obtain

$$\hat{G}_p(k) = \frac{\hat{I}_p(k)}{1 - \hat{J}_p(k)} = \frac{\hat{I}_p(k)}{-\hat{\Delta}_k \hat{J}_p(0) + \hat{I}_p(0)/\chi_p}, \quad (3.2.46)$$

where we have used the symmetry $\hat{J}_p(k) = \hat{J}_p(-k)$ to obtain $-\hat{\Delta}_k \hat{J}_p(0) = \hat{J}_p(0) - \hat{J}_p(k)$. Suppose $-\sum_{n=0}^{\infty} \hat{\Delta}_k \hat{\pi}_p^{(n)}(0) \equiv \sum_{n=0}^{\infty} \sum_x (1 - \cos k \cdot x) \pi_p^{(n)}(x)$ is smaller than $1 - \hat{D}(k)$ in order to ensure $-\hat{\Delta}_k \hat{J}_p(0) \geq 0$. Then, $\hat{G}_p(k)$ is bounded as³

$$0 \leq \hat{G}_p(k) \leq \frac{\hat{I}_p(k)}{-\hat{\Delta}_k \hat{J}_p(0)}. \quad (3.2.49)$$

Since $p \geq 1$, this implies

$$g_2(p) \leq \begin{cases} \sup_k \left(1 + \frac{-\hat{\Delta}_k \hat{\Pi}_p(0)}{1 - \hat{D}(k)} \right)^{-1} & [\text{SAW}], \\ \sup_k \left(1 + \frac{1}{\hat{I}_p(k)} \frac{-\hat{\Delta}_k \hat{\Pi}_p(0)}{1 - \hat{D}(k)} \right)^{-1} & [\text{percolation}], \end{cases} \quad (3.2.50)$$

³For percolation, the non-negativity of $\hat{G}_p(k)$ is elementary and proven in [8, Lemma 3.3]. The actual proof goes as follows. First, by translation-invariance, we can use any vertex y to rewrite $\hat{G}_p(k)$ as

$$\hat{G}_p(k) = \sum_x e^{ik \cdot x} \mathbb{P}_p(o \longleftrightarrow x) = \sum_x e^{ik \cdot x} \mathbb{P}_p(y \longleftrightarrow x + y) = \mathbb{E}_p \left[\sum_z e^{ik \cdot (z-y)} \mathbb{1}_{\{y \longleftrightarrow z\}} \right]. \quad (3.2.47)$$

Then, by using the identity $1 = \sum_y \mathbb{1}_{\{y \in \mathcal{C}(o)\}} / |\mathcal{C}(o)|$, where $\mathcal{C}(o)$ is the set of vertices connected from o , we can rewrite the rightmost expression as

$$\mathbb{E}_p \left[\frac{1}{|\mathcal{C}(o)|} \sum_{y \in \mathcal{C}(o)} \sum_z e^{ik \cdot (z-y)} \mathbb{1}_{\{y \longleftrightarrow z\}} \right] = \mathbb{E}_p \left[\frac{1}{|\mathcal{C}(o)|} \sum_{y, z \in \mathcal{C}(o)} e^{ik \cdot (z-y)} \right] = \mathbb{E}_p \left[\left| \frac{1}{\sqrt{|\mathcal{C}(o)|}} \sum_{z \in \mathcal{C}(o)} e^{ik \cdot z} \right|^2 \right] \geq 0. \quad (3.2.48)$$

where the supremum near $k = 0$ should be interpreted as the supremum over the limit as $|k| \rightarrow 0$.

(iii) To evaluate $g_3(p)$, we want to use Lemma 3.2.2. To do so for percolation, we first notice that, by using $\hat{I}_p(k)p\hat{D}(k) = \hat{J}_p(k)$ and (3.2.46), we obtain

$$\hat{G}_p(k)p\hat{D}(k) = \frac{\hat{J}_p(k)}{1 - \hat{J}_p(k)} = \frac{1}{1 - \hat{J}_p(k)} - 1 \equiv \hat{A}_p(k) - 1, \quad (3.2.51)$$

hence $\hat{\Delta}_k(\hat{G}_p(l)p\hat{D}(l)) = \hat{\Delta}_k\hat{A}_p(l)$. As a result, $g_3(p)$ for both models can be written as

$$g_3(p) = \sup_{k,l} \frac{|\hat{\Delta}_k\hat{A}_p(l)|}{\hat{U}(k,l)}. \quad (3.2.52)$$

Then, noting $\hat{A}_p(k) = (-\hat{\Delta}_k\hat{J}_p(0) + \hat{I}_p(0)/\chi_p)^{-1} \geq 0$, by Lemma 3.2.2 with $a(x) = J_p(x)$, we obtain

$$\begin{aligned} g_3(p) \leq \sup_{k,l} \frac{1 - \hat{D}(k)}{\hat{U}(k,l)} & \left(\frac{\hat{A}_p(l+k) + \hat{A}_p(l-k)}{2} \hat{A}_p(l) \frac{|\hat{\Delta}_k\hat{J}_p(l)|}{1 - \hat{D}(k)} \right. \\ & \left. + 4\hat{A}_p(l+k)\hat{A}_p(l-k) \frac{-\hat{\Delta}_l|\widehat{J_p}|(0)}{1 - \hat{J}_p(l)} \frac{-\hat{\Delta}_k|\widehat{J_p}|(0)}{1 - \hat{D}(k)} \right), \end{aligned} \quad (3.2.53)$$

where

$$|\widehat{J_p}|(k) = \sum_{x \in \mathbb{L}^d} e^{ik \cdot x} |J_p(x)|. \quad (3.2.54)$$

We can further bound $|\hat{\Delta}_k\hat{J}_p(l)|$ and $-\hat{\Delta}_k|\widehat{J_p}|(0) \equiv |\widehat{J_p}|(0) - |\widehat{J_p}|(k) \geq 0$ in terms of sums of $|\hat{\Delta}_k\hat{\pi}_p^{(n)}(0)|$. However, to simplify the exposition, we refrain from doing so for now and postpone it to later section.

So far, we have assumed that $\sum_{n=0}^{\infty} \hat{\pi}_p^{(n)}(0)$ and $-\sum_{n=0}^{\infty} \hat{\Delta}_k\hat{\pi}_p^{(n)}(0)$ are small enough to carry out the above computations. Sufficient conditions to this assumption are

$$\sum_{n=1}^{\infty} \hat{\pi}_p^{(n)}(0) < \infty, \quad \sup_k \sum_{n=1}^{\infty} \frac{-\hat{\Delta}_k\hat{\pi}_p^{(n)}(0)}{1 - \hat{D}(k)} < 1 \quad (3.2.55)$$

for SAW, and

$$\sum_{n=0}^{\infty} \hat{\pi}_p^{(n)}(0) + \sup_k \sum_{n=0}^{\infty} \frac{-\hat{\Delta}_k\hat{\pi}_p^{(n)}(0)}{1 - \hat{D}(k)} < 1 \quad (3.2.56)$$

for percolation. These conditions are to be verified eventually. ■

Step 2. As shown in (3.2.45), (3.2.50) and (3.2.53), the bootstrapping functions $\{g_i(p)\}_{i=1}^3$ are bounded in terms of sums of $\hat{\pi}_p^{(n)}(0)$ and sums of $|\hat{\Delta}_k\hat{\pi}_p^{(n)}(0)|$. In the second step, we evaluate those lace-expansion coefficients in terms of smaller diagrams, such as

$$L_p = \|(pD)^{*2} * G_p\|_{\infty}, \quad B_p = \|(pD)^{*2} * G_p^{*2}\|_{\infty}, \quad T_p = \|(pD)^{*2} * G_p^{*3}\|_{\infty}. \quad (3.2.57)$$

For example, we can bound $\hat{\pi}_p^{(n)}$ for $n \geq 2$ as

$$0 \leq \hat{\pi}_p^{(n)}(0) \leq \begin{cases} B_p(p\|D\|_\infty + L_p)r^{n-2} & [\text{SAW}], \\ (1 + \frac{1}{2}B_p + T_p)^2 r \rho^{n-1} & [\text{percolation}], \end{cases} \quad (3.2.58)$$

where

$$r = p\|D\|_\infty + L_p + B_p, \quad \rho = \left(1 + \frac{1}{2}B_p + T_p\right)(r + T_p) + T_p(2r + T_p) \quad (3.2.59)$$

See Sections 3.3 for the proof of the above inequality and the bound on $\hat{\pi}_p^{(1)}(0)$ for SAW. See [49] for the proof of the above inequality and the bounds on $\hat{\pi}_p^{(0)}(0)$ and $\hat{\pi}_p^{(1)}(0)$ for percolation. It will also be shown that the amplitude of $|\hat{\Delta}_k \hat{\pi}_p^{(n)}(0)|/(1 - \hat{D}(k))$ is bounded in a similar fashion, with the common ratio r for SAW and ρ for percolation. Therefore, the assumptions made in Step 1 hold if L_p, B_p, T_p and other diagrams in the bounds are small enough. ■

Step 3. In the final step, we investigate the aforesaid diagrams and prove that, by choosing appropriate values for $\{K_i\}_{i=1}^3$, those diagrams are indeed small enough for SAW on $\mathbb{L}^{d \geq 6}$ and for percolation on $\mathbb{L}^{d \geq 9}$.

(i) For $p = 1$, we only need to use the trivial inequality $G_1(x) \leq S_1(x)$, $x \in \mathbb{L}^d$, for both models to obtain that, for $d > 2$ (as mentioned earlier, $\hat{S}_1(k) \equiv (1 - \hat{D}(k))^{-1}$ is well-defined in a proper limit when $d > 2$),

$$L_1 \leq \|D^{*2} * S_1\|_\infty = \int_{\mathbb{T}^d} \frac{\hat{D}(k)^2}{1 - \hat{D}(k)} \frac{d^d k}{(2\pi)^d} = (D^{*2} * S_1)(o) \equiv \varepsilon_1. \quad (3.2.60)$$

Similarly, we obtain

$$B_1 \leq \varepsilon_2, \quad T_1 \leq \varepsilon_3. \quad (3.2.61)$$

Consulting with Table 3.1 in Section 3.2.1, we can see that, even in $d_c + 1$ dimensions, r and ρ in (3.2.59) are small enough for the bootstrapping functions $\{g_i(p)\}_{i=1}^3$ to be convergent.

(ii) The strategy for $p \in (1, p_c)$ is different from that for $p = 1$, because there is no *a priori* bound on G_p in terms of S_1 . Here, we use the assumptions $g_i(p) \leq K_i$, $i = 1, 2, 3$, to evaluate the diagrams. For example,

$$L_p \leq p^2 \int_{\mathbb{T}^d} \hat{D}(k)^2 |\hat{G}_p(k)| \frac{d^d k}{(2\pi)^d} \leq K_1^2 K_2 \underbrace{\int_{\mathbb{T}^d} \frac{\hat{D}(k)^2}{1 - \hat{D}(k)} \frac{d^d k}{(2\pi)^d}}_{=\varepsilon_1}. \quad (3.2.62)$$

Similarly,

$$B_p \leq K_1^2 K_2^2 \varepsilon_2, \quad T_p \leq K_1^2 K_2^3 \varepsilon_3. \quad (3.2.63)$$

As a result, r and ρ in (3.2.59) become functions of $\{K_i\}_{i=1,2}$. If we choose their values appropriately, then we can derive the improved bound $g_1(p) < K_1$ for all $d \geq d_c + 1$. To improve the bounds on $\{g_i(p)\}_{i=2,3}$, we also have to control K_3 . This is the worst enemy that keeps us from going down to $d_c + 1$ dimensions. In [27], we will make all-out efforts to overcome this problem. ■

3.2.6 Organization

In the rest of this chapter, we prove the above propositions in detail. We focus on the lace expansion analysis for SAW and omit the full details for percolation. See [49].

In Section 3.3, we prove Propositions 3.2.4, 3.2.5, and 3.2.8 for SAW as follows. In Section 3.3.1, we explain the derivation of the lace expansion (Proposition 3.2.8) for SAW. In Section 3.3.2, we prove bounds on the lace-expansion coefficients in terms of basic diagrams, as briefly explained in *Step 2* in Section 3.2.5. In Section 3.3.4, we prove bounds on those basic diagrams in terms of RW quantities, as explained in *Step 3* in Section 3.2.5. Applying them to the bounds on the bootstrapping functions $\{g_i(p)\}_{i=1}^3$ obtained in *Step 1* in Section 3.2.5, we prove Propositions 3.2.4–3.2.5 on $\mathbb{L}^{d \geq 6}$. Finally, in Section 3.3.5, we provide further discussion to potentially improve our results.

3.3 Lace-expansion analysis for self-avoiding walk

In this section, we prove Propositions 3.2.4–3.2.8 for SAW. First, in Section 3.3.1, we explain the derivation of the lace expansion, Proposition 3.2.8, for SAW. In Section 3.3.2, we prove bounds on the lace-expansion coefficients in terms of basic diagrams, such as L_p and B_p . Finally, in Section 3.3.4, we prove bounds on those basic diagrams in terms of RW loops and RW bubbles and use them to prove Propositions 3.2.4–3.2.5 on $\mathbb{L}^{d \geq 6}$. We close this section by addressing potential elements for extending the result to 5 dimensions, in Section 3.3.5.

3.3.1 Derivation of the lace expansion

Proposition 3.2.8 for SAW is restated as follows.

Proposition 3.3.1 (Lace expansion for SAW). *For any $p < p_c$ and $N \in \mathbb{N}$, there are nonnegative functions $\{\pi_p^{(n)}\}_{n=1}^N$ on \mathbb{L}^d such that, if we define $\Pi_p^{(N)}$ as*

$$\Pi_p^{(N)}(x) = \sum_{n=1}^N (-1)^n \pi_p^{(n)}(x), \quad (3.3.1)$$

then we obtain the recursion equation

$$G_p(x) = \delta_{o,x} + ((pD + \Pi_p^{(N)}) * G_p)(x) + (-1)^{N+1} R_p^{(N+1)}(x), \quad (3.3.2)$$

where the remainder $R_p^{(N)}$ obeys the bound

$$0 \leq R_p^{(N)}(x) \leq (\pi_p^{(N)} * G_p)(x). \quad (3.3.3)$$

Sketch proof of Proposition 3.3.1. First, we derive the first expansion, i.e., (3.3.2) for $N = 1$. For notational convenience, we use

$$P(\omega) = p^{|\omega|} \prod_{j=1}^{|\omega|} D(\omega_j - \omega_{j-1}). \quad (3.3.4)$$

Then, by splitting the sum in (3.2.5) into two depending on whether $|\omega|$ is zero or positive, we obtain

$$G_p(x) = \delta_{o,x} + \sum_{\substack{\omega \in \Omega(o,x) \\ (|\omega| \geq 1)}} P(\omega) = \delta_{o,x} + \sum_y pD(y) \sum_{\omega \in \Omega(y,x)} P(\omega) \mathbb{1}_{\{o \notin \omega\}}. \quad (3.3.5)$$

This is depicted as

$$o \bullet \text{---} \bullet x = \delta_{o,x} + o \bullet \blacksquare \text{---} \bullet x \quad (3.3.6)$$

where the rectangle next to the origin represents that there is a bond from o to a neighboring vertex y , which is summed over \mathbb{L}^d and unlabeled in the picture, and the dashed two-sided arrow represents mutual avoidance between o and SAWs from y to x , which corresponds to the indicator $\mathbb{1}_{\{o \notin \omega\}}$ in (3.3.5). Using the identity $\mathbb{1}_{\{o \notin \omega\}} = 1 - \mathbb{1}_{\{o \in \omega\}}$ due to the inclusion-exclusion relation, we complete the first expansion as

$$\begin{aligned} G_p(x) &= \delta_{o,x} + o \bullet \blacksquare \text{---} \bullet x - \underbrace{o \bullet \blacksquare \text{---} \bullet x}_{\equiv R_p^{(1)}(x)} \\ &= \delta_{o,x} + (pD * G_p)(x) - R_p^{(1)}(x). \end{aligned} \quad (3.3.7)$$

Next, we expand the remainder $R_p^{(1)}(x)$ to complete the first expansion. Splitting each SAW from y (summed over \mathbb{L}^d and unlabeled in the picture) to x through o into two SAWs, $\omega_1 \in \Omega(y, o)$ and $\omega_2 \in \Omega(o, x)$ (in red), we can rewrite $R_p^{(1)}(x)$ as

$$R_p^{(1)}(x) = o \bullet \blacksquare \text{---} \bullet x \quad (3.3.8)$$

where the dashed two-sided arrow implies that the concatenation of ω_1 and ω_2 in this order, denoted $\omega_1 \circ \omega_2$, is SAW. Using the identity $\mathbb{1}_{\{\omega_1 \circ \omega_2 \text{ is SAW}\}} = 1 - \mathbb{1}_{\{\omega_1 \circ \omega_2 \text{ is not SAW}\}}$,

we obtain

$$\begin{aligned}
R_p^{(1)}(x) &= o \text{ --- } x - o \text{ --- } x \\
&\quad \underbrace{\hspace{10em}}_{\equiv R_p^{(2)}(x)} \\
&= \sum_y \underbrace{\bigcirc_{o=y}}_{\equiv \pi_p^{(1)}(y)} G_p(x-y) - R_p^{(2)}(x), \tag{3.3.9}
\end{aligned}$$

where the precise definition of $\pi_p^{(1)}(x)$ is the following:

$$\pi_p^{(1)}(x) = (pD * G_p)(o) \delta_{o,x}. \tag{3.3.10}$$

Since $R_p^{(2)}(x)$ is nonnegative, this also implies (3.3.3) for $N = 1$. This completes the first expansion.

To show how to derive the higher-order expansion coefficients, we further demonstrate the expansion of the remainder $R_p^{(2)}(x)$. Since $\omega_1 \circ \omega_2$ is not SAW, there must be at least one vertex other than o where ω_2 hits ω_1 . Take the first such vertex, say, $z \neq o$, which is summed over \mathbb{L}^d and unlabeled in the following picture, and split $\omega_2 \in \Omega(o, x)$ into two SAWs, $\omega_{21} \in \Omega(o, z)$ and $\omega_{22} \in \Omega(z, x)$ (in blue), so that $\omega_1 \cap \omega_{21} = \{o, z\}$. Then, we can rewrite $R_p^{(2)}(x)$ as

$$R_p^{(2)}(x) = o \text{ --- } x \tag{3.3.11}$$

where the dashed two-sided arrow between the red ω_{21} and the blue ω_{22} implies that the concatenation $\omega_{21} \circ \omega_{22}$ is SAW. Using the identity $\mathbb{1}_{\{\omega_{21} \circ \omega_{22} \text{ is SAW}\}} = 1 - \mathbb{1}_{\{\omega_{21} \circ \omega_{22} \text{ is not SAW}\}}$, we obtain

$$\begin{aligned}
R_p^{(2)}(x) &= o \text{ --- } x - o \text{ --- } x \\
&\quad \underbrace{\hspace{10em}}_{\equiv R_p^{(3)}(x)}
\end{aligned}$$

$$= \sum_y \underbrace{\left(\begin{array}{c} y \\ \bigcirc \\ o \end{array} \right)}_{\equiv \pi_p^{(2)}(y)} G_p(x-y) - R_p^{(3)}(x), \quad (3.3.12)$$

where the precise definition of $\pi_p^{(2)}(x)$ is the following:

$$\pi_p^{(2)}(x) = (1 - \delta_{o,x}) \sum_{\omega_1, \omega_2, \omega_3 \in \Omega(o,x)} P(\omega_1)P(\omega_2)P(\omega_3) \prod_{i \neq j} \mathbb{1}_{\{\omega_i \cap \omega_j = \{o,x\}\}}. \quad (3.3.13)$$

Since $R_p^{(3)}(x)$ is nonnegative, this implies (3.3.3) for $N = 2$, as required.

By repeated application of inclusion-exclusion relations, we obtain the lace expansion (3.3.2), with the lace-expansion coefficients depicted as

$$\pi_p^{(3)}(x) = \begin{array}{c} \text{Diagram 1} \\ o \quad x \end{array}, \quad \pi_p^{(4)}(x) = \begin{array}{c} \text{Diagram 2} \\ o \quad x \end{array}, \quad \pi_p^{(5)}(x) = \begin{array}{c} \text{Diagram 3} \\ o \quad x \end{array}, \quad \dots \quad (3.3.14)$$

where the slashed line segments represent SAWs with length ≥ 0 , while the others represent SAWs with length ≥ 1 . The unlabeled vertices are summed over \mathbb{L}^d . Due to the construction explained above, the red line segments avoid the black ones, the blue ones avoid the red ones, the yellow ones avoid the blue ones, and so on. We complete the sketch proof of Proposition 3.3.1. \blacksquare

3.3.2 Diagrammatic bounds on the expansion coefficients

As explained in *Step 1* in Section 3.2.5, the bootstrapping functions $\{g_i(p)\}_{i=1}^3$ are bounded in terms of sums of $\hat{\pi}_p^{(n)}(0)$ and $|\hat{\Delta}_k \hat{\pi}_p^{(n)}(0)|$. In this subsection, we prove bounds on those quantities in terms of basic diagrams, such as L_p and B_p in (3.2.57), as briefly explained in *Step 2* in Section 3.2.5. Recall that

$$L_p = \|(pD)^{*2} * G_p\|_\infty, \quad B_p = \|(pD)^{*2} * G_p^{*2}\|_\infty, \quad r = p\|D\|_\infty + L_p + B_p. \quad (3.3.15)$$

We also define

$$B'_p = \|(pD)^{*4} * G_p^{*2}\|_\infty, \quad \hat{W}_p(k) = \sup_x (1 - \cos k \cdot x) G_p(x). \quad (3.3.16)$$

Lemma 3.3.2 (Diagrammatic bounds on the expansion coefficients). *The expansion coefficients $\hat{\pi}_p^{(n)}(0) \equiv \sum_x \pi_p^{(n)}(x)$ and $|\hat{\Delta}_k \hat{\pi}_p^{(n)}(0)| \equiv \sum_x (1 - \cos k \cdot x) \pi_p^{(n)}(x)$, both nonnegative, obey the following bounds:*

$$\hat{\pi}_p^{(n)}(0) \leq \begin{cases} L_p & [n = 1], \\ B_p(p\|D\|_\infty + L_p)r^{n-2} & [n \geq 2], \end{cases} \quad (3.3.17)$$

$$|\hat{\Delta}_k \hat{\pi}_p^{(n)}(0)| \leq \begin{cases} B_p^2 \hat{W}_p(k) m^2 r^{2m-2} & [n = 2m + 1], \\ B_p^2 \hat{W}_p(k) m(m-1) r^{2m-3} + B_p \hat{W}_p(k) m r^{2m-2} & [n = 2m]. \end{cases} \quad (3.3.18)$$

For $|\hat{\Delta}_k \hat{\pi}_p^{(2)}(0)|$, in particular, the following bound also holds:

$$|\hat{\Delta}_k \hat{\pi}_p^{(2)}(0)| \leq \frac{3B_p}{2^d} p(1 - \hat{D}(k)) + B'_p \hat{W}_p(k). \quad (3.3.19)$$

Remark 3.3.3. As shown in (3.3.61) and (3.3.56) in the next subsection, $\|\hat{W}_p/(1-\hat{D})\|_\infty$ could be relatively large, compared to L_p, B_p and r . Therefore, if we want to have a good bound on $|\hat{\Delta}_k \hat{\pi}_p^{(n)}(0)|/(1-\hat{D}(k))$, we should have a small multiplicative factor to $\hat{W}_p(k)$. By (3.3.18), that multiplicative factor is at most $\lfloor \frac{n}{2} \rfloor^2 B_p r^{n-2}$ for $n \geq 2$ (it is zero for $n = 1$, due to the definition of $\pi_p^{(1)}$) and the dominant contribution comes from the case of $n = 2$, i.e., B_p . In (3.3.19), on the other hand, the multiplicative factor to $\hat{W}_p(k)$ is B'_p , which is potentially much smaller than B_p . This can be seen by comparing the RW versions of B_p and B'_p , which are the RW bubble ε_2 and

$$\varepsilon'_2 = (D^{*4} * S_1^2)(o) = \sum_{n=2}^{\infty} (2n-3) D^{*2n}(o). \quad (3.3.20)$$

Table 3.2 summarizes the bounds on those RW bubbles that are evaluated as explained in Section 3.2.1.

Table 3.2: Comparison of upper bounds on the RW bubbles for $4 \leq d \leq 9$.

	$d = 4$	$d = 5$	$d = 6$	$d = 7$	$d = 8$	$d = 9$
ε_2	∞	0.178332	0.044004	0.015302	0.006156	0.002678
ε'_2	∞	0.115931	0.018708	0.004302	0.001161	0.000344

The amount of extra work caused by the use of (3.3.19) instead of using only (3.3.18) is quite small. However, this is the key to be able to go down to 6 dimensions. We will get back to this point in Section 3.3.5.

Sketch proof of Lemma 3.3.2. In the following, we repeatedly use the trivial inequality

$$G_p(x) \mathbb{1}_{\{x \neq o\}} \leq (pD * G_p)(x). \quad (3.3.21)$$

For example,

$$\hat{\pi}_p^{(1)}(0) = \sum_{x \neq o} pD(x) G_p(x) \leq ((pD)^{*2} * G_p)(o) \leq L_p. \quad (3.3.22)$$

For $n \geq 2$, we first decompose $\hat{\pi}_p^{(n)}(0)$ by using subadditivity and then repeatedly apply (3.3.21) to obtain (3.3.17). For example,

$$\begin{aligned} \hat{\pi}_p^{(2)}(0) = \text{Diagram} &\leq \left(\sum_{x \neq o} G_p(x)^2 \right) \left(\sup_{x \neq o} G_p(x) \right) \\ &\stackrel{(3.3.21)}{\leq} \underbrace{((pD)^{*2} * G_p^{*2})(o)}_{\leq B_p} \left(\sup_{x \neq o} (pD * G_p)(x) \right), \end{aligned} \quad (3.3.23)$$

and

$$\begin{aligned}
\hat{\pi}_p^{(5)}(0) &= \text{Diagram: A semi-circle with a horizontal base. Inside, there are three triangles meeting at a central point. The left triangle is red, the middle is blue, and the right is yellow. The base is divided into three segments by the projections of the central point. The left segment is red, the middle is blue, and the right is yellow. The central point is labeled 'o' at the bottom left corner of the diagram.} \\
&\leq \left(\sum_{x \neq o} G_p(x)^2 \right) \left(\sup_{x \neq o} \sum_{y \neq x} G_p(y) G_p(x-y) \right)^3 \left(\sup_{x \neq o} G_p(x) \right) \\
&\stackrel{(3.3.21)}{\leq} B_p \left(\sup_x (pD * G_p^{*2})(x) \right)^3 \left(\sup_x (pD * G_p)(x) \right). \tag{3.3.24}
\end{aligned}$$

In general, $\hat{\pi}_p^{(n)}(0)$ for $n \geq 2$ is bounded by the right-most expression with the power 3 replaced by $n-2$. Notice that, by omitting the spatial variables, we have

$$pD * G_p = pD * (\delta + (1-\delta)G_p) \stackrel{(3.3.21)}{\leq} pD + (pD)^{*2} * G_p, \tag{3.3.25}$$

where δ is the Kronecker delta, hence

$$\sup_x (pD * G_p)(x) \leq p\|D\|_\infty + \|(pD)^{*2} * G_p\|_\infty = p\|D\|_\infty + L_p. \tag{3.3.26}$$

Similarly, we have

$$\begin{aligned}
pD * G_p^{*2} &= pD * G_p * (\delta + (1-\delta)G_p) \\
&\stackrel{(3.3.21)}{\leq} pD * G_p + (pD)^{*2} * G_p^{*2} \\
&= pD * (\delta + (1-\delta)G_p) + (pD)^{*2} * G_p^{*2} \\
&\stackrel{(3.3.21)}{\leq} pD + (pD)^{*2} * G_p + (pD)^{*2} * G_p^{*2}, \tag{3.3.27}
\end{aligned}$$

hence

$$\begin{aligned}
\sup_x (pD * G_p^{*2})(x) &\leq p\|D\|_\infty + \|(pD)^{*2} * G_p\|_\infty + \|(pD)^{*2} * G_p^{*2}\|_\infty \\
&= p\|D\|_\infty + L_p + B_p \equiv r. \tag{3.3.28}
\end{aligned}$$

This completes the proof of (3.3.17).

Next, we prove (3.3.18) for $n = 2m+1$. Since $\pi_p^{(1)}(x)$ is proportional to $\delta_{o,x}$ and therefore $\hat{\Delta}_k \hat{\pi}_p^{(1)}(0) \equiv 0$, we can assume $m \geq 1$. To bound $|\hat{\Delta}_k \hat{\pi}_p^{(2m+1)}(0)| \equiv \sum_x (1 - \cos k \cdot x) \pi_p^{(2m+1)}(x)$ for $m \geq 1$, we first identify the diagram vertices along the lowest diagram path from o to x , say, y_1, \dots, y_{m-1} , and then split x into $\{y_j - y_{j-1}\}_{j=1}^m$, where $y_0 = o$ and $y_m = x$. For example,

$$|\hat{\Delta}_k \hat{\pi}_p^{(5)}(0)| = \sum_{y_1, y_2} \left(1 - \cos \sum_{j=1,2} k \cdot (y_j - y_{j-1}) \right) \text{Diagram: A semi-circle with a horizontal base. Inside, there are three triangles meeting at a central point. The left triangle is red, the middle is blue, and the right is yellow. The base is divided into three segments by the projections of the central point. The left segment is red, the middle is blue, and the right is yellow. The central point is labeled 'y_0=o' at the bottom left corner of the diagram. The rightmost point is labeled 'y_2'. The point where the red and blue triangles meet is labeled 'y_1' at the bottom.} \tag{3.3.29}$$

Then, by using (3.2.28) and subadditivity, we obtain

$$\begin{aligned}
|\hat{\Delta}_k \hat{\pi}_p^{(5)}(0)| &\leq 2 \sum_{y_1, y_2} \left((1 - \cos k \cdot y_1) + (1 - \cos k \cdot (y_2 - y_1)) \right) \\
&\quad \times \left(G_p(y_1) \text{ (diagram 1)} + G_p(y_2 - y_1) \text{ (diagram 2)} \right) \\
&\leq 2\hat{W}_p(k) \left(\text{diagram 1} + \text{diagram 2} \right). \tag{3.3.30}
\end{aligned}$$

Each remaining diagram is bounded, by following similar decomposition to (3.3.23)–(3.3.24) and then using (3.3.28), by $B_p^2 r^2$, yielding the desired bound on $|\hat{\Delta}_k \hat{\pi}_p^{(5)}(0)|$. In general,

$$\begin{aligned}
|\hat{\Delta}_k \hat{\pi}_p^{(2m+1)}(0)| &\leq m\hat{W}_p(k) \times \left(m \text{ diagrams, each bounded by } B_p^2 r^{2m-2} \right) \\
&\leq B_p^2 \hat{W}_p(k) m^2 r^{2m-2}, \tag{3.3.31}
\end{aligned}$$

as required.

To prove (3.3.18) for $n = 2m$, we follow the same line as above for $n = 2m + 1$. To bound $|\hat{\Delta}_k \hat{\pi}_p^{(2m)}(0)| \equiv \sum_x (1 - \cos k \cdot x) \pi_p^{(2m)}(x)$, we first identify the diagram vertices along the lowest diagram path from o to x , say, y_1, \dots, y_{m-1} , and then split x into $\{y_j - y_{j-1}\}_{j=1}^m$, where $y_0 = o$ and $y_m = x$. For example,

$$|\hat{\Delta}_k \hat{\pi}_p^{(4)}(0)| = \sum_{y_1, y_2} \left(1 - \cos \sum_{j=1,2} k \cdot (y_j - y_{j-1}) \right) \text{ (diagram)} \tag{3.3.32}$$

Then, by using (3.2.28) and subadditivity, we obtain

$$\begin{aligned}
|\hat{\Delta}_k \hat{\pi}_p^{(4)}(0)| &\leq 2 \sum_{y_1, y_2} \left((1 - \cos k \cdot y_1) + (1 - \cos k \cdot (y_2 - y_1)) \right) \\
&\quad \times \left(G_p(y_1) \text{ (diagram 1)} + G_p(y_2 - y_1) \text{ (diagram 2)} \right) \\
&\leq 2\hat{W}_p(k) \left(\text{diagram 1} + \text{diagram 2} \right). \tag{3.3.33}
\end{aligned}$$

Following similar decomposition to (3.3.23)–(3.3.24) and using (3.3.28), we can bound the first diagram by $B_p^2 r$, while the second diagram is bounded by $B_p r^2$, yielding the desired bound on $|\hat{\Delta}_k \hat{\pi}_p^{(4)}(0)|$. In general,

$$\begin{aligned}
|\hat{\Delta}_k \hat{\pi}_p^{(2m)}(0)| &\leq m\hat{W}_p(k) \times \left(\left((m-1) \text{ diagrams, each bounded by } B_p^2 r^{2m-3} \right) \right. \\
&\quad \left. + \left(1 \text{ diagram, bounded by } B_p r^{2m-2} \right) \right) \\
&\leq B_p^2 \hat{W}_p(k) m(m-1) r^{2m-3} + B_p \hat{W}_p(k) m r^{2m-2}, \tag{3.3.34}
\end{aligned}$$

as required.

To prove the bound (3.3.19) on $|\hat{\Delta}_k \hat{\pi}_p^{(2)}(0)|$, we recall the definition (3.3.13) and divide $\pi_p^{(2)}(x)$ into $\pi_p^{(2),=1}(x)$ and $\pi_p^{(2),\geq 2}(x)$, where

$$\pi_p^{(2),=1}(x) = (1 - \delta_{o,x}) \sum_{\substack{\omega_1, \omega_2, \omega_3 \in \Omega(o,x) \\ (\exists i: |\omega_i|=1)}} P(\omega_1)P(\omega_2)P(\omega_3) \prod_{i \neq j} \mathbb{1}_{\{\omega_i \cap \omega_j = \{o,x\}\}}, \quad (3.3.35)$$

$$\pi_p^{(2),\geq 2}(x) = (1 - \delta_{o,x}) \sum_{\substack{\omega_1, \omega_2, \omega_3 \in \Omega(o,x) \\ (\forall i: |\omega_i| \geq 2)}} P(\omega_1)P(\omega_2)P(\omega_3) \prod_{i \neq j} \mathbb{1}_{\{\omega_i \cap \omega_j = \{o,x\}\}}. \quad (3.3.36)$$

Then, by symmetry, the contribution from $\pi_p^{(2),=1}(x)$ is bounded as

$$\begin{aligned} |\hat{\Delta}_k \hat{\pi}_p^{(2),=1}(0)| &\leq 3 \sum_{x \sim o} (1 - \cos k \cdot x) p D(x) \underbrace{\left(\sum_{\omega \in \Omega(o,x)} P(\omega) \right)^2}_{\leq (pD * G_p)(x)} \\ &\leq 3 \left(\sup_{x \sim o} (pD * G_p)(x)^2 \right) p \sum_x (1 - \cos k \cdot x) D(x) \\ &= 3 \underbrace{\left(\frac{1}{2^d} \sum_{x \sim o} (pD * G_p)(x)^2 \right)}_{\leq B_p} p (1 - \hat{D}(k)), \end{aligned} \quad (3.3.37)$$

while the contribution from $\pi_p^{(2),\geq 2}(x)$ is easily bounded as

$$\begin{aligned} |\hat{\Delta}_k \hat{\pi}_p^{(2),\geq 2}(0)| &\leq \sum_x (1 - \cos k \cdot x) \left(\sum_{\substack{\omega \in \Omega(o,x) \\ (|\omega| \geq 2)}} P(\omega) \right)^3 \\ &\leq \underbrace{\sum_x ((pD)^{*2} * G_p)(x)^2}_{\leq B'_p} \underbrace{\left(\sup_x (1 - \cos k \cdot x) G_p(x) \right)}_{=\hat{W}_p(k)}, \end{aligned} \quad (3.3.38)$$

This completes the proof of Lemma 3.3.2. ■

3.3.3 Diagrammatic bounds on the bootstrapping functions

Let

$$\hat{\Pi}_p^{\text{odd}}(k) = \sum_{m=0}^{\infty} \hat{\pi}_p^{(2m+1)}(k), \quad \hat{\Pi}_p^{\text{even}}(k) = \sum_{m=1}^{\infty} \hat{\pi}_p^{(2m)}(k). \quad (3.3.39)$$

Suppose that $r \equiv p\|D\|_{\infty} + L_p + B_p < 1$. Then, by Lemma 3.3.2, we obtain the following bounds on the above infinite series.

Lemma 3.3.4. *Suppose that $r < 1$. Then, we have*

$$0 \leq \hat{\Pi}_p^{\text{odd}}(0) \leq L_p + B_p(p\|D\|_\infty + L_p) \frac{r}{1-r^2}, \quad (3.3.40)$$

$$0 \leq \hat{\Pi}_p^{\text{even}}(0) \leq B_p(p\|D\|_\infty + L_p) \frac{1}{1-r^2}, \quad (3.3.41)$$

$$\sup_k \frac{|\hat{\Delta}_k \hat{\Pi}_p^{\text{odd}}(0)|}{1 - \hat{D}(k)} \leq \frac{B_p^2(1+r^2)}{(1-r^2)^3} \left\| \frac{\hat{W}_p}{1 - \hat{D}} \right\|_\infty, \quad (3.3.42)$$

$$\sup_k \frac{|\hat{\Delta}_k \hat{\Pi}_p^{\text{even}}(0)|}{1 - \hat{D}(k)} \leq \frac{3B_p}{2^d} p + \left(B'_p + B_p^2 \frac{2r}{(1-r^2)^3} + B_p \frac{r^2(2-r^2)}{(1-r^2)^2} \right) \left\| \frac{\hat{W}_p}{1 - \hat{D}} \right\|_\infty. \quad (3.3.43)$$

Proof. Non-negativity for (3.3.40) and (3.3.41) is trivial because each $\hat{\pi}_p^{(n)}(k)$ is non-negative. By using Lemma 3.3.2, we calculate geometric series, for example,

$$\hat{\Pi}_p^{\text{odd}}(0) \leq L_p + B_p(p\|D\|_\infty + L_p) \sum_{m=0}^{\infty} r^{2m-1} = L_p + B_p(p\|D\|_\infty + L_p) \frac{r}{1-r^2}. \quad (3.3.44)$$

We can obtain (3.3.41) in the same way. For (3.3.42) and (3.3.43), we take the supremum of $\hat{W}_p(k)/1 - \hat{D}(k)$ over $k \in \mathbb{L}^d$. Then, we calculate geometric series again, for example,

$$\sup_k \frac{|\hat{\Delta}_k \hat{\Pi}_p^{\text{odd}}(0)|}{1 - \hat{D}(k)} \leq B_p^2 \left(\sup_k \frac{\hat{W}_p(k)}{1 - \hat{D}(k)} \right) \sum_{m=0}^{\infty} m^2 r^{2m-2} = \frac{B_p^2(1+r^2)}{(1-r^2)^3} \left\| \frac{\hat{W}_p}{1 - \hat{D}} \right\|_\infty. \quad (3.3.45)$$

We can obtain (3.3.43) in the same way. This completes the proof of Lemma 3.3.4. \blacksquare

Applying these bounds to (3.2.45), (3.2.50) and (3.2.53), we obtain the following bounds on the bootstrapping functions $\{g_i(p)\}_{i=1}^3$.

Lemma 3.3.5. *Suppose $r < 1$ and that $L_p, B_p, B'_p, \|\hat{W}_p/(1 - \hat{D})\|_\infty$ are so small that the two inequalities in (3.2.55) hold. Then, we have*

$$g_1(p) \leq 1 + L_p + \frac{B_p(p\|D\|_\infty + L_p)r}{1-r^2}, \quad (3.3.46)$$

$$g_2(p) \leq \left(1 - \frac{B_p^2(1+r^2)}{(1-r^2)^3} \left\| \frac{\hat{W}_p}{1 - \hat{D}} \right\|_\infty \right)^{-1}, \quad (3.3.47)$$

$$g_3(p) \leq \max\{g_2(p), 1\}^3 \times \left(\left(1 + \frac{3B_p}{2^d} \right) p + \left(B'_p + \frac{B_p^2}{(1-r^2)(1-r)^2} + \frac{B_p r^2(2-r^2)}{(1-r^2)^2} \right) \left\| \frac{\hat{W}_p}{1 - \hat{D}} \right\|_\infty \right)^2. \quad (3.3.48)$$

Proof. The bounds on $g_1(p)$ and $g_2(p)$ are easy; since $\hat{\Pi}_p(0) = \hat{\Pi}_p^{\text{even}}(0) - \hat{\Pi}_p^{\text{odd}}(0)$ and $-\hat{\Delta}_k \hat{\Pi}_p(0) = |\hat{\Delta}_k \hat{\Pi}_p^{\text{even}}(0)| - |\hat{\Delta}_k \hat{\Pi}_p^{\text{odd}}(0)|$, we obtain

$$g_1(p) \stackrel{(3.2.45)}{\leq} 1 + \hat{\Pi}_p^{\text{odd}}(0) \stackrel{(3.3.40)}{\leq} 1 + L_p + \frac{B_p(p\|D\|_\infty + L_p)r}{1-r^2}, \quad (3.3.49)$$

$$g_2(p) \stackrel{(3.2.50)}{\leq} \sup_k \left(1 - \frac{|\hat{\Delta}_k \hat{\Pi}_p^{\text{odd}}(0)|}{1 - \hat{D}(k)} \right)^{-1} \stackrel{(3.3.42)}{\leq} \left(1 - \frac{B_p^2(1+r^2)}{(1-r^2)^3} \left\| \frac{\hat{W}_p}{1 - \hat{D}} \right\|_\infty \right)^{-1}. \quad (3.3.50)$$

For $g_3(p)$, since $\hat{G}_p(k) = \hat{A}_p(k) \equiv 1/(1 - \hat{J}_p(k))$ for SAW and $|\hat{G}_p(k)| \leq g_2(p)\hat{S}_1(k) \equiv g_2(p)/(1 - \hat{D}(k))$, we obtain

$$\begin{aligned}
g_3(p) &\stackrel{(3.2.53)}{\leq} \sup_{k,l} \frac{1 - \hat{D}(k)}{\hat{U}(k,l)} \left(\frac{\hat{S}_1(l+k) + \hat{S}_1(l-k)}{2} \hat{S}_1(l) g_2(p)^2 \frac{|\hat{\Delta}_k \hat{J}_p(l)|}{1 - \hat{D}(k)} \right. \\
&\quad \left. + 4 \hat{S}_1(l+k) \hat{S}_1(l-k) g_2(p)^3 \frac{-\hat{\Delta}_l |\widehat{J}_p|(0)}{1 - \hat{D}(l)} \frac{-\hat{\Delta}_k |\widehat{J}_p|(0)}{1 - \hat{D}(k)} \right) \\
&\stackrel{(3.2.13)}{\leq} \max\{g_2(p), 1\}^3 \max \left\{ \sup_{k,l} \frac{|\hat{\Delta}_k \hat{J}_p(l)|}{1 - \hat{D}(k)}, \left(\sup_k \frac{-\hat{\Delta}_k |\widehat{J}_p|(0)}{1 - \hat{D}(k)} \right)^2 \right\}. \tag{3.3.51}
\end{aligned}$$

Since $J_p = pD + \Pi_p$ for SAW, we have

$$\begin{aligned}
\frac{|\hat{\Delta}_k \hat{J}_p(l)|}{1 - \hat{D}(k)} &= \frac{1}{1 - \hat{D}(k)} \left| \sum_x (1 - \cos k \cdot x) e^{il \cdot x} (pD(x) + \Pi_p(x)) \right| \\
&\leq \frac{1}{1 - \hat{D}(k)} \sum_x (1 - \cos k \cdot x) (pD(x) + \Pi_p^{\text{odd}}(x) + \Pi_p^{\text{even}}(x)) \\
&\leq p + \frac{|\hat{\Delta}_k \hat{\Pi}_p^{\text{even}}(0)|}{1 - \hat{D}(k)} + \frac{|\hat{\Delta}_k \hat{\Pi}_p^{\text{odd}}(0)|}{1 - \hat{D}(k)}, \tag{3.3.52}
\end{aligned}$$

which is larger than 1, since $p \geq 1$. It is easy to check that $-\hat{\Delta}_k |\widehat{J}_p|(0)/(1 - \hat{D}(k))$ obeys the same bound. Therefore, by using (3.3.42)–(3.3.43), we obtain

$$\begin{aligned}
g_3(p) &\leq \max\{g_2(p), 1\}^3 \left(p + \sup_k \frac{|\hat{\Delta}_k \hat{\Pi}_p^{\text{even}}(0)|}{1 - \hat{D}(k)} + \sup_k \frac{|\hat{\Delta}_k \hat{\Pi}_p^{\text{odd}}(0)|}{1 - \hat{D}(k)} \right)^2 \\
&\leq \max\{g_2(p), 1\}^3 \\
&\quad \times \left(\left(1 + \frac{3B_p}{2^d} \right) p + \left(B'_p + \frac{B_p^2}{(1-r^2)(1-r)^2} + \frac{B_p r^2 (2-r^2)}{(1-r^2)^2} \right) \left\| \frac{\hat{W}_p}{1 - \hat{D}} \right\|_\infty \right)^2, \tag{3.3.53}
\end{aligned}$$

as required. ■

Remark 3.3.6. If we do not use B'_p , then $g_3(p)$ is bounded as

$$g_3(p) \leq \max\{g_2(p), 1\}^3 \left(p + \left(\frac{B_p^2}{(1-r^2)(1-r)^2} + \frac{B_p}{(1-r^2)^2} \right) \left\| \frac{\hat{W}_p}{1 - \hat{D}} \right\|_\infty \right)^2, \tag{3.3.54}$$

which works in dimensions $d \geq 7$, but does not work in 6 dimension.

3.3.4 Bounds on diagrams in terms of random-walk quantities

In this subsection, we evaluate the diagrams for $p \in [1, p_c)$ and complete the proof of Propositions 3.2.4–3.2.5.

First, we evaluate the diagrams for $p \in (1, p_c)$ under the bootstrapping assumptions.

Lemma 3.3.7. *Let $d \geq 5$ and $p \in (1, p_c)$ and suppose that $g_i(p) \leq K_i$, $i = 1, 2, 3$, for some constants $\{K_i\}_{i=1}^3$. Then, we have*

$$L_p \leq K_1^2 K_2 \varepsilon_1, \quad B_p \leq K_1^2 K_2^2 \varepsilon_2, \quad B'_p \leq K_1^4 K_2^2 \varepsilon'_2, \quad (3.3.55)$$

$$\left\| \frac{\hat{W}_p}{1 - \hat{D}} \right\|_{\infty} \leq 5K_3(1 + 2\varepsilon_1 + \varepsilon_2). \quad (3.3.56)$$

Proof. The first two inequalities in (3.3.55) have already been explained in (3.2.62)–(3.2.63). Similarly, by using $g_i(p) \leq K_i$, $i = 1, 2$, we have

$$B'_p \leq p^4 \int_{\mathbb{T}^d} \hat{D}(k)^4 \hat{G}_p(k)^2 \frac{d^d k}{(2\pi)^d} \leq K_1^4 K_2^2 \underbrace{\int_{\mathbb{T}^d} \frac{\hat{D}(k)^4}{(1 - \hat{D}(k))^2} \frac{d^d k}{(2\pi)^d}}_{=(D^{*4} * S_1^{*2})(o)} = K_1^4 K_2^2 \varepsilon'_2. \quad (3.3.57)$$

For (3.3.56), we use $g_3(p) \leq K_3$ to obtain

$$0 \leq (1 - \cos k \cdot x) G_p(x) = \int_{\mathbb{T}^d} (-\hat{\Delta}_k \hat{G}_p(l)) e^{il \cdot x} \frac{d^d l}{(2\pi)^d} \leq K_3 \int_{\mathbb{T}^d} \hat{U}(k, l) \frac{d^d l}{(2\pi)^d}, \quad (3.3.58)$$

uniformly in x and k . Then, by (3.2.13) and using the Schwarz inequality, the right-hand side is further bounded by

$$5K_3(1 - \hat{D}(k)) \int_{\mathbb{T}^d} \hat{S}_1(l)^2 \frac{d^d l}{(2\pi)^d} = 5K_3(1 - \hat{D}(k)) S_1^{*2}(o). \quad (3.3.59)$$

Since $S_1^{*2}(o) = \sum_{n=0}^{\infty} (2n+1) D^{*2n}(o) = 1 + 2\varepsilon_1 + \varepsilon_2$ (see (3.2.3)), this completes the proof of Lemma 3.3.7. \blacksquare

Next, we evaluate the diagrams at $p = 1$ by using the trivial inequality $G_1(x) \leq S_1(x)$. Here, we do not need the bootstrapping assumptions.

Lemma 3.3.8. *Let $d \geq 5$ and $p = 1$. Then, we have*

$$L_1 \leq \varepsilon_1, \quad B_1 \leq \varepsilon_2, \quad B'_1 \leq \varepsilon'_2, \quad (3.3.60)$$

$$\left\| \frac{\hat{W}_1}{1 - \hat{D}} \right\|_{\infty} \leq 5(1 + 2\varepsilon_1 + \varepsilon_2). \quad (3.3.61)$$

Proof. The first two inequalities in (3.3.60) have already been explained in (3.2.60)–(3.2.61). Similarly, by the trivial inequality $G_1(x) \leq S_1(x)$, we have

$$B'_1 \leq \|D^{*4} * S_1^{*2}\|_{\infty} = \int_{\mathbb{T}^d} \frac{\hat{D}(k)^4}{(1 - \hat{D}(k))^2} \frac{d^d k}{(2\pi)^d} = \varepsilon'_2. \quad (3.3.62)$$

Also, by following the same line as (3.3.58)–(3.3.59), we obtain

$$\begin{aligned}
(1 - \cos k \cdot x)G_p(x) &\leq (1 - \cos k \cdot x)S_1(x) = \int_{\mathbb{T}^d} (-\hat{\Delta}_k \hat{S}_1(l)) e^{il \cdot x} \frac{d^d l}{(2\pi)^d} \\
&\leq \int_{\mathbb{T}^d} \hat{U}(k, l) \frac{d^d l}{(2\pi)^d} \\
&\leq 5(1 - \hat{D}(k))(1 + 2\varepsilon_1 + \varepsilon_2). \tag{3.3.63}
\end{aligned}$$

This completes the proof of (3.3.61). ■

Proof of Proposition 3.2.4. Since ε_1 and ε_2 are finite for $d \geq 5$ (see Table 3.1 in Section 3.2.1) and decreasing in d (because $D^{*2n}(o) \equiv \left(\binom{2n}{n} 2^{-2n}\right)^d$ on \mathbb{L}^d is decreasing in d), we have

$$r = \|D\|_\infty + L_1 + B_1 \stackrel{(3.3.60)}{\leq} 2^{-d} + \varepsilon_1 + \varepsilon_2 \leq \begin{cases} 0.257 & [d = 5], \\ 0.081 & [d \geq 6]. \end{cases} \tag{3.3.64}$$

In addition, by (3.3.40)–(3.3.43) and Lemma 3.3.8 (see also Table 3.2 in Section 3.3.2), we have

$$\sum_{n=1}^{\infty} \hat{\pi}_1^{(n)}(0) \leq \begin{cases} 0.066 & [d = 5], \\ 0.023 & [d \geq 6], \end{cases} \quad \sup_k \sum_{n=1}^{\infty} \frac{-\hat{\Delta}_k \hat{\pi}_1^{(n)}(0)}{1 - \hat{D}(k)} \leq \begin{cases} 1.331 & [d = 5], \\ 0.120 & [d \geq 6], \end{cases} \tag{3.3.65}$$

which imply that the inequalities in (3.2.55) hold for all $d \geq 6$ (but not for $d = 5$). Then, by Lemma 3.3.5, we obtain

$$g_1(1) \leq 1 + \varepsilon_1 + \frac{\varepsilon_2(2^{-d} + \varepsilon_1)r}{1 - r^2} \leq 1.021, \tag{3.3.66}$$

$$g_2(1) \leq \left(1 - 5(1 + 2\varepsilon_1 + \varepsilon_2) \frac{\varepsilon_2^2(1 + r^2)}{(1 - r^2)^3}\right)^{-1} \leq 1.012, \tag{3.3.67}$$

$$\begin{aligned}
g_3(1) &\leq (1.011)^3 \left(1 + \frac{3\varepsilon_2}{2^d} + 5(1 + 2\varepsilon_1 + \varepsilon_2) \left(\varepsilon_2' + \frac{\varepsilon_2^2}{(1 - r^2)(1 - r)^2} + \frac{\varepsilon_2 r^2(2 - r^2)}{(1 - r^2)^2}\right)\right)^2 \\
&\leq 1.301. \tag{3.3.68}
\end{aligned}$$

Proposition 3.2.4 holds as long as $K_1 > 1.021$, $K_2 > 1.012$ and $K_3 > 1.301$. ■

Proof of Proposition 3.2.5. Let

$$K_1 = K_2 = 1.03, \quad K_3 = 1.79, \tag{3.3.69}$$

so that Proposition 3.2.4 holds for $d \geq 6$. Using Table 3.1 in Section 3.2.1, we have

$$r \stackrel{(3.3.55)}{\leq} K_1 2^{-d} + K_1^2 K_2 \varepsilon_1 + K_1^2 K_2^2 \varepsilon_2 \leq 0.088. \tag{3.3.70}$$

In addition, by (3.3.40)–(3.3.43) and Lemma 3.3.7 (see also Table 3.2 in Section 3.3.2), we have

$$\sum_{n=1}^{\infty} \hat{\pi}_p^{(n)}(0) \leq 0.025, \quad \sup_k \sum_{n=1}^{\infty} \frac{-\hat{\Delta}_k \hat{\pi}_p^{(n)}(0)}{1 - \hat{D}(k)} \leq 0.257, \quad (3.3.71)$$

which imply that the inequalities in (3.2.55) hold. Then, similarly to (3.3.66)–(3.3.68), we obtain

$$g_1(p) \leq 1 + K_1^2 K_2 \varepsilon_1 + \frac{K_1^2 K_2^2 \varepsilon_2 (K_1 2^{-d} + K_1^2 K_2 \varepsilon_1) r}{1 - r^2} \leq 1.023 < K_1, \quad (3.3.72)$$

$$g_2(p) \leq \left(1 - 5K_3(1 + 2\varepsilon_1 + \varepsilon_2) \frac{K_1^4 K_2^4 \varepsilon_2^2 (1 + r^2)}{(1 - r^2)^3} \right)^{-1} \leq 1.026 < K_2, \quad (3.3.73)$$

$$\begin{aligned} g_3(p) &\leq (1.025)^3 \left(\left(1 + \frac{3K_1^2 K_2^2 \varepsilon_2}{2^d} \right) K_1 + 5K_3(1 + 2\varepsilon_1 + \varepsilon_2) \right. \\ &\quad \times \left. \left(K_1^4 K_2^2 \varepsilon_2' + \frac{K_1^4 K_2^4 \varepsilon_2^2}{(1 - r^2)(1 - r)^2} + \frac{K_1^2 K_2^2 \varepsilon_2 r^2 (2 - r^2)}{(1 - r^2)^2} \right) \right)^2 \\ &\leq 1.789 < K_3. \end{aligned} \quad (3.3.74)$$

This completes the proof of Proposition 3.2.5. ■

3.3.5 Further discussion

We have been able to prove convergence of the lace expansion for SAW on $\mathbb{L}^{d \geq 6}$ in full detail, in such a small number of pages, rather easily. This is due to the simple structure of the BCC lattice \mathbb{L}^d and the choice of the bootstrapping functions $\{g_i(p)\}_{i=1}^3$ (and thanks to the extra effort explained in the remark after Lemma 3.3.2). Of course, if we follow the same analysis as Hara and Slade [55, 56], we should be able to extend the result to 5 dimensions. But, then, the amount of work and the level of technicality would be almost the same, and it would not make the survey paper [49] attractive or accessible to beginners. Instead of following the analysis of [55, 56], we keep the material as simple as possible and just summarize elements by which we could improve our analysis. Those elements are the following.

1. Apparently, the largest contribution comes from $|\hat{\Delta}_k \hat{\pi}_p^{(2)}(0)|$. To improve its bound, we introduced an extra diagram, i.e., $B_p' \equiv \|(pD)^{*4} * G_p^{*2}\|_{\infty}$. As a result, we were able to improve the applicable range from $d \geq 7$ to $d \geq 6$. It is natural to guess that the introduction of longer bubbles, like $B_p^{(n)} \equiv \|(pD)^{*2n} * G_p^{*2}\|_{\infty}$, could result in the desired applicable range $d \geq 5$. Indeed, its RW counterpart $(D^{*2n} * S_1^{*2})(o)$ gets smaller as n increases. However, since $B_p^{(n)}$ has the exponentially growing factor p^{2n} , there must be an optimal $n_* \in \mathbb{N}$ at which $B_p^{(n)}$ attains its minimum. So far, our naive computation failed to achieve convergence of the lace expansion in $\mathbb{L}^{d \geq 5}$ by merely introducing $B_p^{(n)}$ up to $n = 3$.

2. The reason why we introduced B'_p is because the current bound on $\|\hat{W}_p/(1 - \hat{D})\|_\infty$ in (3.3.61) and (3.3.56) is not small. In particular, the relatively large factor 5 in (3.3.61) and (3.3.56) is due to the use of the Schwarz inequality, as explained in the proof of Lemma 3.2.7. Therefore, if we could achieve a better bound on (3.2.16) instead of (3.2.15), hopefully without using the Schwarz inequality, it would be of great help.
3. In (3.3.46)–(3.3.47), we discarded the contributions from $\hat{\Pi}_p^{\text{even}}(0)$ and $|\hat{\Delta}_k \hat{\Pi}_p^{\text{even}}(0)|$. By Lemma 3.3.2, we can speculate $\hat{\Pi}_p^{\text{even}}(0) \leq \hat{\Pi}_p^{\text{odd}}(0)$ and $|\hat{\Delta}_k \hat{\Pi}_p^{\text{even}}(0)| \geq |\hat{\Delta}_k \hat{\Pi}_p^{\text{odd}}(0)|$. This means that, if we include their effect into computation, then $g_1(p)$ could be much closer to 1 (see (3.2.45)) and $g_2(p)$ could be even smaller than 1 (see (3.2.50)), and as a result, we could achieve the desired applicable limit $d \geq 5$. However, to make use of those even terms, we must also control lower bounds on $g_1(p)$ and $g_2(p)$, and to do so, we need nontrivial lower bounds on the lace-expansion coefficients. Heading towards this direction would significantly increase the amount of work and technical details, as in [55, 56], which is against our motivation of the survey paper [49].
4. We evaluated $\hat{G}_p(k)$ by $\hat{S}_1(k) \equiv (1 - \hat{D}(k))^{-1}$ uniformly in $k \in \mathbb{T}^d$, i.e., in both infrared and ultraviolet regimes. However, doing so in the ultraviolet regime (i.e., bounding $G_p(x)$ by $S_1(x)$ for small x) is not efficient, and as a result, it requires d to be relatively large. To overcome this problem, we may want to incorporate the idea of ultraviolet regularization, first introduced in [8] for percolation. This approach has never been investigated in the previous lace-expansion work, but it could provide a natural way to analyze in dimensions close to d_c .

Chapter 4

The mean-field behavior for the quantum Ising model

4.1 Background for the quantum Ising model

In Section 2, we investigated phase transition and critical behavior for the classical Ising model. However, if we want to understand the real magnetic phenomena, we must take account of the quantum effect (and the Coulomb force) by means of quantum mechanics. We skip many physical motivation for the definition of the quantum Ising model since those are not issues we would like to address in this thesis. Although there are lots of quantum mechanical models (e.g., the quantum Heisenberg model [40]), we only focus on the d -dimensional transverse field quantum Ising model.

Our main interest is to investigate the quantum effect to phase transition or critical behavior. Since there must be a difference from the classical system, we are interested in where and how the quantum effect shows up (e.g., on the critical temperature and the critical exponents?). As explained in Chapter 1, one of the ways to identify the critical exponents is to derive the differential inequalities. The differential inequalities of the classical Ising model are derived by using the graphical representation called the random-current representation as introduced in Chapter 2.

There are two well-known graphical representations for the quantum Ising model. In [7] and [46], the random-current representation (and also the Fortuin-Kasteleyn representation) for the quantum Ising model were introduced. A key property for the random-current representation is the so-called switching lemma, see Lemma 2.3.6. However there was no switching lemma for the quantum setting in [7] and [46]. In [28], Crawford and Ioffe invented the switching lemma and derived the differential inequalities for the spontaneous magnetization.

In [17], Björnberg and Grimmett introduced the random-parity representation which is very similar to the random-current representation for the classical Ising model. This representation also possesses the switching lemma. They considered the space-time Ising model first and made the random-parity representation for that model. The physical quantities for the quantum Ising model can be the special case of ones for the space-time Ising model. Thus, they can show the results for the quantum Ising model as by-products of the space-time Ising model. In [16], Björnberg established an infrared bound

by assuming reflection-positivity and showed the mean-field behavior for the susceptibility by deriving the differential inequalities and using its infrared bound to show the finiteness of the bubble-diagram. He showed that the bubble-diagram is finite either $\beta < \infty$ and $d > 4$ or $\beta = \infty$ and $d > 3$, where $\beta > 0$ is the inverse temperature, which means that the upper critical dimension are different between positive temperature and zero temperature.

Both representations are defined on the continuous time line and obtained based on Poisson point processes. The reason why we consider the continuous time line comes from the definition of the space-time Ising model for the random-parity representation, and the Lie-Trotter formula for the random-current representation for the quantum Ising model. Thus, the representations are quite similar but somehow different from the classical random-current representation on a discrete lattice.

In [17], [16] and [28], they consider the following Hamiltonian,

$$\hat{H}_{\lambda,h,\delta}(\hat{\sigma}) = -\lambda \sum_{x,y \in \Lambda} \hat{\sigma}_x^{(3)} \hat{\sigma}_y^{(3)} - h \sum_{x \in \Lambda} \hat{\sigma}_x^{(3)} - \delta \sum_{x \in \Lambda} \hat{\sigma}_x^{(1)}, \quad (4.1.1)$$

with the parameter of coupling constants $\lambda > 0$, the intensity of the external magnetic field $h > 0$ and the quantum effect $\delta \geq 0$ (see the next section for the precise definitions). They are interested in the critical behavior with varying the ratio between the parameters λ and δ for fixed temperature $\beta > 0$. However, we are also interested in critical behavior when varying the temperature. We would like to investigate the critical temperature with fixing the quantum effect $\delta \geq 0$. From the point of view of the classical models, the estimate of the critical temperature in dimensions above the upper critical dimension can be obtained by the lace expansion analysis [62]. Thus, our final goal is to invent the lace expansion for the quantum Ising model and to analyze the behavior of the critical temperature, which would be the first application of the lace expansion for the quantum mechanical models. This is an ongoing project with Kamijima and Sakai.

Before considering the lace expansion of the quantum Ising model, it is important to check the mean-field behaviors for some order parameters with varying the temperature. There is a well-known result by Suzuki and Trotter [87], which tells us that we can regard the d -dimensional quantum Ising model as the $(d+1)$ -dimensional classical one with adjusting the coupling constants. Thus, we can use the random-current representation of the classical Ising model. We will introduce the detailed setting in the next section and prove the mean-field behavior of the susceptibility by using the Suzuki-Trotter transformation in the analogical strategy of [2, 3, 6].

4.2 Setting and preliminaries

4.2.1 Definition of the quantum Ising model

We consider the quantum Ising model on a finite set $\Lambda \subset \mathbb{Z}^d$. We define the Pauli spin-1/2 matrices as, for any $x \in \Lambda$,

$$\hat{\sigma}_x^{(1)} = \begin{pmatrix} 0 & 1 \\ 1 & 0 \end{pmatrix}, \quad \hat{\sigma}_x^{(3)} = \begin{pmatrix} 1 & 0 \\ 0 & -1 \end{pmatrix}, \quad (4.2.1)$$

(although there is one more matrix $\hat{\sigma}_x^{(2)}$, it does not feature in the definition of the quantum Ising model) and also the Hamiltonian of the quantum Ising model as

$$\hat{H}_{h,\delta}(\hat{\sigma}) = - \sum_{x,y \in \Lambda} J_{x,y} \hat{\sigma}_x^{(3)} \hat{\sigma}_y^{(3)} - h \sum_{x \in \Lambda} \hat{\sigma}_x^{(3)} - \delta \sum_{x \in \Lambda} \hat{\sigma}_x^{(1)}, \quad (4.2.2)$$

where $\{J_{x,y}\}$ is a collection of translation-invariant and summable coupling constants between two Pauli-spins, $h > 0$ is the intensity of the external magnetic field, and $\delta \geq 0$ is a parameter for the intensity of the transverse-field which represents the quantum effect. We define the correlation function of an operator \hat{A} on the Hilbert space $\mathcal{H} = \bigotimes_{x \in \Lambda} \mathbb{C}^2$ as

$$\langle \hat{A} \rangle_{\beta,h,\delta;\Lambda} = \frac{1}{Z_{\beta,h,\delta;\Lambda}} \text{Tr}[\hat{A} e^{-\beta \hat{H}_{h,\delta}(\hat{\sigma})}], \quad (4.2.3)$$

where $Z_{\beta,h,\delta;\Lambda}$ is the partition function defined by $\text{Tr}[e^{-\beta \hat{H}_{h,\delta}(\hat{\sigma})}]$ and $\beta > 0$ is a parameter for the inverse temperature.

We define the free-energy density on a finite set Λ and the infinite-volume limit of it by

$$f_{\beta,h,\delta;\Lambda} = -\frac{1}{\beta} \frac{1}{|\Lambda|} \log Z_{\beta,h,\delta;\Lambda}, \quad f_{\beta,h,\delta} = \lim_{\Lambda \uparrow \mathbb{Z}^d} f_{\beta,h,\delta;\Lambda}, \quad (4.2.4)$$

where $|\Lambda|$ is the cardinality of a finite set Λ . The basic quantity is the magnetization defined by

$$m(\beta, h, \delta) = -\frac{\partial}{\partial h} f_{\beta,h,\delta}. \quad (4.2.5)$$

We also define the spontaneous magnetization by

$$m_s(\beta, \delta) = \lim_{h \downarrow 0} m(\beta, h, \delta). \quad (4.2.6)$$

The main quantity we will investigate is the susceptibility $\chi(\beta, \delta)$ defined by

$$\chi(\beta, \delta) = \lim_{h \downarrow 0} \frac{\partial}{\partial h} m(\beta, h, \delta) = -\lim_{h \downarrow 0} \frac{\partial^2}{\partial h^2} f_{\beta,h,\delta}. \quad (4.2.7)$$

We have defined some physical quantities based on the classical statistical mechanics. To analyze those quantities with the quantum effect $\delta \geq 0$, we might think that whether we can still use the same strategy as the classical one. The Suzuki-Trotter transformation as below enables us to do that.

4.2.2 The Suzuki-Trotter transformation

The Suzuki-Trotter (ST) transformation [87] is a well-know result for the quantum Ising model. By using the ST transformation, we can regard the quantum Ising model on \mathbb{Z}^d as the classical Ising model on $\mathbb{Z}^d \times (\mathbb{N} \cup \{0\})$ with ferromagnetic coupling constants between two classical spins on $\mathbb{Z}^d \times (\mathbb{N} \cup \{0\})$. Let $[l] = \{0, 1, \dots, l-1\}$ be a torus with circumference l .

Proposition 4.2.1 (The Suzuki-Trotter transformation[87]).

$$Z_{\beta,h,\delta;\Lambda} = \lim_{l \uparrow \infty} \left(\frac{1}{2} \sinh \frac{2\beta\delta}{l} \right)^{\frac{l|\Lambda|}{2}} \sum_{\boldsymbol{\sigma} = \{\sigma_{x,t}\}_{x \in \Lambda, t \in [l]}} e^{-H^{ST}(\boldsymbol{\sigma})}, \quad (4.2.8)$$

where $H^{ST}(\boldsymbol{\sigma})$ for $\boldsymbol{\sigma} \in \{\pm 1\}^{\Lambda \times [l]}$ is defined by

$$H^{ST}(\boldsymbol{\sigma}) = - \sum_{x,y \in \Lambda} \sum_{t \in [l]} \frac{\beta J_{x,y}}{l} \sigma_{x,t} \sigma_{y,t} - \sum_{x \in \Lambda} \sum_{t \in [l]} \frac{\beta h}{l} \sigma_{x,t} - \sum_{x \in \Lambda} \sum_{t \in [l]} K_{\beta,\delta,l} \sigma_{x,t} \sigma_{x,t+1}, \quad (4.2.9)$$

and

$$K_{\beta,\delta,l} = \frac{1}{2} \log \coth \frac{\beta\delta}{l}. \quad (4.2.10)$$

Moreover,

$$\langle \hat{\sigma}_o^{(3)} \rangle_{\beta,h,\delta;\Lambda} = \lim_{l \uparrow \infty} \langle \sigma_{o,0} \rangle_{\beta,h,\delta;\Lambda,l} := \lim_{l \uparrow \infty} \frac{\sum_{\boldsymbol{\sigma}} \sigma_{o,0} e^{-H^{ST}(\boldsymbol{\sigma})}}{\sum_{\boldsymbol{\sigma}} e^{-H^{ST}(\boldsymbol{\sigma})}}. \quad (4.2.11)$$

$$\langle \hat{\sigma}_o^{(3)} \hat{\sigma}_x^{(3)} \rangle_{\beta,h,\delta;\Lambda} = \lim_{l \uparrow \infty} \langle \sigma_{o,0} \sigma_{x,0} \rangle_{\beta,h,\delta;\Lambda,l} := \lim_{l \uparrow \infty} \frac{\sum_{\boldsymbol{\sigma}} \sigma_{o,0} \sigma_{x,0} e^{-H^{ST}(\boldsymbol{\sigma})}}{\sum_{\boldsymbol{\sigma}} e^{-H^{ST}(\boldsymbol{\sigma})}}. \quad (4.2.12)$$

Proof of Proposition 4.2.1. We first show the identity for $Z_{\beta,h,\delta;\Lambda}$ in (4.2.8). We introduce the following notation for simplicity,

$$\hat{H}_{h,\delta}^c(\hat{\sigma}) = - \sum_{x,y \in \Lambda} J_{x,y} \hat{\sigma}_x^{(3)} \hat{\sigma}_y^{(3)} - h \sum_{x \in \Lambda} \hat{\sigma}_x^{(3)}, \quad \hat{H}_{h,\delta}^q(\hat{\sigma}) = -\delta \sum_{x \in \Lambda} \hat{\sigma}_x^{(1)}, \quad (4.2.13)$$

so that

$$\hat{H}_{h,\delta}(\hat{\sigma}) = \hat{H}_{h,\delta}^c(\hat{\sigma}) + \hat{H}_{h,\delta}^q(\hat{\sigma}). \quad (4.2.14)$$

By using the Lie-Trotter product formula,

$$\begin{aligned} Z_{\beta,h,\delta;\Lambda} &= \lim_{l \uparrow \infty} \text{Tr} \left[\left(e^{-\frac{\beta}{l} \hat{H}_{h,\delta}^c(\hat{\sigma})} e^{-\frac{\beta}{l} \hat{H}_{h,\delta}^q(\hat{\sigma})} \right)^l \right] \\ &= \lim_{l \uparrow \infty} \sum_{\Psi_0} \left\langle \Psi_0 \left| \left(e^{-\frac{\beta}{l} \hat{H}_{h,\delta}^c(\hat{\sigma})} e^{-\frac{\beta}{l} \hat{H}_{h,\delta}^q(\hat{\sigma})} \right)^l \right| \Psi_0 \right\rangle, \end{aligned} \quad (4.2.15)$$

where $\langle \cdot |$ and $|\cdot \rangle$ are bra and ket vectors, respectively, and $\langle \cdot | \cdot \rangle$ is an inner product on $\mathcal{H} = \bigotimes_{x \in \Lambda} \mathbb{C}^2$. We choose Ψ as an orthonormal basis on \mathcal{H} , defined by $\bigotimes_{x \in \Lambda} \psi_{\sigma_{x,0}}$ for $\sigma_{x,0} \in \{\pm 1\}$, and $\psi_{+1} = {}^t(1, 0)$ and $\psi_{-1} = {}^t(0, -1)$, respectively. Note that $\psi_{\pm 1}$ are the eigenvector of $\hat{\sigma}_x^{(3)}$ corresponding to eigenvalues ± 1 , respectively. Next, we use the identity

$\sum_{\Psi_j} |\Psi_j\rangle \langle \Psi_j| = I$ for $j = 1, \dots, l-1$, where I is an identity operator. Then, the sum at the right-hand side in (4.2.15) becomes

$$\sum_{\Psi_0, \dots, \Psi_{l-1}} \langle \Psi_0 | e^{-\frac{\beta}{l} \hat{H}_{h,\delta}^c(\hat{\sigma})} e^{-\frac{\beta}{l} \hat{H}_{h,\delta}^q(\hat{\sigma})} | \Psi_1 \rangle \langle \Psi_1 | e^{-\frac{\beta}{l} \hat{H}_{h,\delta}^c(\hat{\sigma})} e^{-\frac{\beta}{l} \hat{H}_{h,\delta}^q(\hat{\sigma})} | \Psi_2 \rangle \langle \Psi_2 | \dots \\ \dots | \Psi_{l-1} \rangle \langle \Psi_{l-1} | e^{-\frac{\beta}{l} \hat{H}_{h,\delta}^c(\hat{\sigma})} e^{-\frac{\beta}{l} \hat{H}_{h,\delta}^q(\hat{\sigma})} | \Psi_0 \rangle. \quad (4.2.16)$$

Noting that Ψ_0 is a family of eigenvectors of $\hat{\sigma}_x^{(3)}$, the first factor in the above sum equals

$$\langle \Psi_0 | e^{-\frac{\beta}{l} \hat{H}_{h,\delta}^c(\hat{\sigma})} e^{-\frac{\beta}{l} \hat{H}_{h,\delta}^q(\hat{\sigma})} | \Psi_1 \rangle \\ = \exp \left(- \sum_{x,y \in \Lambda} \sum_{t \in [l]} \frac{\beta J_{x,y}}{l} \sigma_{x,t} \sigma_{y,t} - \sum_{x \in \Lambda} \sum_{t \in [l]} \frac{\beta h}{l} \sigma_{x,t} \right) \langle \Psi_0 | e^{-\frac{\beta}{l} \hat{H}_{h,\delta}^q(\hat{\sigma})} | \Psi_1 \rangle. \quad (4.2.17)$$

The second factor in (4.2.17) becomes

$$\prod_{x \in \Lambda} \langle \Psi_0 | e^{\frac{\beta \delta}{l} \hat{\sigma}_x^{(1)}} | \Psi_1 \rangle = \prod_{x \in \Lambda} \left(\sum_{k: \text{even}} \frac{(\frac{\beta \delta}{l})^k}{k!} \delta_{\sigma_{x,0}, \sigma_{x,1}} + \sum_{k: \text{odd}} \frac{(\frac{\beta \delta}{l})^k}{k!} \delta_{\sigma_{x,0}, -\sigma_{x,1}} \right) \\ = \prod_{x \in \Lambda} \left(\cosh \frac{\beta \delta}{l} \delta_{\sigma_{x,0}, \sigma_{x,1}} + \sinh \frac{\beta \delta}{l} \delta_{\sigma_{x,0}, -\sigma_{x,1}} \right) \\ = \prod_{x \in \Lambda} \frac{e^{\frac{\beta \delta}{l} + \sigma_{x,0} \sigma_{x,1}} e^{-\frac{\beta \delta}{l}}}{2}. \quad (4.2.18)$$

Then we can find $a = \left(\frac{1}{2} \sinh \frac{2\beta \delta}{l} \right)^{1/2}$ and $b = \frac{1}{2} \log \coth \frac{\beta \delta}{l}$ such that,

$$\frac{e^{\frac{\beta \delta}{l} + \sigma_{x,0} \sigma_{x,1}} e^{-\frac{\beta \delta}{l}}}{2} = a e^{b \sigma_{x,0} \sigma_{x,1}}. \quad (4.2.19)$$

The other factors in (4.2.16) are calculated in the same way and then we obtain (4.2.8). For the ST transformation for correlation functions of a single spin in (4.2.11), the slight difference is just replacing the first factor in (4.2.16) by $\langle \Psi_0 | \hat{\sigma}_o^{(3)} e^{-\frac{\beta}{l} \hat{H}_{h,\delta}^c(\hat{\sigma})} e^{-\frac{\beta}{l} \hat{H}_{h,\delta}^q(\hat{\sigma})} | \Psi_1 \rangle$. Thus, we just have $\sigma_{o,0}$ in front of the exponential term in (4.2.17). To obtain the ST transformation for correlation functions of two spins in (4.2.12) can be treated in the same way. This completes the proof of Proposition 4.2.1. \blacksquare

4.2.3 The random-current representation, the source-switching lemma and the correlation inequalities

We introduce the random-current representation in the current setting. A current configuration $\mathbf{n} \equiv \{n_b\}$ is a set of nonnegative integers on bonds $b \in \mathbb{B}_{\Lambda,l} \equiv \{\{X, Y\} \subset \Lambda \times [l] : J_{u,v} > 0\}$ or $B \in \mathbb{G}_{\Lambda,l} \equiv \{\{X, g\} : X \in \Lambda \times [l]\}$, where g is an imaginary ghost site. Given a current configuration \mathbf{n} , we define the source set $\partial \mathbf{n}$ as

$$\partial \mathbf{n} = \left\{ V \in \Lambda \times [l] \cup \{g\} : \sum_{b \ni V} n_b \text{ is odd} \right\}, \quad (4.2.20)$$

and the weight functions $w(\mathbf{n})$ as

$$w(\mathbf{n}) = \prod_{b \in \mathbb{B}_{\Lambda, l}} \frac{(\tilde{J}_b)^{n_b}}{n_b!} \prod_{b' \in \mathbb{G}_{\Lambda, l}} \frac{(\beta h/l)^{n_{b'}}}{n_{b'}!}, \quad (4.2.21)$$

where

$$\tilde{J}_b = \begin{cases} \frac{\beta J_{x,y}}{l} & \text{if } b = \{(x, t), (y, t)\}, \\ K_{\beta, \delta, l} & \text{if } b = \{(x, t), (x, t+1)\}. \end{cases} \quad (4.2.22)$$

For any subset $A \subset \Lambda \times [l]$, we define $\sigma_A := \prod_{X \in A} \sigma_X$. We omit the dependance of the parameters for abbreviation, e.g., $\langle\langle \sigma_A \rangle\rangle = \langle\langle \sigma_A \rangle\rangle_{\beta, \delta; \Lambda, l}$. Then, we obtain the following random current representation.

For any subsets $A, B \subset \Lambda \times [l]$ such that $|A|$ is odd and $|B|$ is even,

$$\sum_{\sigma} e^{-H^{\text{ST}}(\sigma)} = 2^{l|\Lambda|} \underbrace{\sum_{\partial \mathbf{n} = \emptyset} w(\mathbf{n})}_{=: \tilde{Z}}, \quad \langle\langle \sigma_A \rangle\rangle = \sum_{\partial \mathbf{n} = A \cup \{g\}} \frac{w(\mathbf{n})}{\tilde{Z}}, \quad \langle\langle \sigma_B \rangle\rangle = \sum_{\partial \mathbf{n} = B} \frac{w(\mathbf{n})}{\tilde{Z}}. \quad (4.2.23)$$

Given a current configuration $\mathbf{n} = \{n_b\}$, we say that X is \mathbf{n} -connected to Y , denoted $X \xleftrightarrow{\mathbf{n}} Y$ if either $X = Y \in \Lambda \times [l] \cup \{g\}$ or there is a path from X to Y consisting of bonds $b \in \mathbb{B}_{\Lambda, l} \cup \mathbb{G}_{\Lambda, l}$ with $n_b > 0$.

The most important feature of the random-current representation is the so-called source-switching lemma (e.g., [79, Lemma 2.3]). We state the version we use in this section. This is an immediate consequence from the source-switching lemma (but we just call this lemma the source-switching lemma).

Lemma 4.2.2 (Consequence from the source-switching lemma, [79]). *For any subset $A \subset \Lambda \times [l] \cup \{g\}$, any $X, Y \in \Lambda \times [l]$ and any function f on current configurations,*

$$\sum_{\substack{\partial \mathbf{n} = A \\ \partial \mathbf{m} = \emptyset}} w(\mathbf{n}) w(\mathbf{m}) \mathbb{1}\{X \xleftrightarrow{\mathbf{n} + \mathbf{m}} Y\} f(\mathbf{n} + \mathbf{m}) = \sum_{\substack{\partial \mathbf{n} = A \Delta \{X\} \Delta \{Y\} \\ \partial \mathbf{m} = \{X\} \Delta \{Y\}}} w(\mathbf{n}) w(\mathbf{m}) f(\mathbf{n} + \mathbf{m}). \quad (4.2.24)$$

For a proof, we refer to [79, Lemma 2.3].

Next, we list up the some correlation inequalities related to this thesis. We just abbreviate the dependance of Λ and l in correlation functions in order to simplify their notations, e.g., $\langle\langle \sigma_A \rangle\rangle_{\beta, \delta} = \langle\langle \sigma_A \rangle\rangle_{\beta, \delta; \Lambda, l}$.

Proposition 4.2.3 (The Griffiths 1st inequality [41],[42],[43]). *For any subset $A \subset \Lambda \times [l]$,*

$$\langle\langle \sigma_A \rangle\rangle \geq 0. \quad (4.2.25)$$

Proof. By using the random-current representation in (4.2.23), we can immediately show the non-negativity of the correlation function since the weight function $w(\mathbf{n})$ is non-negative. ■

Proposition 4.2.4 (The Griffiths 2nd inequality [41],[42],[43]). *For any subset $A, B \subset \Lambda \times [l]$,*

$$\langle\langle \sigma_A; \sigma_B \rangle\rangle \geq 0, \quad (4.2.26)$$

where $\langle\langle f; g \rangle\rangle := \langle\langle fg \rangle\rangle - \langle\langle f \rangle\rangle \langle\langle g \rangle\rangle$ called a truncated correlation function.

Proof. We give a sketch proof only for the case $A = \{X, Y\}$ and $B = \{Z, W\}$ for $X, Y, Z, W \in \Lambda \times [l]$. By using the random-current representation in (4.2.23) and the source-switching lemma (4.2.24),

$$\langle\langle \sigma_X \sigma_Y; \sigma_Z \sigma_W \rangle\rangle = \sum_{\substack{\partial \mathbf{n} = \{X\} \Delta \{Y\} \Delta \{Z\} \Delta \{W\} \\ \partial \mathbf{m} = \emptyset}} \frac{w(\mathbf{n})w(\mathbf{m})}{\tilde{Z}^2} \underbrace{(1 - \mathbb{1}[Z \xleftrightarrow{\mathbf{n}+\mathbf{m}} W])}_{\geq 0}. \quad (4.2.27)$$

Thus, the desired inequality holds by the non-negativity of the weight function. \blacksquare

Proposition 4.2.5 (Lebowitz' inequality [68]). *For $X, Y, Z, W \in \Lambda \times [l]$,*

$$\langle\langle \sigma_X \sigma_Y; \sigma_Z \sigma_W \rangle\rangle \leq \langle\langle \sigma_X \sigma_Z \rangle\rangle \langle\langle \sigma_Y \sigma_W \rangle\rangle + \langle\langle \sigma_X \sigma_W \rangle\rangle \langle\langle \sigma_Y \sigma_Z \rangle\rangle. \quad (4.2.28)$$

For a proof, we refer to [68]. See also the proof of Lemma 4.3.2 in the next section.

Proposition 4.2.6 (The Griffiths-Hurst-Sherman inequality [44]). *For $X, Y, Z \in \Lambda \times [l]$,*

$$\begin{aligned} & \langle\langle \sigma_X \sigma_Y \sigma_Z \rangle\rangle - \langle\langle \sigma_X \rangle\rangle \langle\langle \sigma_Y \sigma_Z \rangle\rangle - \langle\langle \sigma_Y \rangle\rangle \langle\langle \sigma_X \sigma_Z \rangle\rangle \\ & - \langle\langle \sigma_Z \rangle\rangle \langle\langle \sigma_X \sigma_Y \rangle\rangle + 2 \langle\langle \sigma_X \rangle\rangle \langle\langle \sigma_Y \rangle\rangle \langle\langle \sigma_Z \rangle\rangle \geq 0. \end{aligned} \quad (4.2.29)$$

For a proof, we refer to [44].

Proposition 4.2.7 (The Aizenman-Graham inequality [6]). *For $X, Y, Z, W \in \Lambda \times [l]$,*

$$\begin{aligned} \langle\langle \sigma_X \sigma_Y; \sigma_Z \sigma_W \rangle\rangle & \geq \langle\langle \sigma_X \sigma_Z \rangle\rangle \langle\langle \sigma_Y \sigma_W \rangle\rangle + \langle\langle \sigma_X \sigma_W \rangle\rangle \langle\langle \sigma_Y \sigma_Z \rangle\rangle \\ & - \sum_{U, V \in \Lambda \times [l]} \tanh \tilde{J}_{U, V} \langle\langle \sigma_X \sigma_Y; \sigma_U \sigma_V \rangle\rangle \langle\langle \sigma_Z \sigma_V \rangle\rangle \langle\langle \sigma_W \sigma_V \rangle\rangle \\ & - \langle\langle \sigma_X \sigma_Y \rangle\rangle \langle\langle \sigma_X \sigma_Z \rangle\rangle \langle\langle \sigma_X \sigma_W \rangle\rangle - \langle\langle \sigma_X \sigma_Y \rangle\rangle \langle\langle \sigma_Y \sigma_Z \rangle\rangle \langle\langle \sigma_Y \sigma_W \rangle\rangle. \end{aligned} \quad (4.2.30)$$

For a proof, we refer to [6] and [58].

4.2.4 The magnetization and the susceptibility

First, we rewrite the definition of the magnetization $m(\beta, h, \delta)$ as follows.

Proposition 4.2.8. *For any $\beta, h > 0$ and $\delta \geq 0$,*

$$m(\beta, h, \delta) = \lim_{\Lambda \uparrow \mathbb{Z}^d} \frac{1}{|\Lambda|} \sum_{x \in \Lambda} \langle \hat{\sigma}_x^{(3)} \rangle_{\beta, h, \delta; \Lambda}. \quad (4.2.31)$$

Proof. First, we need to assure that we can change the order between the derivative with respect to h and the limit of Λ . By the ST transformation for the partition function in Proposition 4.2.1, we can regard the partition function as one of the classical and ferromagnetic Ising model. By using the continuity of a logarithmic function and noting that the constant factor in front of the sum over spin configurations σ in (4.2.8) does not depend on h , the second derivative of $f_{\beta,h,\delta;\Lambda}$ with respect to h is non-positive by the Griffiths 2nd inequality in Proposition 4.2.4. Thus, the function $f_{\beta,h,\delta;\Lambda}$ is convex with respect to h . Therefore, we can assure the change of the order between h and Λ and then,

$$m(\beta, h, \delta) = -\lim_{\Lambda \uparrow \mathbb{Z}^d} \frac{\partial}{\partial h} f_{\beta,h,\delta;\Lambda} = \lim_{\Lambda \uparrow \mathbb{Z}^d} \frac{1}{\beta} \frac{1}{|\Lambda|} \frac{\frac{\partial}{\partial h} Z_{\beta,h,\delta;\Lambda}}{Z_{\beta,h,\delta;\Lambda}}. \quad (4.2.32)$$

The derivative with respect to h in the numerator in the left-hand side above is

$$\begin{aligned} \frac{\partial}{\partial h} Z_{\beta,h,\delta;\Lambda} &= \text{Tr} \left[\frac{\partial}{\partial h} e^{-\beta \hat{H}_{h,\delta}} \right] = \text{Tr} \left[\sum_{n=0}^{\infty} \frac{\beta^n}{n!} \frac{\partial}{\partial h} (-\hat{H}_{h,\delta})^n \right] \\ &= \text{Tr} \left[\sum_{n=1}^{\infty} \frac{\beta^n}{n!} \sum_{k=1}^n (-\hat{H}_{h,\delta})^{k-1} \frac{\partial}{\partial h} (-\hat{H}_{h,\delta}) (-\hat{H}_{h,\delta})^{n-k} \right] \\ &= \sum_{n=1}^{\infty} \frac{\beta^n}{n!} \sum_{k=1}^n \text{Tr} \left[\sum_{x \in \Lambda} \hat{\sigma}_x^{(3)} (-\hat{H}_{h,\delta})^{n-1} \right] \\ &= \beta \sum_{x \in \Lambda} \text{Tr} [\hat{\sigma}_x^{(3)} e^{-\beta \hat{H}_{h,\delta}}], \end{aligned} \quad (4.2.33)$$

where, in the fourth equality, we have used the fact that the trace is invariant under cyclic permutations. Thus, the magnetization (4.2.32) is equal to

$$\lim_{\Lambda \uparrow \mathbb{Z}^d} \frac{1}{|\Lambda|} \sum_{x \in \Lambda} \frac{1}{Z_{\beta,h,\delta;\Lambda}} \text{Tr} [\hat{\sigma}_x^{(3)} e^{-\beta \hat{H}_{h,\delta}}] = \lim_{\Lambda \uparrow \mathbb{Z}^d} \frac{1}{|\Lambda|} \sum_{x \in \Lambda} \langle \hat{\sigma}_x^{(3)} \rangle_{\beta,h,\delta;\Lambda}. \quad (4.2.34)$$

■

Remark 4.2.9. If we choose Λ as a torus, by its periodicity

$$m(\beta, h, \delta) = \lim_{\Lambda \uparrow \mathbb{Z}^d} \frac{1}{|\Lambda|} \sum_{x \in \Lambda} \langle \hat{\sigma}_x^{(3)} \rangle_{\beta,h,\delta;\Lambda} = \lim_{\Lambda \uparrow \mathbb{Z}^d} \langle \hat{\sigma}_o^{(3)} \rangle_{\beta,h,\delta;\Lambda}. \quad (4.2.35)$$

From now on, we assume that Λ is a torus as mentioned in the above remark. In principle, we define the following quantities related to the susceptibility $\chi(\beta, \delta)$;

$$\chi_{\Lambda,l}^P(\beta, \delta) := \beta \sum_{x \in \Lambda} \frac{1}{l} \sum_{t \in [l]} \langle \langle \sigma_{o,0} \sigma_{x,t} \rangle \rangle_{\beta,\delta;\Lambda,l}, \quad \chi^P(\beta, \delta) := \lim_{\Lambda \uparrow \mathbb{Z}^d} \lim_{l \uparrow \infty} \chi_{\Lambda,l}^P(\beta, \delta), \quad (4.2.36)$$

where the superscript P means that the both domains of the space and time are periodic.

Now we are prepared to define the critical temperature $\beta_c = \beta_c(\delta)$ and the critical exponent γ for the periodic susceptibility $\chi^P(\beta, \delta)$ as,

$$\beta_c(\delta) = \inf \{ \beta > 0 : \chi^P(\beta, \delta) = \infty \}, \quad \chi^P(\beta, \delta) \underset{\beta \uparrow \beta_c}{\asymp} (\beta_c - \beta)^{-\gamma}, \quad (4.2.37)$$

where $f \asymp g$ means that f is bounded above and below by g with some constants in the prescribed limit. If we know the monotonicity of $\chi^P(\beta, \delta)$ with respect to β , then $\beta_c(\delta) = \sup\{\beta > 0 : \chi^P(\beta, \delta) < \infty\}$. Unfortunately, we have only proved the monotonicity for sufficiently small $\delta \geq 0$.

Although it seems to be weird to define such a periodic susceptibility, the reason comes from the technical reason about the change of order among some limits, and the analogy of the classical Ising model. In fact, we can obtain the equality between the susceptibilities $\chi(\beta, \delta)$ and $\chi^P(\beta, \delta)$ in the high temperature phase $\beta < \beta_c$ as follows.

Proposition 4.2.10. *For any $\beta < \beta_c$ and $\delta \geq 0$,*

$$\chi(\beta, \delta) = \chi^P(\beta, \delta). \quad (4.2.38)$$

Proof. By Proposition 4.2.8 and Remark 4.2.9, we obtain

$$\chi(\beta, \delta) = \lim_{h \downarrow 0} \frac{\partial}{\partial h} \lim_{\Lambda \uparrow \mathbb{Z}^d} \langle \hat{\sigma}_o^{(3)} \rangle_{\beta, h, \delta; \Lambda}. \quad (4.2.39)$$

Here, we use the ST transformation for $\langle \hat{\sigma}_o^{(3)} \rangle_{\beta, h, \delta; \Lambda}$,

$$\frac{\partial}{\partial h} \lim_{\Lambda \uparrow \mathbb{Z}^d} \lim_{l \uparrow \infty} \langle \sigma_{o,0} \rangle_{\beta, h, \delta; \Lambda, l}. \quad (4.2.40)$$

Note that the function $\langle \sigma_{o,0} \rangle_{\beta, h, \delta; \Lambda, l}$ is a classical and ferromagnetic single spin expectation. We would like to change the order between the derivative with respect to h and the limits of Λ and l . If we take the derivative of $\langle \sigma_{o,0} \rangle_{\beta, h, \delta; \Lambda, l}$ with respect to h at first,

$$\frac{\partial}{\partial h} \langle \sigma_{o,0} \rangle_{\beta, h, \delta; \Lambda, l} = \sum_{x \in \Lambda} \sum_{t \in [l]} \frac{\beta}{l} \langle \sigma_{o,0}; \sigma_{x,t} \rangle_{\beta, h, \delta; \Lambda, l}. \quad (4.2.41)$$

By the trivial inequality $\langle \sigma_{o,0}; \sigma_{x,t} \rangle_{\beta, h, \delta; \Lambda, l} \leq 1$, the right-hand side in (4.2.41) is uniformly bounded above in h and l . Thus, we can assure the change of order between h and l . Since the function $\langle \sigma_{o,0} \rangle_{\beta, h, \delta; \Lambda, l}$ is convex with respect to h by the GHS inequality in Proposition 4.2.6, we can also assure the change of order between h and Λ . Therefore, we obtain

$$\chi(\beta, \delta) = \beta \lim_{h \downarrow 0} \lim_{\Lambda \uparrow \mathbb{Z}^d} \lim_{l \uparrow \infty} \sum_{x \in \Lambda} \frac{1}{l} \sum_{t \in [l]} \langle \sigma_{o,0}; \sigma_{x,t} \rangle_{\beta, h, \delta; \Lambda, l}. \quad (4.2.42)$$

Moreover, we would like to change the order between the limits of h and of Λ and l . Again by the GHS inequality in Proposition 4.2.6, the truncated two-point function is a monotonically decreasing function with respect to h . Therefore, the right-hand side in (4.2.42) is bounded above by

$$\beta \lim_{h \downarrow 0} \lim_{\Lambda \uparrow \mathbb{Z}^d} \lim_{l \uparrow \infty} \sum_{x \in \Lambda} \frac{1}{l} \sum_{t \in [l]} \langle \sigma_{o,0}; \sigma_{x,t} \rangle_{\beta, h, \delta; \Lambda, l} \leq \beta \lim_{\Lambda \uparrow \mathbb{Z}^d} \lim_{l \uparrow \infty} \sum_{x \in \Lambda} \frac{1}{l} \sum_{t \in [l]} \langle \sigma_{o,0} \sigma_{x,t} \rangle_{\beta, \delta; \Lambda, l}, \quad (4.2.43)$$

uniformly in h since the right-hand side is finite for $\beta < \beta_c$ (note that $h = 0$ in the right-hand side and there is no truncation since the single spin expectation is 0 due to the

periodicity). The truncated two-point function with $h > 0$ has the exponential decay, which implies that the left-hand side in (4.2.43) is bounded above uniformly in Λ and l . Therefore, we can assure the change of order between those limits and finally obtain the equality for $\chi(\beta, \delta)$ in (4.2.38) as required. ■

Therefore, it suffices to consider $\chi^P(\beta, \delta)$ instead of $\chi(\beta, \delta)$ in the high temperature phase $\beta < \beta_c$. In the next section, we will derive the differential inequalities for $\chi^P(\beta, \delta)$, which are much easier to deal with compared to $\chi(\beta, \delta)$.

Remark 4.2.11. We focus on the high temperature phase. In the low temperature phase, the right-hand side in (4.2.43) is not finite anymore. Thus, we cannot use $\chi^P(\beta, \delta)$ as an expression for $\chi(\beta, \delta)$. For the classical Ising model, we have the decent expression for the susceptibility such as the sum of truncated two-point function under the plus-boundary condition with no magnetic field for all temperature. However, for the quantum Ising model, we do not have the same expression since we lose some good properties like the commutativity for spin operators, the right continuity of the correlation function with respect to h and the boundary-independence of the infinite-volume limit (by the ST transformation, we must choose the periodic boundary for the time line axis $[l]$).

Before closing this subsection, we give an expected result for the spontaneous magnetization $m_s(\beta, \delta)$ as follows.

Proposition 4.2.12. *For any $\beta < \beta_c$ and $\delta \geq 0$,*

$$m_s(\beta, \delta) = 0. \quad (4.2.44)$$

Proof. By Remark 4.2.9 and the SK transformation for the single spin expectation, the spontaneous magnetization $m_s(\beta, \delta)$ becomes

$$0 \leq m_s(\beta, \delta) = \lim_{h \downarrow 0} \lim_{\Lambda \uparrow \mathbb{Z}^d} \langle \hat{\sigma}_o^{(3)} \rangle_{\beta, h, \delta; \Lambda} = \lim_{h \downarrow 0} \lim_{\Lambda \uparrow \mathbb{Z}^d} \lim_{l \uparrow \infty} \langle \langle \sigma_{o,0} \rangle \rangle_{\beta, h, \delta; \Lambda, l} \quad (4.2.45)$$

By using the trivial equality $\langle \langle \sigma_{o,0} \rangle \rangle_{\beta, \delta; \Lambda, l} = 0$ due to the periodicity (note that $h = 0$), the right-hand side in (4.2.45) becomes

$$\begin{aligned} \lim_{h \downarrow 0} \lim_{\Lambda \uparrow \mathbb{Z}^d} \lim_{l \uparrow \infty} \int_0^h \frac{d}{dh'} \langle \langle \sigma_{o,0} \rangle \rangle_{\beta, h', \delta; \Lambda, l} dh' &= \beta \lim_{h \downarrow 0} \lim_{\Lambda \uparrow \mathbb{Z}^d} \lim_{l \uparrow \infty} \sum_{x \in \Lambda} \frac{1}{l} \sum_{t \in [l]} \int_0^h \langle \langle \sigma_{o,0} \sigma_{x,t} \rangle \rangle_{\beta, h', \delta; \Lambda, l} dh' \\ &\leq \beta \lim_{h \downarrow 0} h \lim_{\Lambda \uparrow \mathbb{Z}^d} \lim_{l \uparrow \infty} \underbrace{\sum_{x \in \Lambda} \frac{1}{l} \sum_{t \in [l]} \langle \langle \sigma_{o,0} \sigma_{x,t} \rangle \rangle_{\beta, \delta; \Lambda, l}}_{= \chi^P(\beta, \delta)}, \end{aligned} \quad (4.2.46)$$

where we have used the GHS inequality in Proposition 4.2.6 at the above inequality. Therefore, $m_s(\beta, \delta) = 0$ since $\chi^P(\beta, \delta) < \infty$ for $\beta < \beta_c$. This completes the proof. ■

4.3 Mean-field behavior of the susceptibility

As explained in the above section, we would like to identify the value of γ in high dimensions. Would the value be the same as the classical value 1 or affected by quantum effect δ ? The answer lies in the next subsection.

4.3.1 The main results

We define the following quantity, which is called the space-time bubble diagram.

$$B_{\Lambda,l} := \sum_{x \in \Lambda, t \in [l]} \frac{1}{l} \langle\langle \sigma_{o,0} \sigma_{x,t} \rangle\rangle_{\beta,\delta;\Lambda,l}^2, \quad B = \lim_{\Lambda \uparrow \mathbb{Z}^d} \lim_{l \uparrow \infty} B_{\Lambda,l}. \quad (4.3.1)$$

In the following theorem, we assume that the limit B of the space-time bubble diagram $B_{\Lambda,l}$ as $\Lambda \uparrow \infty$ and $l \uparrow \infty$ is bounded and sufficiently small. See Remark 4.3.3.

Theorem 4.3.1. *Let the spin-spin coupling be non-negative and summable. For the ferromagnetic Ising model with the sufficiently small quantum effect $\delta \geq 0$, sufficiently small the space-time bubble diagram B and for $0 < \beta < \beta_c(\delta)$, the following holds.*

(a) *We have the lower bound for the susceptibility,*

$$\chi(\beta, \delta) \geq \frac{C_1}{\beta_c - \beta}. \quad (4.3.2)$$

where $0 < C_1 < \infty$ is a constant. Thus, if the critical exponent γ exists, then $\gamma \leq 1$.

(b) *We have the upper bound for the susceptibility,*

$$\chi(\beta, \delta) \leq \frac{C_2}{\beta_c - \beta}, \quad (4.3.3)$$

where $0 < C_2 < \infty$ is a constant. Thus, if the critical exponent γ exists, then $\gamma \geq 1$.

In the following two subsections, we will prove each item in the above theorem.

4.3.2 Proof of the item (a) in Theorem 4.3.1.

We abbreviate the dependance of the parameters in correlation functions in order to simplify their notations, e.g., $\langle\langle \sigma_{o,0} \sigma_{x,t} \rangle\rangle = \langle\langle \sigma_{o,0} \sigma_{x,t} \rangle\rangle_{\beta,\delta;\Lambda,l}$. Although our results hold for summable coupling constants, from now on, we only consider the nearest-neighbor coupling constants (i.e., $J_{x,y} = 1$ if $|x - y| = 1$ and $J_{x,y} = 0$ otherwise) for simplicity.

Proof of the item (a) in Theorem 4.3.1. Taking the derivative of the two-point function $\langle\langle \sigma_{o,0} \sigma_{x,t} \rangle\rangle$ with respect to β ,

$$\begin{aligned} & \frac{\partial}{\partial \beta} \langle\langle \sigma_{o,0} \sigma_{x,t} \rangle\rangle \\ &= \sum_{u,v \in \Lambda} \sum_{s \in [l]} \frac{J_{u,v}}{l} \langle\langle \sigma_{o,0} \sigma_{x,t}; \sigma_{u,s} \sigma_{v,s} \rangle\rangle + \sum_{u \in \Lambda} \sum_{s \in [l]} \frac{\partial K_{\beta,\delta,l}}{\partial \beta} \langle\langle \sigma_{o,0} \sigma_{x,t}; \sigma_{u,s} \sigma_{u,s+1} \rangle\rangle. \end{aligned} \quad (4.3.4)$$

Thus, we have the following expression for the derivative of the susceptibility,

$$\begin{aligned} & \frac{\partial}{\partial \beta} \left(\frac{\chi_{\Lambda,l}^P(\beta, \delta)}{\beta} \right) \\ &= \sum_{\substack{x \in \Lambda, \\ u,v \in \Lambda}} \sum_{\substack{t,s \in [l]}} \frac{J_{u,v}}{l^2} \langle\langle \sigma_{o,0} \sigma_{x,t}; \sigma_{u,s} \sigma_{v,s} \rangle\rangle + \sum_{x,u \in \Lambda} \sum_{t,s \in [l]} \frac{1}{l} \frac{\partial K_{\beta,\delta,l}}{\partial \beta} \langle\langle \sigma_{o,0} \sigma_{x,t}; \sigma_{u,s} \sigma_{u,s+1} \rangle\rangle. \end{aligned} \quad (4.3.5)$$

Remembering the definition of $K_{\beta,\delta,l}$ in Proposition 4.2.1,

$$\frac{\partial K_{\beta,\delta,l}}{\partial \beta} = \frac{\partial}{\partial \beta} \frac{1}{2} \log \coth \frac{\beta \delta}{l} = -\frac{\delta}{l \sinh \frac{2\beta \delta}{l}}. \quad (4.3.6)$$

Thus, together with the Griffiths 2nd inequality in Proposition 4.2.4, the second term is non-positive. To ignore the second term gives us the upper bound for the derivative $\frac{\partial}{\partial \beta} \langle \sigma_{o,0} \sigma_{x,t} \rangle$. For the first term, we can use Lebowitz' inequality in Proposition 4.2.5 as below,

$$\langle \sigma_{o,0} \sigma_{x,t}; \sigma_{u,s} \sigma_{v,s} \rangle \leq \langle \sigma_{o,0} \sigma_{u,s} \rangle \langle \sigma_{x,t} \sigma_{v,s} \rangle + \langle \sigma_{o,0} \sigma_{v,s} \rangle \langle \sigma_{x,t} \sigma_{u,s} \rangle. \quad (4.3.7)$$

Thus,

$$\begin{aligned} \frac{\partial}{\partial \beta} \left(\frac{\chi_{\Lambda,l}^P(\beta, \delta)}{\beta} \right) &\leq \sum_{\substack{x \in \Lambda \\ u, v \in \Lambda}} \frac{1}{l^2} \sum_{s, t \in [l]} \left(J_{u,v} \langle \sigma_{o,0} \sigma_{u,s} \rangle \langle \sigma_{x,t} \sigma_{v,s} \rangle + J_{u,v} \langle \sigma_{o,0} \sigma_{v,s} \rangle \langle \sigma_{x,t} \sigma_{u,s} \rangle \right) \\ &= \sum_{u, v \in \Lambda} \frac{1}{l} \sum_{s \in [l]} J_{u,v} \left(\langle \sigma_{o,0} \sigma_{u,s} \rangle \sum_{x \in \Lambda} \frac{1}{l} \sum_{t \in [l]} \langle \sigma_{x,t} \sigma_{v,s} \rangle + \langle \sigma_{o,0} \sigma_{v,s} \rangle \sum_{x \in \Lambda} \frac{1}{l} \sum_{t \in [l]} \langle \sigma_{x,t} \sigma_{u,s} \rangle \right) \\ &= 2 \left(\frac{\chi_{\Lambda,l}^P(\beta, \delta)}{\beta} \right) \left(\sum_{u \in \Lambda} \frac{1}{l} \sum_{s \in [l]} \langle \sigma_{o,0} \sigma_{u,s} \rangle \sum_{v \in \Lambda} J_{u,v} \right) = 4d \left(\frac{\chi_{\Lambda,l}^P(\beta, \delta)}{\beta} \right)^2, \end{aligned} \quad (4.3.8)$$

where we have used the non-positivity of the second term in (4.3.5) and Lebowitz' inequality at the inequality, and translation-invariance at the second equality. Therefore, we obtain the following differential inequality,

$$\frac{\partial}{\partial \beta} \left(\frac{\chi_{\Lambda,l}^P(\beta, \delta)}{\beta} \right)^{-1} \geq -4d. \quad (4.3.9)$$

By integrating (4.3.9) from β_1 to β_2 ($\beta_1 < \beta_c < \beta_2$),

$$\left(\frac{\chi_{\Lambda,l}^P(\beta_2, \delta)}{\beta_2} \right)^{-1} - \left(\frac{\chi_{\Lambda,l}^P(\beta_1, \delta)}{\beta_1} \right)^{-1} \geq -4d(\beta_2 - \beta_1). \quad (4.3.10)$$

After taking the limits as $\Lambda \uparrow \mathbb{Z}^d$ and $l \uparrow \infty$, we have $\chi^P(\beta_2, \delta) = \infty$ by the definition of the critical temperature β_c and the monotonicity with respect to β . We can only show the monotonicity for sufficiently small δ by (4.3.35) in the proof of the item (b) in Theorem 4.3.1 in the next subsection. Thus, (4.3.10) gives us

$$\frac{\beta_1}{\chi^P(\beta_1, \delta)} \leq 4d(\beta_2 - \beta_1). \quad (4.3.11)$$

Since the above inequality holds for any $\beta_1 (< \beta_c)$ and $\beta_2 (> \beta_c)$ and also the equality (4.2.38), then we finally obtain for any $\beta < \beta_c$ and $\delta > 0$,

$$\chi(\beta, \delta) \geq \frac{\beta}{4d(\beta_c - \beta)}. \quad (4.3.12)$$

■

4.3.3 Proof of the item (b) in Theorem 4.3.1.

Proof of the item (b) in Theorem 4.3.1. Now, we need to obtain the lower bound for the derivative $\frac{\partial}{\partial \beta} \langle \sigma_{o,0} \sigma_{x,t} \rangle$ in (4.3.4). To do that, we use the Aizenman-Graham (AG) inequality in Proposition 4.2.7 for the first term in (4.3.4) as follows;

$$\begin{aligned} \langle \sigma_{o,0} \sigma_{x,t}; \sigma_{u,s} \sigma_{v,s} \rangle &\geq \langle \sigma_{o,0} \sigma_{u,s} \rangle \langle \sigma_{x,t} \sigma_{v,s} \rangle + \langle \sigma_{o,0} \sigma_{v,s} \rangle \langle \sigma_{x,t} \sigma_{u,s} \rangle \\ &\quad - \tanh \tilde{J}_{X,Y} \sum_{X,Y \in \Lambda \times [l]} \langle \sigma_{o,0} \sigma_{x,t}; \sigma_X \sigma_Y \rangle \langle \sigma_{u,s} \sigma_Y \rangle \langle \sigma_{v,s} \sigma_Y \rangle \\ &\quad - \langle \sigma_{o,0} \sigma_{x,t} \rangle \langle \sigma_{o,0} \sigma_{u,s} \rangle \langle \sigma_{o,0} \sigma_{v,s} \rangle - \langle \sigma_{o,0} \sigma_{x,t} \rangle \langle \sigma_{x,t} \sigma_{u,s} \rangle \langle \sigma_{x,t} \sigma_{v,s} \rangle. \end{aligned} \quad (4.3.13)$$

Remember that

$$\tilde{J}_{X,Y} = \begin{cases} \frac{\beta J_{x,y}}{l} & \text{if } X = (x, t), Y = (y, t), \\ K_{\beta, \delta, l} & \text{if } X = (x, t), Y = (x, t+1). \end{cases} \quad (4.3.14)$$

We say that (X, Y) is a spatial bond for the first case and a temporal bond for the latter case. By using the AG inequality, we have the lower bound consisting of six terms for the derivative of the susceptibility in (4.3.5). We define those six terms by,

$$M_1 = \sum_{x \in \Lambda, t \in [l]} \frac{1}{l} \sum_{\substack{u, v \in \Lambda \\ s \in [l]}} \frac{J_{u,v}}{l} \langle \sigma_{o,0} \sigma_{u,s} \rangle \langle \sigma_{x,t} \sigma_{v,s} \rangle, \quad (4.3.15)$$

$$M_2 = \sum_{x \in \Lambda, t \in [l]} \frac{1}{l} \sum_{\substack{u, v \in \Lambda \\ s \in [l]}} \frac{J_{u,v}}{l} \langle \sigma_{o,0} \sigma_{v,s} \rangle \langle \sigma_{x,t} \sigma_{u,s} \rangle, \quad (4.3.16)$$

$$M_3 = - \sum_{x \in \Lambda, t \in [l]} \frac{1}{l} \sum_{\substack{u, v \in \Lambda \\ s \in [l]}} \frac{J_{u,v}}{l} \tanh \tilde{J}_{X,Y} \sum_{X,Y \in \Lambda \times [l]} \langle \sigma_{o,0} \sigma_{x,t}; \sigma_X \sigma_Y \rangle \langle \sigma_{u,s} \sigma_Y \rangle \langle \sigma_{v,s} \sigma_Y \rangle, \quad (4.3.17)$$

$$M_4 = - \sum_{x \in \Lambda, t \in [l]} \frac{1}{l} \sum_{\substack{u, v \in \Lambda \\ s \in [l]}} \frac{J_{u,v}}{l} \langle \sigma_{o,0} \sigma_{x,t} \rangle \langle \sigma_{o,0} \sigma_{u,s} \rangle \langle \sigma_{o,0} \sigma_{v,s} \rangle, \quad (4.3.18)$$

$$M_5 = - \sum_{x \in \Lambda, t \in [l]} \frac{1}{l} \sum_{\substack{u, v \in \Lambda \\ s \in [l]}} \frac{J_{u,v}}{l} \langle \sigma_{o,0} \sigma_{x,t} \rangle \langle \sigma_{x,t} \sigma_{u,s} \rangle \langle \sigma_{x,t} \sigma_{v,s} \rangle, \quad (4.3.19)$$

$$M_6 = \sum_{x, u \in \Lambda} \sum_{t, s \in [l]} \frac{\partial K_{\beta, \delta, l}}{\partial \beta} \langle \sigma_{o,0} \sigma_{x,t}; \sigma_{u,s} \sigma_{u,s+1} \rangle, \quad (4.3.20)$$

such that

$$\frac{\partial}{\partial \beta} \left(\frac{\chi_{\Lambda, l}^P(\beta, \delta)}{\beta} \right) \geq \sum_{j=1}^6 M_j. \quad (4.3.21)$$

Note that M_6 has already showed up in (4.3.5).

By following the same computation in (4.3.8),

$$M_1 + M_2 = 4d \left(\frac{\chi_{\Lambda, l}^P(\beta, \delta)}{\beta} \right)^2. \quad (4.3.22)$$

Next, we evaluate M_4 .

$$\begin{aligned}
M_4 &= - \sum_{x \in \Lambda, t \in [l]} \frac{1}{l} \sum_{\substack{u, v \in \Lambda \\ s \in [l]}} \frac{J_{u,v}}{l} \langle\langle \sigma_{o,0} \sigma_{x,t} \rangle\rangle \langle\langle \sigma_{o,0} \sigma_{u,s} \rangle\rangle \langle\langle \sigma_{o,0} \sigma_{v,s} \rangle\rangle \\
&= - \underbrace{\sum_{x \in \Lambda, t \in [l]} \frac{1}{l} \langle\langle \sigma_{o,0} \sigma_{x,t} \rangle\rangle}_{= \chi_{\Lambda,l}^P(\beta, \delta) / \beta} \sum_{\substack{u, v \in \Lambda \\ s \in [l]}} \frac{J_{u,v}}{l} \langle\langle \sigma_{o,0} \sigma_{u,s} \rangle\rangle \langle\langle \sigma_{o,0} \sigma_{v,s} \rangle\rangle.
\end{aligned} \tag{4.3.23}$$

By using the Schwarz inequality for the second sum, M_4 is bounded below by

$$\begin{aligned}
M_4 &\geq - \frac{\chi_{\Lambda,l}^P(\beta, \delta)}{\beta} \left(\sum_{\substack{u, v \in \Lambda \\ s \in [l]}} \frac{J_{u,v}}{l} \langle\langle \sigma_{o,0} \sigma_{u,s} \rangle\rangle^2 \right)^{1/2} \left(\sum_{\substack{u, v \in \Lambda \\ s \in [l]}} \frac{J_{u,v}}{l} \langle\langle \sigma_{o,0} \sigma_{v,s} \rangle\rangle^2 \right)^{1/2} \\
&= -2d\beta B_{\Lambda,l} \frac{\chi_{\Lambda,l}^P(\beta, \delta)}{\beta}.
\end{aligned} \tag{4.3.24}$$

Since the contribution from M_5 is the same by the symmetry,

$$M_4 + M_5 \geq -4d\beta B_{\Lambda,l} \frac{\chi_{\Lambda,l}^P(\beta, \delta)}{\beta}. \tag{4.3.25}$$

We give more careful consideration to M_3 . We split the sum into two cases; either (X, Y) is a spatial bond or (X, Y) is a temporal bond. The contribution from the spatial case is

$$\begin{aligned}
&- \sum_{x \in \Lambda, t \in [l]} \frac{1}{l} \sum_{\substack{u, v \in \Lambda \\ s \in [l]}} \frac{J_{u,v}}{l} \sum_{\substack{w, z \in \Lambda \\ s' \in [l]}} \tanh \frac{J_{w,z}}{l} \langle\langle \sigma_{o,0} \sigma_{x,t}; \sigma_{w,s'} \sigma_{z,s'} \rangle\rangle \langle\langle \sigma_{u,s} \sigma_{z,s'} \rangle\rangle \langle\langle \sigma_{v,s} \sigma_{z,s'} \rangle\rangle \\
&\geq - \sum_{x \in \Lambda, t \in [l]} \frac{1}{l} \sum_{\substack{w, z \in \Lambda \\ s' \in [l]}} \frac{J_{w,z}}{l} \langle\langle \sigma_{o,0} \sigma_{x,t}; \sigma_{w,s'} \sigma_{z,s'} \rangle\rangle \underbrace{\sum_{\substack{u, v \in \Lambda \\ s \in [l]}} \frac{J_{u,v}}{l} \langle\langle \sigma_{u,s} \sigma_{z,s'} \rangle\rangle \langle\langle \sigma_{v,s} \sigma_{z,s'} \rangle\rangle}_{\leq 2d\beta B_{\Lambda,l}},
\end{aligned} \tag{4.3.26}$$

where we have used that $\tanh x \leq x$. By the identity (4.3.5) for $\frac{\partial}{\partial \beta} \left(\frac{\chi_{\Lambda,l}^P(\beta, \delta)}{\beta} \right)$, (4.3.26) is bounded below by

$$-2d\beta B_{\Lambda,l} \frac{\partial}{\partial \beta} \left(\frac{\chi_{\Lambda,l}^P(\beta, \delta)}{\beta} \right) + 2d\beta B_{\Lambda,l} \underbrace{\sum_{x \in \Lambda, t \in [l]} \frac{1}{l} \sum_{u \in \Lambda, s \in [l]} \frac{\partial K_{\beta, \delta, l}}{\partial \beta} \langle\langle \sigma_{o,0} \sigma_{x,t}; \sigma_{u,s} \sigma_{u,s+1} \rangle\rangle}_{= M_6}. \tag{4.3.27}$$

Therefore, together with M_6 , the contribution from the spatial case and M_6 is

$$-2d\beta B_{\Lambda,l} \frac{\partial}{\partial \beta} \left(\frac{\chi_{\Lambda,l}^P(\beta, \delta)}{\beta} \right) + (2d\beta B_{\Lambda,l} + 1) M_6. \tag{4.3.28}$$

Next, we need to deal with the truncated four-point function in M_6 . To obtain the lower bound, we need to bound it above since $\frac{\partial K_{\beta,\delta,l}}{\partial \beta}$ is non-positive. Although we naively would like to use Lebowitz' inequality in Proposition 4.2.5, we need to extract the extra factor $\frac{1}{l}$. To do that, we use the following lemma. The proof will be given at the end of this subsection.

Lemma 4.3.2. *For any finite subset $\Lambda \subset \mathbb{Z}^d$ and $l \in \mathbb{Z}_+$,*

$$\begin{aligned} \langle\langle \sigma_{o,0} \sigma_{x,t}; \sigma_{u,s} \sigma_{u,s+1} \rangle\rangle_{\beta,\delta;\Lambda,l} &\leq \frac{4\beta\delta}{l} \left(\langle\langle \sigma_{o,0} \sigma_{u,s} \rangle\rangle_{\beta,\delta;\Lambda,l} \langle\langle \sigma_{x,t} \sigma_{u,s+1} \rangle\rangle_{\beta,\delta;\Lambda,l} \right. \\ &\quad \left. + \langle\langle \sigma_{o,0} \sigma_{u,s+1} \rangle\rangle_{\beta,\delta;\Lambda,l} \langle\langle \sigma_{x,t} \sigma_{u,s} \rangle\rangle_{\beta,\delta;\Lambda,l} \right). \end{aligned} \quad (4.3.29)$$

By using this lemma, the second term in (4.3.28) is bounded below by

$$\begin{aligned} -(2d\beta B_{\Lambda,l} + 1) \frac{4\beta\delta^2}{l \sinh \frac{2\beta\delta}{l}} \sum_{x \in \Lambda, t \in [l]} \frac{1}{l} \sum_{u \in \Lambda, s \in [l]} \frac{1}{l} \left(\langle\langle \sigma_{o,0} \sigma_{u,s} \rangle\rangle_{\beta,\delta;\Lambda,l} \langle\langle \sigma_{x,t} \sigma_{u,s+1} \rangle\rangle_{\beta,\delta;\Lambda,l} \right. \\ \left. + \langle\langle \sigma_{o,0} \sigma_{u,s+1} \rangle\rangle_{\beta,\delta;\Lambda,l} \langle\langle \sigma_{x,t} \sigma_{u,s} \rangle\rangle_{\beta,\delta;\Lambda,l} \right). \end{aligned} \quad (4.3.30)$$

By using translation-invariance, this becomes

$$-(2d\beta B_{\Lambda,l} + 1) \frac{8\beta\delta^2}{l \sinh \frac{2\beta\delta}{l}} \left(\frac{\chi_{\Lambda,l}^P(\beta, \delta)}{\beta} \right)^2 \geq -4\delta(2d\beta B_{\Lambda,l} + 1) \left(\frac{\chi_{\Lambda,l}^P(\beta, \delta)}{\beta} \right)^2, \quad (4.3.31)$$

where we have used that $\sinh x \geq x$.

Now, we go back to the estimate for the temporal case in M_3 . Noting that $\tanh K_{\beta,\delta,l} = \frac{1 - \tanh \frac{\beta\delta}{l}}{1 + \tanh \frac{\beta\delta}{l}}$, the contribution from the temporal case is

$$\begin{aligned} &\underbrace{- \frac{1 - \tanh \frac{\beta\delta}{l}}{1 + \tanh \frac{\beta\delta}{l}} \sum_{x \in \Lambda, t \in [l]} \frac{1}{l} \sum_{\substack{u,v \in \Lambda \\ s \in [l]}} \frac{J_{u,v}}{l} \sum_{w \in \Lambda, s' \in [l]} \langle\langle \sigma_{o,0} \sigma_{x,t}; \sigma_{w,s'} \sigma_{w,s'+1} \rangle\rangle \langle\langle \sigma_{u,s} \sigma_{w,s'+1} \rangle\rangle \langle\langle \sigma_{v,s} \sigma_{w,s'+1} \rangle\rangle}_{\leq 1} \\ &\geq - \sum_{x \in \Lambda, t \in [l]} \frac{1}{l} \sum_{w \in \Lambda, s' \in [l]} \langle\langle \sigma_{o,0} \sigma_{x,t}; \sigma_{w,s'} \sigma_{w,s'+1} \rangle\rangle \underbrace{\sum_{\substack{u,v \in \Lambda \\ s \in [l]}} \frac{J_{u,v}}{l} \langle\langle \sigma_{u,s} \sigma_{w,s'+1} \rangle\rangle \langle\langle \sigma_{v,s} \sigma_{w,s'+1} \rangle\rangle}_{\leq 2dB_{\Lambda,l}}. \end{aligned} \quad (4.3.32)$$

Here, we also use the Lemma 4.3.2 for the second sum on the right-hand side above. Then this is bounded below by

$$\begin{aligned} &-8d\beta\delta B_{\Lambda,l} \sum_{x \in \Lambda, t \in [l]} \frac{1}{l} \sum_{w \in \Lambda, s' \in [l]} \frac{1}{l} \left(\langle\langle \sigma_{o,0} \sigma_{u,s} \rangle\rangle \langle\langle \sigma_{x,t} \sigma_{u,s+1} \rangle\rangle + \langle\langle \sigma_{o,0} \sigma_{u,s+1} \rangle\rangle \langle\langle \sigma_{x,t} \sigma_{u,s} \rangle\rangle \right) \\ &\geq -16d\beta\delta B_{\Lambda,l} \left(\frac{\chi_{\Lambda,l}^P(\beta, \delta)}{\beta} \right)^2. \end{aligned} \quad (4.3.33)$$

Thus, together (4.3.31) and (4.3.33),

$$M_3 + M_6 \geq -2d\beta B_{\Lambda,l} \frac{\partial}{\partial \beta} \left(\frac{\chi_{\Lambda,l}^P(\beta, \delta)}{\beta} \right) - 4\delta(5d\beta\delta B_{\Lambda,l} + 1) \left(\frac{\chi_{\Lambda,l}^P(\beta, \delta)}{\beta} \right)^2. \quad (4.3.34)$$

Therefore, we finally obtain the differential inequality by (4.3.22), (4.3.25) and (4.3.34),

$$\frac{\partial}{\partial \beta} \left(\frac{\chi_{\Lambda,l}^P(\beta, \delta)}{\beta} \right) \geq \frac{4(d - (5d\beta B_{\Lambda,l} + 1)\delta) \left(\frac{\chi_{\Lambda,l}^P(\beta, \delta)}{\beta} \right)^2 - 4dB_{\Lambda,l} \left(\frac{\chi_{\Lambda,l}^P(\beta, \delta)}{\beta} \right)}{1 + 2d\beta B_{\Lambda,l}}. \quad (4.3.35)$$

By solving this differential inequality and taking the limit of Λ and l going to infinity, with the assumption that $B_{\Lambda,l}$ is bounded and $\delta \geq 0$ is sufficiently small (we choose $0 \leq \delta < \frac{d}{5d\beta B_{\Lambda,l} + 1}$ so that the first term in the numerator above can be positive), then we can conclude the desired upper bound for the susceptibility $\chi(\beta, \delta)$. \blacksquare

Remark 4.3.3. In the item in Theorem 4.3.1, we assume the boundedness of the space-time bubble diagram $B_{\Lambda,l}$. It is well-known that for the classical ferromagnetic Ising model if the system satisfies reflection-positivity, then the infrared bound holds, which implies the boundedness of the bubble diagram.

To close this subsection, we provide the proof of Lemma 4.3.2 below.

Proof of Lemma 4.3.2. By using the random-current representation (4.2.23) and the source switching lemma (4.2.24),

$$\begin{aligned} \langle\langle \sigma_{o,0} \sigma_{x,t}; \sigma_{u,s} \sigma_{u,s+1} \rangle\rangle_{\beta, \delta; \Lambda, l} &= \sum_{\substack{\partial \mathbf{n} = \{(o,0), (x,t), \\ (u,s), (u,s+1)\} \\ \partial \mathbf{m} = \emptyset}} \frac{w(\mathbf{n})w(\mathbf{m})}{\tilde{Z}^2} (1 - \mathbb{1}[(o,0) \xleftrightarrow{\mathbf{n}+\mathbf{m}} (x,t)]) \\ &\leq \sum_{\substack{\partial \mathbf{n} = \{(o,0), (x,t), \\ (u,s), (u,s+1)\} \\ \partial \mathbf{m} = \emptyset}} \frac{w(\mathbf{n})w(\mathbf{m})}{\tilde{Z}^2} \mathbb{1}[n_{(u,s), (u,s+1)} = m_{(u,s), (u,s+1)} = 0] \\ &\quad \times (\mathbb{1}[(o,0) \xleftrightarrow{\mathbf{n}+\mathbf{m}} (u,s)] + \mathbb{1}[(o,0) \xleftrightarrow{\mathbf{n}+\mathbf{m}} (u,s+1)]), \end{aligned} \quad (4.3.36)$$

where we have used that if $(o,0)$ and (x,t) are not connected, then by the source constraint $(o,0)$ should be connected to either (u,s) or $(u,s+1)$, and also the currents $n_{(u,s), (u,s+1)}$ and $m_{(u,s), (u,s+1)}$ should be 0. We can insert $1 = \left(\frac{\cosh K_{\beta, \delta, l}}{\cosh K_{\beta, \delta, l}} \right)^2$ as the currents on the bond $(u,s), (u,s+1)$. This does not change the source constraint since cosine hyperbolic function has the even currents. Thus, the right-hand side in (4.3.36) becomes

$$\begin{aligned} &(\cosh K_{\beta, \delta, l})^{-2} \sum_{\substack{\partial \mathbf{n} = \{(o,0), (x,t), \\ (u,s), (u,s+1)\} \\ \partial \mathbf{m} = \emptyset}} \frac{w(\mathbf{n})w(\mathbf{m})}{\tilde{Z}^2} (\mathbb{1}[(o,0) \xleftrightarrow{\mathbf{n}+\mathbf{m}} (u,s)] + \mathbb{1}[(o,0) \xleftrightarrow{\mathbf{n}+\mathbf{m}} (u,s+1)]) \\ &= (\cosh K_{\beta, \delta, l})^{-2} \left(\underbrace{\sum_{\substack{\partial \mathbf{n} = \{(x,t), (u,s+1)\} \\ \partial \mathbf{m} = \{(o,0), (u,s)\}}} \frac{w(\mathbf{n})w(\mathbf{m})}{\tilde{Z}^2}}_{= \langle\langle \sigma_{o,0} \sigma_{u,s} \rangle\rangle \langle\langle \sigma_{x,t} \sigma_{u,s+1} \rangle\rangle} + \underbrace{\sum_{\substack{\partial \mathbf{n} = \{(x,t), (u,s)\} \\ \partial \mathbf{m} = \{(o,0), (u,s+1)\}}} \frac{w(\mathbf{n})w(\mathbf{m})}{\tilde{Z}^2}}_{= \langle\langle \sigma_{o,0} \sigma_{u,s+1} \rangle\rangle \langle\langle \sigma_{x,t} \sigma_{u,s} \rangle\rangle} \right), \end{aligned} \quad (4.3.37)$$

where we have also used the source-switching lemma (4.2.24).

Remembering that $K_{\beta,\delta,l} = \frac{1}{2} \log \coth \frac{\beta\delta}{l}$,

$$(\cosh K_{\beta,\delta,l})^{-2} = \frac{4}{(e^{K_{\beta,\delta,l}} + e^{-K_{\beta,\delta,l}})^2} \leq 4e^{-2K_{\beta,\delta,l}} = 4 \tanh \frac{\beta\delta}{l} \leq \frac{4\beta\delta}{l}. \quad (4.3.38)$$

Therefore, we obtain the desired bound. ■

4.3.4 Further discussion

1. We have the space-time bubble diagram $B_{\Lambda,l}$ in the lower bound for the derivative of the susceptibility and assume its boundedness. As explained in Remark 4.3.3, the infrared bound implies the boundedness of the bubble diagram in high dimensions. If the system satisfies reflection-positivity, then the infrared bound holds for the classical ferromagnetic Ising model. Since we now consider the nearest-neighbor coupling constant for a spatial bond by the definition of the model and for a temporal bond by the ST transformation, the reflection-positivity holds. Thus, it would be possible that we show Gaussian domination and obtain the suitable infrared bound for the Fourier transform of the two-point function $\langle\langle \sigma_{o,0} \sigma_{x,t} \rangle\rangle_{\beta,\delta;\Lambda,l}$. By using its infrared bound, we should be able to show the boundedness of the space-time bubble diagram in high dimensions.
2. In the main theorem, we assume the smallness of δ and B for the monotonicity of $\chi^P(\beta, \delta)$ with respect to β to hold. However, we have not succeeded in showing the monotonicity for any $\delta > 0$. By physical intuition, we believe that the two-point function $\langle\langle \sigma_{o,0} \sigma_{x,t} \rangle\rangle_{\beta,\delta;\Lambda,l}$ is monotonic with respect to β with fixed δ . By taking the derivative and observing the random-current representations for two terms in (4.3.4) more carefully, we expect to show the non-negativity of its derivative. If the monotonicity holds for any $\delta \geq 0$, the item (a) in Theorem 4.3.1 holds for any $\delta \geq 0$ without assuming the smallness of B .
3. As explained in Section 4.1, our final goal is to investigate the critical temperature of the quantum Ising model to observe the quantum effect on the classical system. We have shown that the critical exponent for the quantum susceptibility takes on the same mean-field value as the classical one. Although we cannot rule out the possibility that other critical exponents take on different values from the classical system, we are next interested in the quantum effect on the critical temperature. Since, contrary to the critical exponent, the critical temperature differs depending on the concerned models, we expect that the critical temperature of the quantum system is different from the classical system. One of the ways to estimate the critical temperature in high dimensions is the lace expansion analysis. Sakai [79] invented the lace expansion for the classical Ising model in 2007 by using the random-current representation. Applying the ST transformation and the random-current representation should enable us to do the lace expansion analysis for the quantum Ising model in a similar manner of [79].

Acknowledgements

Thanks to a lot of supports and helps from many people around me, I could accomplished the completion of my Ph.D. First of all, I would like to thank my supervisor Professor Akira Sakai. I first met him when I was a junior in Hokkaido University and got curious about his research field on mathematically-rigorous analysis for phase transition and critical phenomena. Since then, I had belonged to his research group and spent seven years until I finished Ph.D. course. I learned a lot about mathematics and physics, lifestyle as a great researcher, how to make attractive presentation and the way of surviving in real life with a strong brief and spirit. He is the best researcher and educator I have ever met. It is a great treasure for me to have had a lot of discussion, done the joint works and spent time as a student in his research group. I'm full of gratitude.

I would like to thank Professor Markus Heydenreich for the joint work on the Ising 1-arm exponent. He gave precious time for discussion and supported my visits to Ludwig Maximilian University of Munich in München in June of 2016 and September of 2018. It was a great honor to have done the joint work and written a paper with him and Professor Sakai. I also would like to thank Killian Matzke for his hospitality during my stay in München and having many discussion on our individual research.

I would like to thank Professor Gordon Slade for giving a valuable opportunity to study renormalisation group analysis in University of British Columbia in Vancouver from April and June of 2017. The experience to study its method and to have a discussion with him motivated me to study more and broadened my knowledge and research field very widely. I also would like to thank Benjamin Wallace for his hospitality during my stay in Vancouver and having many discussion on the application of renormalisation group analysis to the Ising model and the high-dimensional n -component $|\phi|^4$ model.

I would like to thank Professor Lung-Chi Chen for the joint work on the lace expansion analysis for oriented percolation on the BCC lattice. He gave precious time for discussion and supported my visit to National Chengchi University in Taipei in May of 2018. It is a great honor to have an ongoing project with him and Yoshinori Kamijima.

I would like to thank Eric Ossami Endo, Lucas Affonso and Rodrigo Bissacot for the joint work on the long-range Ising model with decaying magnetic fields. They gave wonderful cultural experiences and fruitful discussion during my visit to University of São Paulo in São Paulo in August of 2018. In particular, I met Eric when I participated in the PIMS summer school in 2017 in Vancouver. It was a lucky to know each other and start the interesting joint work. It was a great honor to invite and host him to visit Hokkaido University in Japan.

I would like to thank all young researchers I met in conferences, workshops and summer schools. They and their research have really stimulated my mathematical curiosity and

motivated me to study as much as (more than?) they do.

I would like to thank all the members in Sakai research group. Their seminars were very nice places to study various kinds of mathematical topics from the basics and to learn how to make a good presentation. In particular, I am grateful to Dr. Yuki Chino. He is the first to have got the Ph.D. in Sakai research group. I learned a lot about his attitude to enjoy the mathematics and research, how to communicate with people very well and a spirit to be an entertainer.

I would like to thank old friends of mine and all the members in Hokkaido University. They always made me relaxed with having a chitchat. I hope that everything will go well for them.

I would like to thank all the staffs in the math department in Hokkaido university. Thanks to their quick and sincere managements, I could concentrate on my research without any trouble.

I would like to thank all the members of Hitachi Hokkaido University Laboratory Hitachi. We had a regular weekly meeting to discuss the Ising machine from mathematical point of view. I did not know that the main research object of mine, the Ising model, could be applied to solve optimization problems in real life, which was very impressing and exciting. It was a nice opportunity to feel a connection between academic and industry.

I would like to thank the Ambitious Leader's Program in Hokkaido University and their members. Thanks to them, I could have a numerous number of experiences to go abroad for studying English and research, to join events involved with companies and to make a wide variety of connections among scientists in a lot of departments such as chemistry, polymer science, engineering, pharmacy and computer science. Through discussion and conversation with them, I found out the cultural difference from mathematics and different points of view from other scientific discipline. I could not have fruitful experienced if I had not belonged to the ALP program.

Finally, I would like to thank my family, in particular my father and mother. They had supported and understood me very much, which finally made the completion of my Ph.D. achieved. Thank you from the bottom of my heart.

I swear that I will return the favor to all the people who have supported me.

Sincere thanks to all of you.

Bibliography

- [1] M. Aizenman. Geometric analysis of ϕ^4 fields and Ising models. *Commun. Math. Phys.* **86** (1982): 1–48.
- [2] M. Aizenman and D.J. Barsky. Sharpness of the phase transition in percolation models. *Commun. Math. Phys.* **108** (1987): 489–526.
- [3] M. Aizenman, D.J. Barsky and R. Fernández. The phase transition in a general class of Ising-type models is sharp. *J. Stat. Phys.* **47** (1987): 343–374.
- [4] M. Aizenman, H. Duminil-Copin and V. Sidoravicius. Random currents and continuity of Ising model’s spontaneous magnetization. *Commun. Math. Phys.* **334** (2015): 719–742.
- [5] M. Aizenman and R. Fernández. On the critical behavior of the magnetization in high-dimensional Ising models. *J. Stat. Phys.* **44** (1986): 393–454.
- [6] M. Aizenman and R. Graham. On the renormalized coupling constant and the susceptibility in ϕ_4^4 field theory and the Ising model in four dimensions. *Nucl. Phys.* **B225** [FS7] (1983): 261–288.
- [7] M. Aizenman and B. Nachtergale. Geometric aspects of quantum spin states. *Commun. Math. Phys.* **164** (1994): 17–63.
- [8] M. Aizenman and C.M. Newman. Tree graph inequalities and critical behavior in percolation models. *J. Stat. Phys.* **36** (1984): 107–143.
- [9] R. Bauerschmidt, D.C. Brydges and G. Slade. Scaling limits and critical behaviour of the 4-dimensional n-component $|\phi|^4$ spin model. *J. Stat. Phys.* **157** (2014): 692–742.
- [10] R. Bauerschmidt, D.C. Brydges and G. Slade. Logarithmic correction for the susceptibility of the 4-dimensional weakly self-avoiding walk: a renormalisation group analysis. *Commun. Math. Phys.* **337** (2015): 817–877.
- [11] R. Bauerschmidt, D.C. Brydges and G. Slade. *Introduction to a Renormalisation Group Method*. Preprint (2018).
- [12] R. Bauerschmidt, H. Duminil-Copin, J. Goodman and G. Slade. Lectures on self-avoiding walks. A chapter in *Probability and Statistical Physics in Two and More Dimensions* (D. Ellwood et al. eds., American Mathematical Society, 2012).

- [13] R. Bissacot, M. Cassandro, L. Cioletti and E. Presutti. Phase transitions in ferromagnetic Ising models with spatially dependent magnetic fields. *Commun. Math. Phys.* **337** (2015): 41–53.
- [14] R. Bissacot, and L. Cioletti. Phase transition in ferromagnetic Ising models with non-uniform external magnetic fields. *J. Stat. Phys.* **139** (2010): 769–778.
- [15] R. Bissacot, E.O. Endo and A.C.D. van Enter. Stability of the phase transition of critical-field Ising model on Cayley trees under inhomogeneous external fields. *Stoch. Process. Their Appl.* **127** (2017):4126–4138.
- [16] J.E. Björnberg. Infrared bound and mean-field behaviour in the quantum Ising model. *Commun. Math. Phys.* **323** (2013): 329–366.
- [17] J.E. Björnberg and G.R. Grimmett. The phase transition of the quantum Ising model is sharp. *J. Stat. Phys.* **136** (2009): 231–273.
- [18] B. Bollobás and O. Riordan. *Percolation* (Cambridge University Press, 2006).
- [19] D. Brydges and T. Spencer. Self-avoiding walk in 5 or more dimensions. *Commun. Math. Phys.* **97** (1985): 125–148.
- [20] L. Cioletti and R. Vila. Graphical representations for Ising and Potts models in general external fields. *Ann. Appl. Probab.* **162** (2016): 81–122.
- [21] S. Chatterjee and J. Hanson. Restricted percolation critical exponents in high dimensions. Preprint (2018): arXiv:1810.03750.
- [22] L.-C. Chen and A. Sakai. Critical behavior and the limit distribution for long-range oriented percolation. I. *Probab. Theory Related Fields* **142** (2008): 151–188.
- [23] L.-C. Chen and A. Sakai. Critical behavior and the limit distribution for long-range oriented percolation. II: Spatial correlation. *Probab. Theory Related Fields* **145** (2009): 435–458.
- [24] L.-C. Chen and A. Sakai. Asymptotic behavior of the gyration radius for long-range self-avoiding walk and long-range oriented percolation. *Ann. Appl. Probab.* **39** (2011): 507–548.
- [25] L.-C. Chen and A. Sakai. Critical two-point functions for long-range statistical-mechanical models in high dimensions. *Ann. Probab.* **43** (2015): 639–681.
- [26] L.-C. Chen and A. Sakai. Critical two-point functions for long-range models with power-law couplings: The marginal case for $d \geq d_c$. Preprint (2018): arXiv:1808.06789.
- [27] L.-C. Chen, S. Handa, M. Heydenreich, Y. Kamijima and A. Sakai. An attempt to prove mean-field behavior for nearest-neighbor percolation in 7 dimensions. In preparation.

- [28] N. Crawford, D. Ioffe. Random current representation for transverse field Ising model. *Commun. Math. Phys.* **296** (2010): 447–474.
- [29] H. Duminil-Copin, S. Goswami and A. Raoufi. Exponential decay of truncated correlations for the Ising model in any dimension for all but the critical temperature. Preprint (2018): arXiv:1808.00439.
- [30] H. Duminil-Copin and V. Tassion. A new proof of the sharpness of the phase transition for Bernoulli percolation and the Ising model. *Commun. Math. Phys.* **343** (2016): 725–745.
- [31] F. J. Dyson. Existence of a phase transition in a one-dimensional Ising ferromagnet. *Commun. Math. Phys.* **12** (1969): 91–107.
- [32] E.O. Endo Gibbs measures for models on lines and trees. Ph.D. Thesis (2018).
- [33] W. Feller. *An Introduction to Probability Theory and Its Applications* (Vol. I, 3rd ed., Wiley, 1968).
- [34] R. Fitzner and R. van der Hofstad. Generalized approach to the non-backtracking lace expansion. To appear in *Probab. Theory Related Fields*.
- [35] R. Fitzner and R. van der Hofstad. Mean-field behavior for nearest-neighbor percolation in $d > 10$. *Electron. J. Probab.* **22** (2017): No. 43. An extended version is available at arXiv:1506.07977.
- [36] S. Friedli and Y. Velenik. *Statistical Mechanics of Lattice Systems: A Concrete Mathematical Introduction* (Cambridge University Press, 2017).
- [37] J. Fröhlich, B. Simon and T. Spencer. Infrared bounds, phase transitions and continuous symmetry breaking. *Commun. Math. Phys.* **50** (1976): 79–95.
- [38] J. Fröhlich and T. Spencer. The phase transition in the one-dimensional Ising model with $1/r^2$ interaction energy. *Commun. Math. Phys.* **84** (1982): 87–101.
- [39] J. Ginibre. General formulation of Griffiths’ inequalities. *Commun. Math. Phys.* **16** (1970): 310–328.
- [40] C. Goldschmidt, D. Ueltschi, P. Windridge, Quantum Heisenberg models and their probabilistic representations. *Commun. Contemp. Math.* **552** (2011): 177–224.
- [41] R.B. Griffiths. Correlations in Ising ferromagnets I. *J. Math. Phys.* **8** (1967): 478–483.
- [42] R.B. Griffiths. Correlations in Ising ferromagnets II. *J. Math. Phys.* **8** (1967): 484–489.
- [43] R.B. Griffiths. Correlations in Ising ferromagnets III. *Commun. Math. Phys.* **6** (1967): 121–127.

- [44] R.B. Griffiths, C.A. Hurst and S. Sherman. Concavity of magnetization of an Ising ferromagnet in a positive external field. *J. Math. Phys.* **11** (1970): 790–795.
- [45] G.R. Grimmett. *Percolation* (2nd ed., Springer, 1999).
- [46] D. Ioffe. Stochastic geometry of classical and quantum Ising models. *Methods of contemporary mathematical statistical physics* (Lecture Notes in Mathematics, Springer, Berlin, 2009)
- [47] E. Ising. Beitrag zur Theorie des Ferromagnetismus. *Zeitschrift für Physik.* **31** (2003): 253–258.
- [48] S. Handa, M. Heydenreich and A. Sakai. Mean-field bound on the 1-arm exponent for Ising ferromagnets in high dimensions. Accepted as a chapter in *Sojourns in Probability and Statistical Physics* (V. Sidoravicius ed., Springer).
- [49] S. Handa, Y. Kamijima and A. Sakai. A survey on the lace expansion for the nearest-neighbor models on the BCC lattice. Preprint (2017): arXiv:1712.05573.
- [50] S. Handa, Y. Kamijima and A. Sakai. Quantum effect on the divergence around the critical temperature of the Ising susceptibility. In preparation.
- [51] T. Hara. Decay of correlations in nearest-neighbour self-avoiding walk, percolation, lattice trees and animals. *Ann. Probab.* **36** (2008): 530–593.
- [52] T. Hara, R. van der Hofstad and G. Slade. Critical two-point functions and the lace expansion for spread-out high-dimensional percolation and related models. *Ann. Probab.* **31** (2003): 349–408.
- [53] T. Hara and G. Slade. On the upper critical dimension of lattice trees and lattice animals. *J. Stat. Phys.* **59** (1990): 1469–1510.
- [54] T. Hara and G. Slade. Mean-field critical behaviour for percolation in high dimensions. *Commun. Math. Phys.* **128** (1990): 333–391.
- [55] T. Hara and G. Slade. Self-avoiding walk in five or more dimensions. I. The critical behaviour. *Commun. Math. Phys.* **147** (1992): 101–136.
- [56] T. Hara and G. Slade. The lace expansion for self-avoiding walk in five or more dimensions. *Rev. Math. Phys.* **4** (1992): 235–327.
- [57] T. Hara and G. Slade. Mean-field behaviour and the lace expansion. *Probability and Phase Transition* (ed., G. R. Grimmett, Kluwer, 1994): 87–122.
- [58] T. Hara and H. Tasaki. 相転移と臨界現象の数理 (共立出版株式会社, 2015年).
- [59] M. Heydenreich and R. van der Hofstad. *Progress in high-dimensional percolation and random graphs* (CRM Short Courses, Springer, 2017).

- [60] M. Heydenreich, R. van der Hofstad and A. Sakai. Mean-field behavior for long- and finite range Ising model, percolation and self-avoiding walk. *J. Stat. Phys.* **132** (2008): 1001–1049.
- [61] M. Heydenreich and L. Kolesnikov. The critical 1-arm exponent for the ferromagnetic Ising model on the Bethe lattice. *J. Math. Phys.* **59** (2018): 043301.
- [62] R. van der Hofstad and A. Sakai. Critical points for spread-out self-avoiding walk, percolation and the contact process above the upper critical dimensions. *Probab. Theory Related Fields* **132** (2005): 438–470.
- [63] T. Hulshof. The one-arm exponent for mean-field long-range percolation. *Electron. J. Probab.* **7** (2015). Paper no. 115.
- [64] Y. Imry and S. K. Ma. Random-filed instability of the ordered state of continuous symmetry. *Phys. Rev. Lett.* **35** (1975): 1399–1401.
- [65] J. Jonasson and J.E. Steif. Amenability and phase transition in the Ising model. *J. Theor. Probab.* **12** (1999): 549–559.
- [66] S. Katsura and M. Takizawa. Bethe lattice and the Bethe approximation. *Progr. Theor. Phys.* **51** (1974): 82–98.
- [67] G. Kozma and A. Nachmias. Arm exponents in high dimensional percolation. *J. Amer. Math. Soc.* **24** (2011): 375–409.
- [68] J.L. Lebowitz. GHS and other inequalities. *Commun. Math. Phys.* **35** (1974): 87–92.
- [69] T.D. Lee and C.N. Yang. Statistical theory of equation of state and phase transitions. II. Lattice gas and Ising model. *Phys. Rev.* **87** (1952): 410–419.
- [70] E.H. Lieb. A refinement of Simon’s correlation inequality. *Commun. Math. Phys.* **77** (1980): 127–135.
- [71] N. Madras and G. Slade. *The Self-Avoiding Walk* (Birkhäuser, 1993).
- [72] M.V. Menshikov. Coincidence of critical points in percolation problems. *Soviet Mathematics, Doklady* **33** (1986): 856–859.
- [73] B.G. Nguyen and W-S. Yang. Triangle condition for oriented percolation in high dimensions. *Ann. Prob.* **21** (1993): 1809–1844.
- [74] L. Onsager. Crystal statistics. I. A two-dimensional model with an order-disorder transition. *Phys. Rev.* **65** (1944): 117–149.
- [75] R. Peierls. On Ising’s model of ferromagnetism. *Proc. Cambridge Phil. Soc.* **32** (1936): 477–481.
- [76] C.J. Preston. *Gibbs States on Countable Sets* (Cambridge University Press, London, 1974).

- [77] A. Sakai. Mean-field critical behavior for the contact process. *J. Stat. Phys.* **104** (2001): 111–143.
- [78] A. Sakai. Mean-field behavior for the survival probability and the percolation point-to-surface connectivity. *J. Stat. Phys.* **117** (2004): 111–130.
- [79] A. Sakai. Lace expansion for the Ising model. *Commun. Math. Phys.* **272** (2007): 283–344.
- [80] A. Sakai. Applications of the lace expansion to statistical-mechanical models. A chapter in *Analysis and Stochastics of Growth Processes and Interface Models* (P. Mörters et al. eds., Oxford University Press, 2008): 123–147.
- [81] A. Sakai. Application of the lace expansion to the φ^4 model. *Commun. Math. Phys.* **336** (2015): 619–648.
- [82] R.H. Schonmann. Multiplicity of phase transitions and mean-field criticality on highly non-amenable graphs. *Commun. Math. Phys.* **219** (2001): 271–322.
- [83] B. Simon. Correlation inequalities and the decay of correlations in ferromagnets. *Commun. Math. Phys.* **77** (1980): 111–126.
- [84] B. Simon and R.B. Griffiths. The $(\phi^4)_2$ field theory as a classical Ising model. *Commun. Math. Phys.* **33** (1973): 145–164.
- [85] A.D. Sokal. An alternate constructive approach to the φ_3^4 quantum field theory, and a possible destructive approach to φ_4^4 . *Ann. Inst. Henri Poincaré Phys. Théorique* **37** (1982): 317–398.
- [86] G. Slade. The lace expansion and its applications. *Lecture Notes in Mathematics* **1879** (2006).
- [87] M. Suzuki. Relationship between d -Dimensional Quantal Spin Systems and $(d + 1)$ -Dimensional Ising Systems: Equivalence, Critical Exponents and Systematic Approximants of the Partition Function and Spin Correlations. *PTP.* **56** (1976): 1454–1469.
- [88] H. Tasaki. Hyperscaling inequalities for percolation. *Commun. Math. Phys.* **113** (1987): 49–65.
- [89] T.T. Wu, B.M. McCoy, C.A. Tracy and E. Barouch. Spin-spin correlation functions for the two-dimensional Ising model: Exact theory in the scaling region. *Phys. Rev. B* **13** (1976): 316–374.
- [90] C.N. Yang. The spontaneous magnetization of a two-dimensional Ising model. *Phys. Rev.* **85** (1952): 808–816.